INFORMATION TO USERS

This material was produced from a microfilm copy of the original document. While the most advanced technological means to photograph and reproduce this document have been used, the quality is heavily dependent upon the quality of the original submitted.

The following explanation of techniques is provided to help you understand markings or patterns which may appear on this reproduction.

1. The sign or "target" for pages apparently lacking from the document photographed is "Missing Page(s)". If it was possible to obtain the missing page(s) or section, they are spliced into the film along with adjacent pages. This may have necessitated cutting thru an image and duplicating adjacent pages to insure you complete continuity.

2. When an image on the film is obliterated with a large round black mark, it is an indication that the photographer suspected that the copy may have moved during exposure and thus cause a blurred image. You will find a good image of the page in the adjacent frame.

3. When a map, drawing or chart, etc., was part of the material being photographed the photographer followed a definite method in "sectioning" the material. It is customary to begin photoing at the upper left hand corner of a large sheet and to continue photoing from left to right in equal sections with a small overlap. If necessary, sectioning is continued again — beginning below the first row and continuing on until complete.

4. The majority of users indicate that the textual content is of greatest value, however, a somewhat higher quality reproduction could be made from "photographs" if essential to the understanding of the dissertation. Silver prints of "photographs" may be ordered at additional charge by writing the Order Department, giving the catalog number, title, author and specific pages you wish reproduced.

5. PLEASE NOTE: Some pages may have indistinct print. Filmed as received.

University Microfilms International
300 North Zeeb Road
Ann Arbor, Michigan 48106 USA
St. John's Road, Tyler's Green
High Wycombe, Bucks, England HP10 8HR

77-17,978

DEDE, Metin, 1936-
SOME STUDIES OF NONLINEAR DYNAMICS
OF BEAMS.

The University of Michigan, Ph.D., 1977
Applied Mechanics

Xerox University Microfilms, Ann Arbor, Michigan 48106

SOME STUDIES ON NONLINEAR DYNAMICS OF BEAMS

by
Metin Dede

A dissertation submitted in partial fulfillment
of the requirements for the degree of
Doctor of Philosophy
(Applied Mechanics)
in The University of Michigan
1977

Doctoral Committee:

Associate Professor Richard A. Scott, Co-Chairman
Professor William J. Anderson, Co-Chairman
Professor Samuel K. Clark
Professor Donald T. Greenwood
Professor Roger D. Low

ACKNOWLEDGEMENTS

The help and assistance of numerous persons contributed to the realization of this endeavor. Most grateful appreciation is extended to my co-advisors Professors Richard A. Scott and William J. Anderson for their invaluable guidance. I would also like to express appreciation to Professors D. T. Greenwood, R. D. Low and S. K. Clark for their suggestions and help. Financial support is gratefully acknowledged from the Rackham School of Graduate Studies, the Department of Applied Mechanics and Engineering Science, The University of Michigan Computing Center, and the Ford Motor Company. Many thanks are due my wife for her untiring encouragement.

TABLE OF CONTENTS

ACKNOWLEDGEMENTS.....ii

LIST OF ILLUSTRATIONS.....iv

LIST OF ABBREVIATIONS.....vii

PART ONE: NONLINEAR-WHIRLING MOTION OF AN INITIALLY BUCKLED BEAM

1.1. Introduction.....1

1.2. Derivations of the Equations of Motion.....3

1.2.1. Relationship between Forces, Moments, and Displacements

1.3. Frequency-Amplitude Relation.....14

1.3.1. Galerkin's Method
1.3.2. Planar Vibration
1.3.3. Nonplanar Vibration

1.4. Stability.....23

1.4.1. Planar Vibration
1.4.2. Nonplanar Vibration

1.5. Numerical Results and Conclusions.....36

PART TWO: STEADY-STATE NONLINEAR VIBRATION OF VISCOELASTIC, LAYERED BEAMS

2.1. Introduction.....44

2.2. Derivation of the Equations of Motion.....46

2.3. Frequency-Amplitude Relation.....57

2.4. Parametric Study.....66

2.5. Experimental Results.....69

REFERENCES.....74

ILLUSTRATIONS.....78

LIST OF ILLUSTRATIONS

Figure		Page
1.1	Initial buckling and deformation of a beam in the x-z plane.....	3
1.2.	Force resultants and moments acting on an infinitesimal beam element in the x-z plane.....	4
1.3.	Force resultants and moments acting on an infinitesimal beam element in the y-z plane.....	5
1.4.	Deformation in the x-z plane.....	7
1.5.	Deformation in the y-z plane.....	7
1.6.	Geometry of cross-section of a beam element.....	9
1.7.	Response and stability regions for planar motion. $m = 1,\ n = 1,\ 2,\ \alpha = .005,\ \beta = .01,\ \lambda = 2,\ \bar{c}_1 \neq 0$.....	78
1.8.	Response and stability regions for planar motion. $m = 1,\ n = 1,\ \alpha = .005,\ \beta = .01,\ \lambda = 4,\ \bar{c}_1 \neq 0$....	79
1.9.	Response and stability regions for planar motion. $m = 1,\ n = 1,\ \alpha = .01,\ \beta = .02,\ \lambda = 2,\ \bar{c}_1 \neq 0$.....	80
1.10.	Response and stability regions for planar motion. $m = 1,\ n = 1,\ \alpha = .01,\ \beta = .02,\ \lambda = 4,\ \bar{c}_1 \neq 0$....	81
1.11.	Stability regions for planar motion. $m = 1,\ n = 1,\ \alpha = .005,\ \beta = .01,\ \lambda = 2,\ 4,\ \bar{c}_1 \neq 0$.....	82
1.12.	Stability regions for planar motion. $m = 1,\ n = 1,\ \alpha = .01,\ \beta = .02,\ \lambda = 2,\ 4,\ \bar{c}_1 \neq 0$.....	83
1.13.	Response and stability regions for planar motion. $m = 1,\ n = 1,\ \alpha = .005,\ \beta = .01,\ \lambda = 1.1,\ \bar{c}_1 = 0$....	84
1.14.	Response and stability regions for planar motion. $m = 1,\ n = 1,\ \alpha = .01,\ \beta = .02,\ \lambda = 1.1,\ \bar{c}_1 = 0$.....	85
1.15.	Response and stability regions for nonplanar motion. $m = 1,\ n = 1,\ \alpha = .005,\ \beta = .01,\ \lambda = 2,\ \bar{c}_1 \neq 0$.....	86

Figure Page

1.16. Response and stability regions for nonplanar motion. $m = 1$, $n = 1$, $\alpha = .005$, $\beta = .01$, $\lambda = 2$, $\bar{c}_1 \neq 0$..... 87

1.17. Response and stability regions for nonplanar motion. $m = 1$, $n = 1$, $\alpha = .01$, $\beta = .02$, $\lambda = 2$, $\bar{c}_1 \neq 0$..... 88

1.18. Response and stability regions for nonplanar motion. $m = 1$, $n = 1$, $\alpha = .01$, $\beta = .02$, $\lambda = 2$, $\bar{c}_1 \neq 0$..... 89

1.19. Response and stability regions for nonplanar motion. $m = 1$, $n = 1$, $\alpha = .005$, $\beta = .01$, $\lambda = 4$, $\bar{c}_1 \neq 0$..... 90

1.20. Response and stability regions for nonplanar motion. $m = 1$, $n = 1$, $\alpha = .005$, $\beta = .01$, $\lambda = 4$, $\bar{c}_1 \neq 0$..... 91

1.21. Response and stability regions for nonplanar motion. $m = 1$, $n = 1$, $\alpha = .01$, $\beta = .02$, $\lambda = 4$, $\bar{c}_1 \neq 0$..... 92

1.22. Response and stability regions for nonplanar motion. $m = 1$, $n = 1$, $\alpha = .01$, $\beta = .02$, $\lambda = 4$, $\bar{c}_1 \neq 0$..... 93

1.23. Response and stability regions for nonplanar motion. $m = 1$, $n = 1$, $\alpha = .005$, $\beta = .01$, $\lambda = 1.1$, $\bar{c}_1 = 0$.... 94

1.24. Response and stability regions for nonplanar motion. $m = 1$, $n = 1$, $\alpha = .005$, $\beta = .01$, $\lambda = 1.1$, $\bar{c}_1 = 0$.... 95

1.25. Response and stability regions for nonplanar motion. $m = 1$, $n = 1$, $\alpha = .01$, $\beta = .02$, $\lambda = 1.1$, $\bar{c}_1 = 0$..... 96

1.26. Response and stability regions for nonplanar motion. $m = 1$, $n = 1$, $\alpha = .01$, $\beta = .02$, $\lambda = 1.1$, $\bar{c}_1 = 0$.... 97

2.1. Shear and bending deformations of an infinitesimal beam element..... 49

2.2. Force resultants and moments acting on an infinitesimal beam element..... 50

2.3. Dynamic mechanical properties of ISPD 111..... 98

2.4. Shear modulus and loss tangent-temperature of ISPD 111 at 100 Hz..... 99

Figure		Page
2.5.	Undamped response. h = .018", b = 1", L = 12".....	100
2.6.	Undamped response. h = .022", b = 1", L = 12".....	101
2.7.	Undamped response. h = .035", b = 1", L = 12".....	102
2.8.	Damped response. h = .018", b = 1", L = 12", t = .008" layer.....	103
2.9.	Damped response. h = .022", b = 1", L = 12", t = .008" layer.....	104
2.10.	Damped response. h = .035", b = 1", L = 12", t = .008" layer.....	105
2.11.	ISPD 111 viscoelastic layer thickness F = .1 lbs., ω = 70 Hz.....	106
2.12.	Experimental test set-up.....	107
2.13.	Excitation force.....	108
2.14.	Response.....	108
2.15.	Calibration curve of proximeter.....	109
2.16.	Jump-beating phenomena.....	110

LIST OF ABBREVIATIONS

A_o	Area of cross section
A_2, A_3, A_4, A_5	Coefficients defined in eqs. (2.28) and (2.35)
A^T	Area of cross section of viscoelastic face layers
$\bar{A}_1$	Frequency dependent amplitude defined in eq. (2.39)
$\bar{A}_2, \bar{A}_3$	Frequency dependent amplitudes defined in eqs. (2.42)
A	Amplitude of nondimensional time dependencies p_m
2a	Width of the beam in Part One
$a_1, a_2, a_3, a_4, a_5, a_6$	Constant coefficients used in eqs. (1.100) and (1.101)
$a_{11}, a_{22}, a_{33}, a_{44}, a_{55}, a_{66}$	Constant coefficients used in eqs. (1.124) and (1.123)
B	Amplitude of nondimensional time dependencies q_n
B_c	Constant material property defined in eq. (2.19)
B_1, B_2, B_3, B_4	Constant coefficients defined in eqs. (2.32) and (2.35)
2b	Depth of the beam in Part One
c	Viscous damping coefficient per unit length
C_1, C_3, C_5, C_7	Coefficients defined in eqs. (2.50)
C_o, C_2, C_4	Coefficients defined in eqs. (1.108)
$\bar{C}_o, \bar{C}_2, \bar{C}_4$	Coefficients defined in eqs. (1.117)
$\bar{c}_1$	Constant amplitude of nondimensional time dependencies p_m
D_c	Constant material property defined in eq. (2.19)

D_o, D_2, D_4	Coefficients defined in eqs. (1.115)
$\bar{D}_o, \bar{D}_2, \bar{D}_4$	Coefficients defined in eqs. (1.119)
E	Young's modulus
E_{ij}	Green's strain measure
$F_1 \cdots F_8$	Coefficients defined in eqs. (2.30) and (2.35)
F_{ox}, F_{oy}	Amplitudes of nondimensional forces F_{x1} and F_{y1} respectively
$F_x(z, t), F_y(z, t)$	External forces per unit length
G_c	Modulus of rigidity of elastic core
h	Thickness of elastic core
I^c	Moment of inertia of elastic core
I_{xx}, I_{yy}	Moments of inertia about x and y axes
K	Constant material property defined in eq. (2.19)
K_1	Integration constant defined in eq. (1.33)
K_o, K_2, K_4	Coefficients defined in eqs. (2.56)
k	Timoshenko shear coefficient
k_x, k_y	Constants defined in eq. (1.55)
L	Length of the beam
ℓ_x, ℓ_y	Constants defined in eq. (1.55)
M_x, M_y	Moments about x and y axes, respectively
N_x, N_y, N_z	Force resultants in x, y, and z directions respectively
P_x, P_y	Nondimensional external forces
p_m, q_n	Time dependencies defined in eqs. (1.44) and (1.45)

Q_x, Q_y	Shear forces in the x-y directions, respectively
Q_1, Q_2	Functions defined in eqs. (1.100)
Q_{11}, Q_{22}	Functions defined in eqs. (1.123)
S_{zz}	Component of stress tensor
t	Time
u, v, w	Displacements at point (x, y, z) defined in eqs. (1.12), (1.13) and (1.14)
$\bar{u}, \bar{v}$	Nondimensional displacements
u_o, v_o, w_o	Displacements of the neutral axes in the x, y, z directions, respectively
W	Frequency dependent amplitude used in eq. (2.36)
ΔW_{cr}	Initial net axial displacement due to first buckling load
x, y, z	Cartesian coordinates
α	$\frac{2b}{L}$ defined in eq. (1.56)
β	$\frac{2a}{L}$ defined in eq. (1.56)
β_2	Constants defined in eq. (2.42)
γ	A Galerkin trial function defined in eq. (2.24)
$\gamma_1, \bar{\gamma}_3$	Constants defined in eq. (2.39) and (2.42)
$\delta p_m, \delta q_n$	Perturbations of p_m and q_n, respectively
$\epsilon_{1x}, \epsilon_{2x}, \alpha_x$ $\epsilon_{1y}, \epsilon_{2y}, \alpha_y$	Coefficients defined in eqs. (1.98)
$\bar{\epsilon}_{1x}, \bar{\epsilon}_{2x}, \beta_{1x}, \beta_{2x}, \bar{\alpha}_x$ $\bar{\epsilon}_{1y}, \bar{\epsilon}_{2y}, \beta_{1y}, \beta_{2y}, \bar{\alpha}_y$	Coefficients defined in eqs. (1.121)
ζ^T	$\frac{G}{\omega} 14.5 \times 10^{-6} \tan \delta$ damping parameter for viscoelastic face layer

η	Time dependence defined in eq. (2. 24)
θ	Slope due to bending
λ	$\Delta W_B / \Delta W_{cR}$ buckling parameter defined in eq. (1. 43)
μ	A Galerkin trial function defined in eq. (2. 24)
ξ	A Galerkin trial function defined in eq. (2. 24)
ρ	Mass density per unit length
σ	Characteristic exponent used in eq. (1. 99)
τ, T	Time dependencies defined in eqs. (2. 24)
ϕ_m	A Galerkin trial function defined in eqs. (1. 51)
ψ_n	A Galerkin trial function defined in eqs. (1. 52)
ω'	Frequency of external force
ω_o	Linear fundamental frequency
ω	Frequency ratio ω' / ω_o

PART ONE

NONLINEAR-WHIRLING MOTION OF AN INITIALLY BUCKLED BEAM

1.1. INTRODUCTION

Nonlinear transverse vibration of a beam whose ends are assumed to remain a fixed distance apart during vibration, has been studied extensively. The nonlinearity is introduced into the equations of motion by the extension of the neutral axis by the restriction of immovable supports. References to early work on the plane vibration of unbuckled beams can be found in the thesis of Ho [1]. Eisley [2] studied the large amplitude vibration of buckled beams and rectangular plates. Min and Eisley [3] examined the theoretical response and stability of free and forced vibration of a simply supported buckled beam. Tseng and Dugundji [4] studied analytically and experimentally a buckled beam with fixed ends, excited by the harmonic motion of its supporting base. Plane response and stability regions were determined.

Early work on out-of-plane motions of strings has been reported by Ames, Lee, Zaiser [5], Ames, Vicario, Jr. [6], Ames, Lee, Vicario, [7], and Shih [ ]. However, few such studies have been reported for beams. In this area, Haight and King [9] examined harmonic plane excitation of a cantilever beam and mentioned that in certain circumstances the response was nonplanar. Rodgers and

Warner [10] studied the dynamic response and out-of-plane stability of thin curved rods excited by a harmonic end force applied normal to the cross-section. More recently Ho, Scott, and Eisley [11, 12] studied the large amplitude nonplanar vibration of a simply supported beam with immovable ends. Hamilton's principle was used to derive the equations of motion and Galerkin's method was employed to reduce the governing nonlinear coupled partial differential equations to coupled ordinary differential equations. Stability analysis showed that under certain circumstances planar motion was unstable to out-of-plane perturbations. It was further found that the ensuing motion could be of the steady state or beating type.

The present study is concerned with the effect of buckling on out-of-plane stability. Governing equations of motion, which are original, were derived using the equilibrium principle and certain kinematic approximations. Galerkin's method is then employed to generate a set of ordinary nonlinear differential equations. Response and stability are investigated by means of an approximate method applied to these equations of motion.

1.2. DERIVATIONS OF THE EQUATIONS OF MOTION

Consider a simply supported symmetric beam initially buckled in the x-z plane*, with the xy axes being in the plane of symmetry.

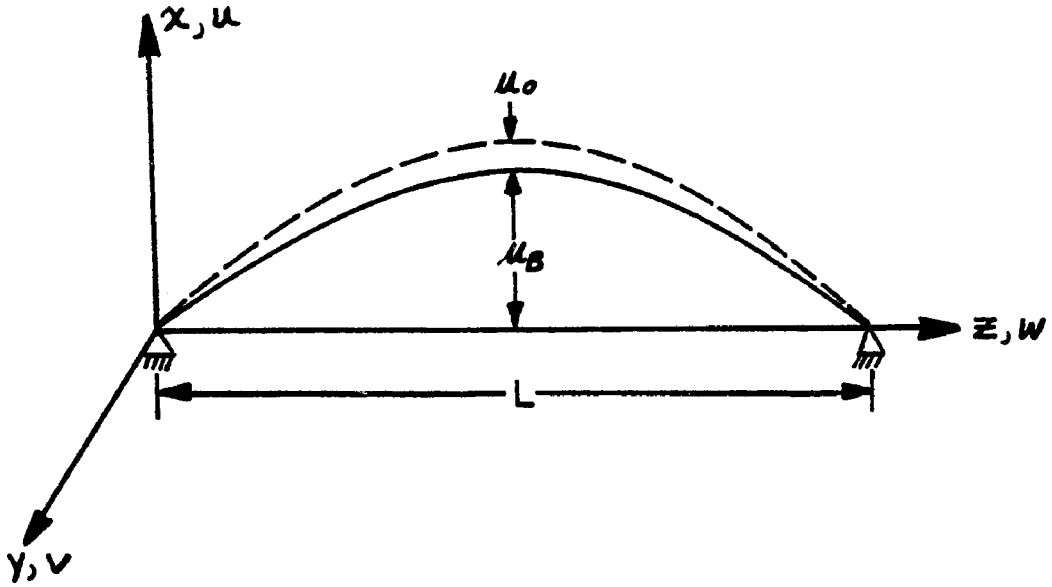


Figure 1.1. Initial buckling and deformation of a beam in the x-z plane.

The distance L between the supports is fixed, after the beam is buckled; u, v and w are displacements of an arbitrary point in the cross-section in the x, y, z directions respectively. The equations of motion for the initially buckled beam will be derived using Lagrangian coordinates (based on undeformed shape) and equilibrium conditions as follows: it is assumed that the forces in the x-z plane and the moments about the y-axis are as given in Figure 1.2. Note in the ensuing equilibrium analysis no distinction is made between the arc length ds and dz.

* This implies $I_{xx} > I_{yy}$ where $I_{xx} = \iint_{A_o} y^2 dA_o$, $I_{yy} = \iint_{A_o} x^2 dA_o$ where A_o is the area of the x-section.

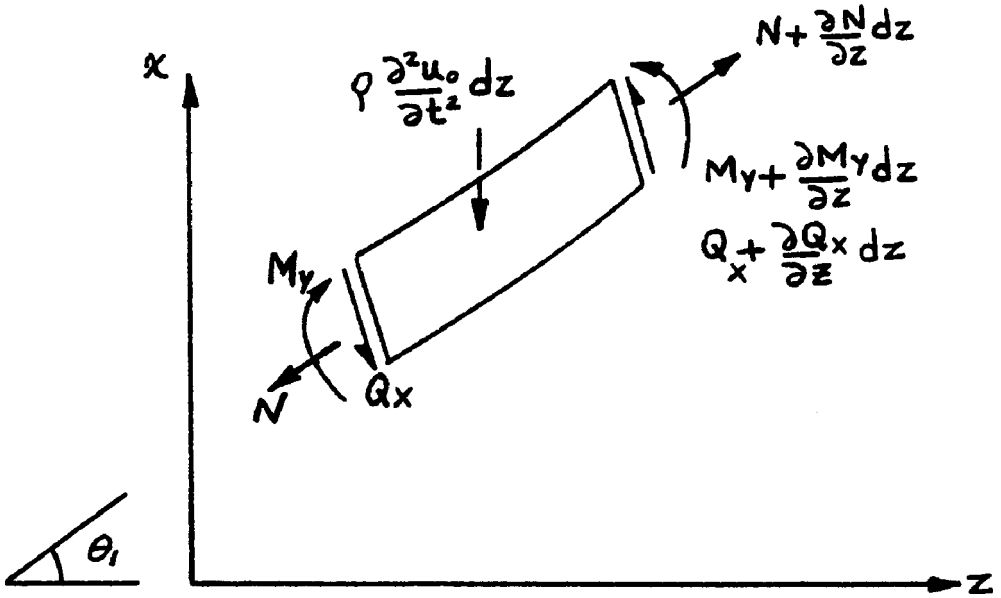


Figure 1. 2. Force resultants and moments acting on an infinitesimal beam element in the x-z plane.

Summation of the forces in the x-direction gives

$$\frac{\partial N_x}{\partial z} + \frac{\partial Q_x}{\partial z} - \rho \frac{\partial^2 u_o}{\partial t^2} - c \frac{\partial u_o}{\partial t} = - F_x(z, t) \qquad (1.1)$$

where ρ is mass per unit length, c is viscous damping coefficient per unit length, F_x is external force and $u = u_o + u_B$, the subscripts o and B denoting a centerline quantity. Also note $\frac{\partial^2 u_B}{\partial t^2} = 0$. Summation of y-axis moments about the centroid gives (on neglecting the rotatory inertia about the y-axis):

$$\frac{\partial M_y}{\partial z} + Q_x = 0 \qquad (1.2)$$

where for small slope (assumed)

$$N_x = N \frac{\partial (u_o + u_B)}{\partial z} \qquad (1.3)$$

$$N_z \cong N \qquad (1.4)$$

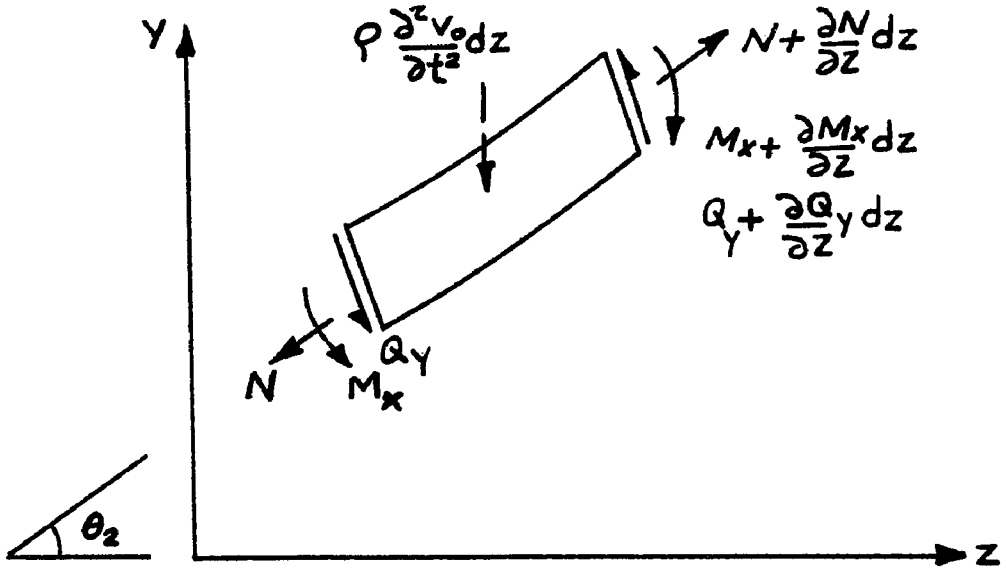


Figure 1.3. Force resultants and moments acting on an infinitesimal beam element in the y-z plane.

The forces in the y-z plane and the moment about the x-axis are shown in Figure 1.3. Summation of forces in the y-direction gives:

$$\frac{\partial N_y}{\partial z} + \frac{\partial Q_y}{\partial z} - \rho \frac{\partial^2 v_o}{\partial t^2} - c \frac{\partial v_o}{\partial t} = - F_y(z,t) \qquad (1.5)$$

$$\text{where } v \equiv v_o \qquad \text{and } N_y = N \frac{\partial v_o}{\partial z} \qquad (1.6)$$

Summation of the x-axis moment about the centroid gives (on neglecting the inertia about the x-axis):

$$\frac{\partial M_x}{\partial z} - Q_y = 0 \qquad (1.7)$$

Summation of forces in the z-direction gives (on neglecting the longitudinal inertia):

$$\frac{\partial N_z}{\partial z} - \frac{\partial}{\partial z}\left(\frac{\partial v_o}{\partial z} Q_y + \frac{\partial u}{\partial z} Q_y\right) = 0 \qquad (1.8)$$

Following the same assumption used by Herrmann [13] and other authors, the horizontal component of shear force is neglected in eq. (1.8) hereafter. Then eq. (1.8) gives

$$N_z = K_1 \quad , \quad \text{a constant.} \qquad (1.9)$$

From eqs. (1.1) and (1.2) Q_x and from eqs. (1.5) and (1.7) Q_y can be eliminated to give

$$\frac{\partial N_x}{\partial z} - \frac{\partial^2 M_y}{\partial z^2} - \rho \frac{\partial^2 u_o}{\partial t^2} - c \frac{\partial u_o}{\partial t} = - F_x(z, t) \qquad (1.10)$$

$$\frac{\partial N_y}{\partial z} + \frac{\partial^2 M_x}{\partial z^2} - \rho \frac{\partial^2 v_o}{\partial t^2} - c \frac{\partial v_o}{\partial t} = - F_y(z, t) \qquad (1.11)$$

1.2.1. RELATIONSHIPS BETWEEN FORCES, MOMENTS, AND DISPLACEMENTS

The assumed deformation pattern is shown in Figures 1.4 and 1.5:

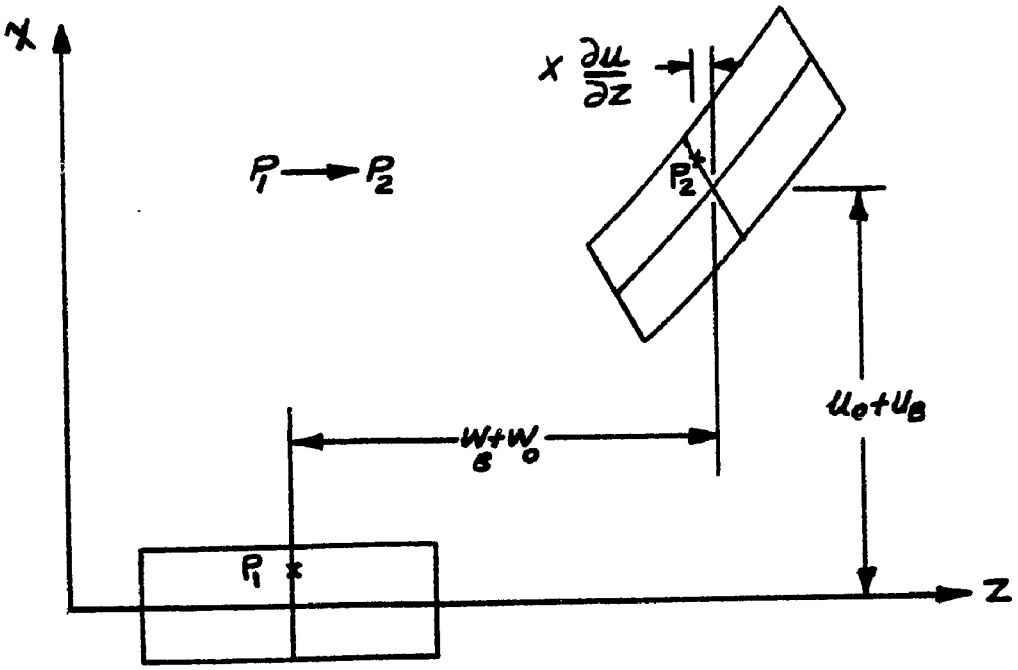
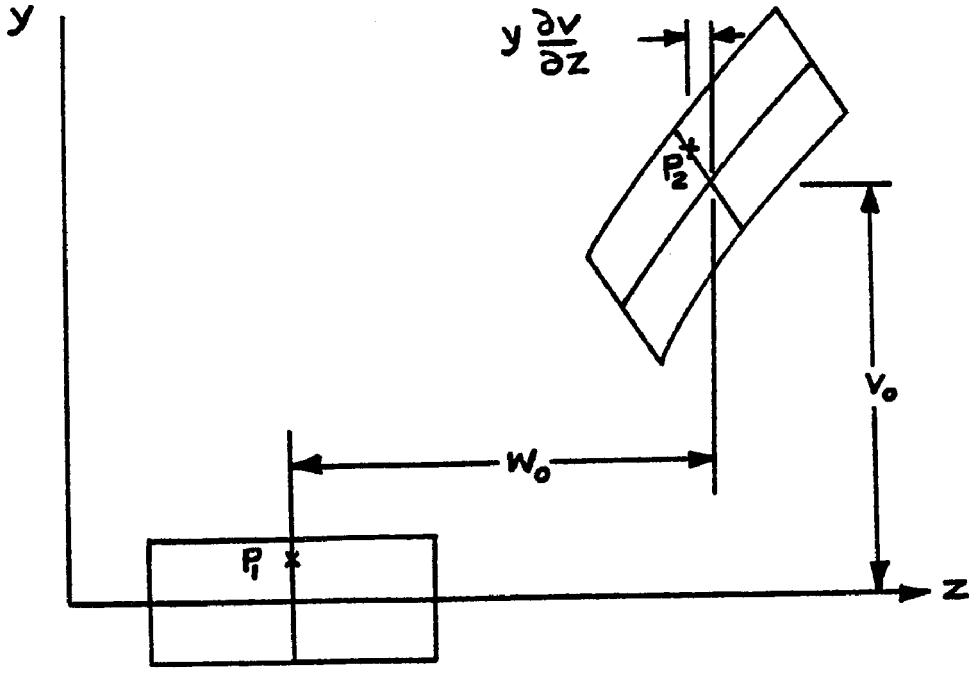


Figure 1.4. Deformation in the x-z plane.



1.5. Deformation in the y-z plane.

where w_B is the initial displacement of the neutral axis in the x-z plane due to buckling. The rotations of the element are taken in the counter-clockwise direction in order to be consistent with the definition of positive slope.

Using Figures 1.4 and 1.5, the displacements can be written:

$$w = w_o + w_B - x\frac{\partial u}{\partial z} - y\frac{\partial v}{\partial z} \tag{1.12}$$

$$u = u_o + u_B \tag{1.13}$$

$$v = v_o \tag{1.14}$$

Nonlinearity is taken into account only through use of Green's strain tensor in the z-direction

$$E_{zz} = \frac{\partial w}{\partial z} + \frac{1}{2}\left[\left(\frac{\partial u}{\partial z}\right)^2 + \left(\frac{\partial v}{\partial z}\right)^2 + \left(\frac{\partial w}{\partial z}\right)^2\right] \tag{1.15}$$

Subsequently, $\left(\frac{\partial w}{\partial z}\right)^2$ is taken to be small and is neglected.

The axial force can be written, on neglecting Poisson's effect and considering only isotropic materials, so that the Kirchhoff stress tensor component is $S_{zz} = E\,E_{zz}$ where E is Young's modulus, and noting again $N \cong N_z$,

$$N_z = \int\int_{A_o} E\,E_{zz}\,d\,A_o \tag{1.16}$$

Taking, for example, a beam of rectangular cross-section (as shown in Figure 1.6) yields

$$N_z = E\int_{-b}^{b}\int_{-a}^{a}\left[\left(\frac{\partial w}{\partial z}\right) + \frac{1}{2}\left\{\left(\frac{\partial u}{\partial z}\right)^2 + \left(\frac{\partial v}{\partial z}\right)^2\right\}\right] dxdy \tag{1.17}$$

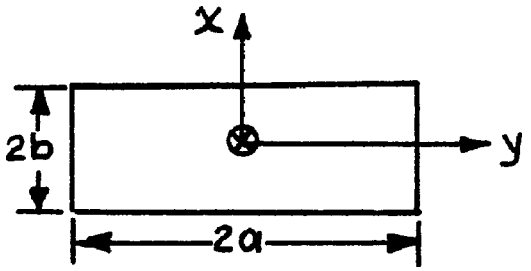


Figure 1.6. Geometry of cross-section of a beam element.

Substituting eqs. (1.12), (1.13) and eq. (1.14) into eq. (1.17) gives

$$N_z = E \int_{-a}^{a} \int_{-b}^{b} \left[\frac{\partial (w_o + w_B)}{\partial z} - x \frac{\partial^2 (u_o + u_B)}{\partial z^2} - y \frac{\partial^2 v_o}{\partial z^2} + \frac{1}{2} \left\{ \left(\frac{\partial (u_o + u_B)}{\partial z} \right)^2 + \left(\frac{\partial v_o}{\partial z} \right)^2 \right\} \right] dA_o \tag{1.18}$$

Carrying out the integrations over x and y results in

$$N_z = E A_o \left[\frac{\partial (w_o + w_B)}{\partial z} + \frac{1}{2} \left\{ \left(\frac{\partial (u_o + u_B)}{\partial z} \right)^2 + \left(\frac{\partial v_o}{\partial z} \right)^2 \right\} \right] \tag{1.19}$$

Note that

$$N_x = N \sin \theta_1 \cong N_z \sin \theta_1 \cong N_z \frac{\partial u}{\partial z} \tag{1.20}$$

and

$$N_y = N \sin \theta_2 \cong N_z \sin \theta_2 \cong N_z \frac{\partial v}{\partial z} \tag{1.21}$$

Further

$$M_x = (2b) \int_{-a}^{a} S_{zz} \, y \, dy \tag{1.22}$$

$$M_y = -(2a) \int_{-b}^{b} S_{zz} \, x \, dx \tag{1.23}$$

or

$$M_x = (2b) \int_{-a}^{a} E\, E_{zz}\, y\, dy \tag{1.24}$$

Substituting eqs. (1.12), (1.13), (1.14) and (1.15) into eq. (1.24) gives

$$M_x = 2b\, E \int_{-a}^{a} \left[\frac{\partial (w_o + w_B)}{\partial z} - x \frac{\partial^2 u}{\partial z^2} - y \frac{\partial^2 v}{\partial z^2} + \frac{1}{2} \left\{ \left(\frac{\partial u}{\partial z} \right)^2 + \left(\frac{\partial v}{\partial z} \right)^2 \right\} \right] y\, dy \tag{1.25}$$

Noting that the cross-section is symmetric, this reduces to:

$$M_x = -2b\, E \int_{-a}^{a} \left(\frac{\partial^2 v}{\partial z^2} \right) y^2\, dy \tag{1.26}$$

$$= -E\, I_{xx} \frac{\partial^2 v_o}{\partial z^2} \tag{1.27}$$

where

$$I_{xx} = \frac{4}{3}\, ba^3 \tag{1.28}$$

Similarly

$$M_y = -2a\, E \int_{-b}^{b} \left[\left(\frac{\partial (w_o + w_B)}{\partial z} - x \frac{\partial^2 u}{\partial z^2} - y \frac{\partial^2 v}{\partial z^2} \right) + \frac{1}{2} \left\{ \left(\frac{\partial u}{\partial z} \right)^2 + \left(\frac{\partial v}{\partial z} \right)^2 \right\} \right] x\, dx = E\, I_{yy} \frac{\partial^2 (u_o + u_B)}{\partial z^2} \tag{1.29}$$

where

$$I_{yy} = \frac{4}{3}\, ab^3 \ . \tag{1.30}$$

By substituting eqs. (1.20), (1.21), (1.26) and (1.29) into eqs. (1.9), (1.10), and (1.11), gives

$$N_z \frac{\partial^2 u}{\partial z^2} - \frac{\partial^2}{\partial z^2} E I_{yy} \left(\frac{\partial^2 u_o}{\partial z^2} + \frac{\partial^2 u_B}{\partial z^2} \right) - \rho \frac{\partial^2 u_o}{\partial t^2} - c \frac{\partial u_o}{\partial t} = - F_x(z, t) \tag{1.31}$$

$$N_z \frac{\partial^2 v_o}{\partial z^2} - \frac{\partial^2}{\partial z^2} E I_{xx} \frac{\partial^2 v_o}{\partial z^2} - \rho \frac{\partial^2 v_o}{\partial t^2} - c \frac{\partial v_o}{\partial t} = - F_y(z, t) \tag{1.32}$$

$$N_z \equiv \left(E A_o \left[\frac{\partial (w_o + w_B)}{\partial z} + \frac{1}{2} \left\{ \left(\frac{\partial (u_o + u_B)}{\partial z} \right)^2 + \left(\frac{\partial v_o}{\partial z} \right)^2 \right\} \right] \right) = K_1 \tag{1.33}$$

The constant K_1, that is to say N_z, can be calculated from eq. (1.33) on integrating from 0 to L:

$$N_z L = E A_o \int_o^L \left\{ \frac{\partial (w_o + w_B)}{\partial z} + \frac{1}{2} \left[\left(\frac{\partial (u_o + u_B)}{\partial z} \right)^2 + \left(\frac{\partial v_o}{\partial z} \right)^2 \right] \right\} dz = \int_o^L K_1 \, dz \tag{1.34}$$

Now consider the first integral in eq. (1.34).

$$\int_o^L \frac{\partial (w_o + w_B)}{\partial z} dz = \left(w_o \Big|_L - w_o \Big|_o \right) + \left(w_B \Big|_L - w_B \Big|_o \right) \tag{1.35}$$

The boundary condition considered here is

$$w_o \Big|_L = w_o \Big|_o = 0 \tag{1.36}$$

which implies that the ends of the beam are held fixed, after buckling has occurred. Then eq. (1.35) gives

$$\int_o^L \frac{\partial}{\partial z}\,(w_o+w_B)\,dz = w_B\Big|_L - w_B\Big|_o \equiv \Delta w_B \tag{1.37}$$

where Δw_B is the net axial displacement due to initial buckling. Then eq. (1.34) gives

$$N_z = \frac{EA_o}{2L}\left(2\Delta w_B + \int_o^L \left[\left(\frac{\partial (u_o+u_B)}{\partial z}\right)^2 + \left(\frac{\partial v_o}{\partial z}\right)^2\right]dz\right) \tag{1.38}$$

Substituting eq. (1.38) into eqs. (1.31) and (1.32) gives

$$\frac{EA_o}{2L}\left\{2\Delta w_B + \int_o^L \left[\left(\frac{\partial (u_o+u_B)}{\partial z}\right)^2 + \left(\frac{\partial v_o}{\partial z}\right)^2\right]dz\right\}\frac{\partial^2 (u_o+u_B)}{\partial z^2}$$

$$-\frac{\partial^2}{\partial z^2}\left\{E I_{yy}\left(\frac{\partial^2 u_o}{\partial z^2} + \frac{\partial^2 u_B}{\partial z^2}\right)\right\} - \rho\frac{\partial^2 u_o}{\partial t^2} - c\frac{\partial u_o}{\partial t}$$

$$= -F_x(z,t) \tag{1.39}$$

$$\frac{EA_o}{2L}\left\{2\Delta w_B + \int_o^L \left[\left(\frac{\partial (u_o+u_B)}{\partial z}\right)^2 + \left(\frac{\partial v_o}{\partial z}\right)^2\right]dz\right\}\frac{\partial^2 v_o}{\partial z^2}$$

$$-\frac{\partial^2}{\partial z^2}\left(E I_{xx}\frac{\partial^2 v_o}{\partial z^2}\right) - \rho\frac{\partial^2 v_o}{\partial t^2} - c\frac{\partial v_o}{\partial t} = -F_y(z,t) \tag{1.40}$$

Note that when $v_o = 0$, eq. (1.39) reduces to Min and Eisley's [3] equation. Further, eqs. (1.39) and (1.40) are the same as those of Ho, Scott, and Eisley [11] when Δw_B is set to zero.

In non-dimensional form eqs. (1.39) and (1.40) may be written:

$$\frac{\partial^2 \bar{u}_o}{\partial \tau^2} + \frac{I_{yy}}{A_o L^2}\left[\frac{\partial^4}{\partial \bar{z}^4}(\bar{u}_o+\bar{u}_B) + \lambda\pi^2\frac{\partial^2}{\partial \bar{z}^2}(\bar{u}_o+\bar{u}_B)\right] - \frac{1}{2}\left\{\int_o^1\left[\left(\frac{\partial \bar{v}_o}{\partial \bar{z}}\right)^2 + \left(\frac{\partial(\bar{u}_o+\bar{u}_B)}{\partial \bar{z}}\right)^2\right]d\bar{z}\right\}\frac{\partial^2 \bar{u}}{\partial \bar{z}^2} + \bar{c}\,\frac{\partial \bar{u}_o}{\partial \tau}$$

$$= F_x\left\{\bar{z}\,L,\ L\left(\frac{\rho}{EA_o}\right)^{1/2}\right\}\frac{L}{A_o E} \equiv F_x(\bar{z},\tau) \qquad (1.41)$$

$$\frac{\partial^2 \bar{v}_o}{\partial \tau^2} + \frac{I_{xx}}{A_o L^2}\left[\frac{\partial^4 \bar{v}_o}{\partial \bar{z}^4} + \lambda\gamma^2\pi^2\frac{\partial^2 \bar{v}_o}{\partial \bar{z}^2}\right] - \frac{1}{2}\left\{\int_o^1\left[\left(\frac{\partial \bar{v}_o}{\partial \bar{z}}\right)^2 + \left(\frac{\partial(\bar{u}_o+\bar{u}_B)}{\partial \bar{z}}\right)^2\right]d\bar{z}\right\}\frac{\partial^2 \bar{v}_o}{\partial \bar{z}^2} + \bar{c}\,\frac{\partial \bar{v}_o}{\partial \tau}$$

$$= F_y\left\{\bar{z}\,L,\ L\left(\frac{\rho}{A_o E}\right)^{1/2}\right\}\frac{L}{A_o E} \equiv F_y(\bar{z},\tau) \qquad (1.42)$$

where

$$\gamma = \left(2b/2a\right)$$

$$\bar{z} = \frac{z}{L}$$

$$\tau = \left(\frac{EA_o}{\rho}\right)^{1/2}\frac{t}{L}$$

$$\bar{u} = \frac{u}{L} \qquad (1.43)$$

$$\bar{v} = \frac{v_o}{L}$$

$$\bar{c} = \frac{c\,L}{(A_o E\rho)^{1/2}}$$

$$\lambda = \frac{\Delta w_B}{\Delta w_{cR}}$$

and $P_{cR} = \pi^2 \dfrac{E I_{yy}}{L^2}$ is the first buckling load and $\Delta w_{cR} = -\dfrac{P_{cR} L}{A_o E}$ is the initial net axial displacement due to the first buckling load.

1.3. FREQUENCY-AMPLITUDE RELATION

Eqs. (1.41) and (1.42) are nonlinear-coupled partial differential equations. An approximate technique, such as Galerkin's method, must be used. Displacements are assumed in the following form:

$$\bar{u}(\bar{z}, \tau) = \sum_{m=1}^{\infty} p_m(\tau)\phi_m(\bar{z}) \tag{1.44}$$

$$\bar{v}(\bar{z}, \tau) = \sum_{n=1}^{\infty} q_n(\tau)\, \psi_n(\bar{z}) \tag{1.45}$$

where $\phi_m(\bar{z})$, $\psi_n(\bar{z})$ are functions of a space variable and must satisfy the boundary conditions of the problem [14],

$$\phi_m(0) = \phi_m(1) = 0 \tag{1.46}$$

$$\psi_n(0) = \psi_n(1) = 0 \tag{1.47}$$

Substituting eqs. (1.44) and (1.45) into eqs. (1.41) and (1.42) gives

$$\sum_{m=1}^{\infty} \ddot{p}_m \phi_m + \frac{I_{yy}}{A_o L^2} \sum_{m=1}^{\infty} \left(\phi_m^{IV} + \pi^2 \lambda \phi_m''\right) \sum_{m=1}^{\infty} p_m - \frac{1}{2} \left\{ \int_0^1 \left[\sum_{n=1}^{\infty} q_n^2 \left(\psi_n'\right)^2 + \sum_{m=1}^{\infty} p_m^2 \left(\phi_m'\right)^2 \right] d\bar{z} \right\} \sum_{m=1}^{\infty} \phi_m'' p_m + \bar{c} \sum_{m=1}^{\infty} \dot{p}_m \phi_m = F_x(\bar{z}, \tau) \tag{1.48}$$

$$\sum_{n=1}^{\infty} \ddot{q}_n \psi_n + \frac{I_{xx}}{A_o L^2} \sum_{m=1}^{\infty} \left(\psi_n^{IV} + \pi^2 \gamma^2 \lambda \psi_n'' \right) \sum_{n=1}^{\infty} q_n - \frac{1}{2} \left\{ \int_o^1 \left[\sum_{n=1}^{\infty} q_n^2 \left(\psi_n' \right)^2 + \sum_{m=1}^{\infty} p_m^2 \left(\phi_m' \right)^2 \right] d\bar{z} \right\} \sum_{m=1}^{\infty} \psi_n'' q_n + \bar{c} \sum_{n=1}^{\infty} \dot{q}_n \psi_n = F_y(\bar{z}, \tau) \tag{1.49}$$

where

$$(\dot{}) = \frac{d}{d\tau}$$
$$(') = \frac{d}{d\bar{z}} \tag{1.50}$$

1.3.1. GALERKIN'S METHOD

Now Galerkin's method will be employed in order to reduce the nonlinear-coupled partial differential equations to ordinary differential equations. For the simply supported beam, the mode shapes of the linear problem are:

$$\phi_m(\bar{z}) = \sin m\pi \bar{z} \tag{1.51}$$

$$\psi_n(\bar{z}) = \sin n\pi \bar{z} \tag{1.52}$$

Eqs. (1.51) and (1.52) satisfy all the boundary conditions of the problem.

Multiplying eq. (1.48) by $\phi_m(\bar{z})$ and eq. (1.49) by $\psi_n(\bar{z})$ and integrating from zero to one with respect to $\bar{z}$, yields

$$\ddot{p}_m + \bar{c}\dot{p}_m + k_x p_m + \ell_x (q_n^2 + p_m^2) p_m = P_{xm} \tag{1.53}$$

$$\ddot{q}_n + \bar{c}\,\dot{q}_n + k_y q_n + \ell_y (q_n^2 + p_m^2) q_n = P_{yn} \tag{1.54}$$

where

$$k_x = \frac{\pi^4}{12}\,\alpha^2 m^2 (m^2 - \lambda)$$

$$k_y = \frac{\pi^4}{12}\,\beta^2 n^2 (n^2 - \gamma^2 \lambda) \tag{1.55}$$

$$\ell_x = m^2 \pi^4 / 4$$

$$\ell_y = n^2 \pi^4 / 4$$

$$P_{xm} = \frac{2L}{A_o E} \int_o^1 F_x\left(\bar{z}\, L;\, L\left[\frac{\rho}{EA_o}\right]\right) \sin m\pi \bar{z}\, d\bar{z}$$

$$P_{yn} = \frac{2L}{A_o E} \int_o^1 F_y\left(\bar{z}\, L;\, L\left[\frac{\rho}{EA_o}\right]\right) \sin n\pi\, \bar{z}\, d\bar{z} \tag{1.56}$$

$$\alpha = (2b/L)$$

$$\beta = (2a/L)$$

Eqs. (1.53) and (1.54) are nonlinear, coupled ordinary differential equations. Note that for an unbuckled beam, i.e., $\lambda = 0$, they reduce to the equations given by Ho, Scott, and Eisley [11, 12]. When $q_n = 0$, then eq. (1.53) reduces to Min and Eisley's [3] equation. There are no known exact solutions to these equations, but approximate solutions are possible. Here the harmonic balance method will be employed [15].

1.3.2 PLANAR VIBRATION

Consider now the special case of forcing in the x-direction only:

$$F_{x1} = F_{ox} \cos\omega\tau, \quad F_{y1} \equiv 0 \tag{1.57}$$

where F_{ox} is a constant and $\omega = \frac{\omega'}{\omega_o}$, ω' being the frequency of the external force and $\omega_o = \left(\frac{\pi A_o}{\rho}\right)^{1/2} \frac{1}{L}$. It is assumed that in certain circumstances the response to such an input will be in the x-direction only, i.e., $q_n \equiv 0$ (planar-vibration). Moreover attention is restricted to the case $m = n = 1$ and $\bar{c} = 0$.

From eq. (1.56)

$$P_{x1} = \frac{4 F_{ox} L}{\pi E A_o} \cos\omega\tau \tag{1.58}$$

Eq. (1.53) then gives the well known Duffing equation

$$\frac{d^2 p_1}{d\tau^2} + k_x p_1 + \ell_x p_1^3 = \frac{4L}{A_o E \pi} F_{ox} \cos\omega\tau \tag{1.59}$$

An approximate solution can be obtained using the harmonic balance technique. Assume

$$p_1 = A \cos\omega\tau + \bar{c}_1 \tag{1.60}$$

It is important to note at this stage that two basic types of response are feasible. One is a "local" vibration about the buckled position (nonsymmetric vibration), and for this case the constant $\bar{c}_1 \neq 0$. The other type is a so-called snap-through* motion (symmetric vibration) for which $\bar{c}_1$ should be set equal to zero. This case must be treated with some caution, though, as pointed out by Tseng and Dungundji [4], since it is unlikely that a perturbation scheme like the

* This phrase is used throughout to denote complete motions about the z-axis.

method of harmonic balance would give accurate results for such violent oscillations. It may, however, work if the initial buckling of the beam is small (i. e., λ is close to unity). Substituting eq. (1.60) into eq. (1.59) and equating the coefficients of $\cos\omega\tau$ give

$$-\omega^2 A + k_x A + \ell_x \left(\frac{3}{4} A^3 + 3 \bar{c}_1^2 A \right) = \frac{4 F_{ox} L}{\pi E A_o} \tag{1.61}$$

The constant terms are

$$k_x \bar{c}_1 + \ell_x \bar{c}_1^3 = 0 \tag{1.62}$$

$$\bar{c}_1 = 0 \quad \text{or} \quad \bar{c}_1 = \left(- \frac{k_x}{\ell_x} \right)^{1/2} \tag{1.63}$$

The case of nonsymmetric vibration is studied first:

$$\bar{c}_1 = \left(- k_x / \ell_x \right)^{1/2} \tag{1.64}$$

Eqs. (1.61) and (1.64) give the frequency amplitude relation:

$$\left(-\omega^2 - 2 k_x \right) A + \frac{3}{4} \ell_x A^3 = \frac{4 L F_{ox}}{A_o \pi E} \tag{1.65}$$

Note from eq. (1.65) on setting $F_{ox} = 0$ and ignoring A^3, that the free vibration frequency of the buckled beam is $\omega' = \omega_o \left(- 2 k_x \right)^{1/2}$.

Next the symmetric vibration case is considered. Eq. (1.61) with $\bar{c}_1 = 0$ gives the following expression for the frequency amplitude relation:

$$\left(- \omega^2 + k_x \right) A + \frac{3}{4} \ell_x A^3 = \frac{4 L F_{ox}}{A_o \pi E} \tag{1.66}$$

As noted previously, λ must be close to unity in order to obtain an accurate result. Both eqs. (1.65) and (1.66) will be explored numerically later.

1.3.3 NONPLANAR VIBRATION

Now the case of nonplanar vibration, that is, the possibility of $q_n \neq 0$, will be examined. Using eq. (1.57), eqs. (1.53) and (1.54) become on setting $\bar{c} = 0$, $P_{y1} = 0$

$$\ddot{p}_1 + k_x p_1 + \ell_x (q_1^2 p_1 + p_1^3) = \frac{4LF_{ox}}{\pi A_o E} \cos\omega\tau \tag{1.67}$$

$$\ddot{q}_1 + k_y q_1 + \ell_y (q_1 p_1^2 + q_1^3) = 0 \tag{1.68}$$

Harmonic balance will now be applied. Assume*

$$p_1 = A \cos\omega\tau + \bar{c}_1 \tag{1.69}$$

$$q_1 = B \cos(\omega\tau + \phi) \tag{1.70}$$

Substituting these expressions into eq. (1.67) and equating the coefficients of $\cos\omega\tau$ to zero gives:

$$(-\omega^2 + k_x + 3\bar{c}_1^2 \ell_x) A + \frac{3}{4} \ell_x A^3 + \frac{1}{4} \ell_x B^2 A(2 + \cos 2\phi) = \frac{4LF_{ox}}{\pi A_o E} . \tag{1.71}$$

Equating the coefficients of $\sin\omega\tau$ to zero gives:

$$\sin 2\phi = 0 \tag{1.72}$$

or $\phi = \mp s\pi/2$ where $s = 0, 1, 2$.

The constant term yields:

$$k_x \bar{c}_1 + \ell_x \bar{c}_1^3 = 0 . \tag{1.73}$$

Similarly, substituting eqs. (1.69) and (1.70) into eq. (1.68) and balancing the coefficients of the same harmonics gives, after some trigonometric manipulations,

---

*Note that there is no constant term in the expression for q_1. This stems from the fact that there was no initial buckling in the y-z plane.

$$(-\omega^2+k_y+\bar{c}_1^2\ell_y)B + \frac{3}{4}B^3\ell_y + \frac{1}{4}\ell_y BA^2(2+\cos 2\phi) = 0 \qquad (1.74)$$

the constant term yields eq. (1.72) again. Eq. (1.73) gives

$$\bar{c}_1 = 0 \text{ or } \bar{c}_1 = (-k_x/\ell_x)^{1/2} . \qquad (1.75)$$

Again $\bar{c}_1 = 0$ corresponds to the case of symmetric (snap-through) vibration and $\bar{c}_1 \neq 0$ corresponds to the case of nonsymmetric vibration.

Consider first the case of nonsymmetric vibrations, $\bar{c}_1 \neq 0$. Eqs. (1.71) and (1.74) with eq. (1.75) become:

$$(-\omega^2-2k_x)A + \frac{3}{4}\ell_x A^3 + \frac{1}{4}\ell_x B^2 A(2+\cos 2\phi) = \frac{4F_{ox}L}{\pi A_o E} \qquad (1.76)$$

$$(-\omega^2+k_y-\frac{\ell_y}{\ell_x}k_x)B + \frac{3}{4}B^3\ell_y + \frac{1}{4}\ell_y BA^2(2+\cos 2\phi) = 0 \qquad (1.77)$$

From eq. (1.77), either B = 0 (which corresponds to the case of planar vibration already studied) or

$$B^2 = -\frac{4}{3\ell_y}(-\omega^2+k_y-\frac{\ell_y}{\ell_x}k_x) - \frac{1}{3}A^2(2+\cos 2\phi) \qquad (1.78)$$

Substituting eq. (1.78) into eq. (1.76) gives the frequency amplitude relation

$$\left[\left(-\omega^2-2k_x\right) - \frac{1}{3}\frac{\ell_x}{\ell_y}(2+\cos 2\phi)\left(-\omega^2+k_y-\frac{\ell_y}{\ell_x}k_x\right)\right]A + \left[\frac{3}{4}\ell_x - \frac{1}{12}\ell_x(2+\cos 2\phi)^2\right]A^3 = \frac{4LF_{ox}}{\pi A_o E} \qquad (1.79)$$

Examining eq. (1.79), it is found that two cases arise, namely

i) $\phi = \mp s\pi/2$ where $s = 0, 2$.

Then eq. (1.79) reduces to

$$A = 4LF_{ox}/\pi A_o E(k_x+k_y) \qquad (1.80)$$

This last equation requires A to be zero when F_{ox} is zero and so

precludes the possibility of large-amplitude free vibrations. Hence, this possibility is unphysical and must be discarded.

ii) $\phi = s\pi/2$ where $s = 1$.

Then eqs. (1.78) and (1.79) give

$$B^2 = -\frac{4}{3\ell_y}(-\omega^2+k_y-k_x) - \frac{1}{3}A^2 \tag{1.81}$$

$$(-\frac{2}{3}\omega^2 - \frac{5}{3}k_x - \frac{1}{3}k_y)A + \frac{2}{3}\ell_x A^3 = \frac{4LF_{ox}}{\pi A_o E} \tag{1.82}$$

Eq. (1.82) can be solved for A and from eq. (1.81) B can be determined.

For the symmetric vibrations (snap-through) $\bar{c}_1 = 0$, eqs. (1.71) and (1.74) give

$$(-\omega^2+k_x)A + \frac{3}{4}\ell_x A^3 + \frac{1}{4}\ell_x B^2 A(2+\cos 2\phi) = \frac{4LF_{ox}}{\pi A_o E} \tag{1.83}$$

$$(-\omega^2+k_y)B + \frac{3}{4}\ell_y B^3 + \frac{1}{4}\ell_y B A^2(2+\cos 2\phi) = 0 \tag{1.84}$$

From eq. (1.84), either $B = 0$ (which corresponds to the case of planar vibration already studied) or

$$B^2 = -\frac{4}{3\ell_y}(-\omega^2+k_y) - \frac{1}{3}A^2(2+\cos 2\phi) \tag{1.85}$$

Substituting eq. (1.85) into eq. (1.83) gives the frequency amplitude relation for symmetric (snap-through) vibration.

$$\left[\left(-\omega^2+k_x\right) - \frac{\ell_x}{3\ell_y}\left(-\omega^2+k_y\right)\left(2+\cos 2\phi\right)\right]A + \left[\frac{3}{4}\ell_x - \frac{\ell_x}{12}\left(2+\cos 2\phi\right)^2\right]A^3 = \frac{4LF_{ox}}{\pi A_o E} \tag{1.86}$$

Again examining eq. (1.86), it is found that two cases arise, namely

i) $\phi = \pm\frac{s\pi}{2}$ where $s = 0, 2$ Then eq. (1.86) reduces to

$$A = \frac{4LF_{ox}}{\pi A_o E (k_x - k_y)} \tag{1.87}$$

This equation again requires A to be zero when F_{ox} is zero and so precludes the possibility of large-amplitude free vibrations. Hence, this possibility is nonphysical and must be discarded. (Same as the unsymmetric vibration case.)

ii) When $\phi = \frac{s\pi}{2}$ where s = 1. Then eqs. (1.85) give:

$$B^2 = -\frac{4}{3\ell_y}(-\omega^2 + k_y) - \frac{1}{3}A^2 \tag{1.88}$$

and eq. (1.86) with $\phi = \frac{\pi}{2}$ gives:

$$(-\frac{2}{3}\omega^2 + k_x - \frac{1}{3}k_y)A + \frac{2}{3}A^3\ell_x = \frac{4F_o L}{\pi A_o E} \tag{1.89}$$

Eq. (1.89) can be solved for A, and from eq. (1.88) B can be determined.

Eqs. (1.81), (1.82), (1.88), and (1.89) will be explored numerically later.

1.4. STABILITY

Eqs. (1.67) and (1.68) are

$$\ddot{p}_1 + k_x p_1 + \ell_x (q_1^2 + p_1^2)\, p_1 = P_{x1} \tag{1.90}$$

$$\ddot{q}_1 + k_y q_1 + \ell_y (q_1^2 + p_1^2)\, q_1 = P_{y1} \tag{1.91}$$

Let a small perturbation be given to the steady-state response by

$$p_1 \longrightarrow \delta p_1 + p_1 \tag{1.92}$$

$$q_1 \longrightarrow \delta q_1 + q_1 \tag{1.93}$$

If δp_1 or δq_1 is unbounded (grow with time), the system is unstable. Substituting eqs. (1.92) and (1.93) into eqs. (1.90) and (1.91) and retaining only the first order terms gives

$$\begin{bmatrix} 1 & 0 \\ 0 & 1 \end{bmatrix} \begin{bmatrix} \delta\ddot{p}_1 \\ \delta\ddot{q}_1 \end{bmatrix} + \begin{bmatrix} \ell_x \left\{ \frac{k_x}{\ell_x} + (3p_1^2 + q_1^2) \right\} & 2\ell_x p_1 q_1 \\ 2\ell_y p_1 q_1 & \ell_y \left\{ \frac{k_y}{\ell_y} + (3q_1^2 + p_1^2) \right\} \end{bmatrix} \begin{bmatrix} \delta p_1 \\ \delta q_1 \end{bmatrix} = \begin{bmatrix} 0 \\ 0 \end{bmatrix} \tag{1.94}$$

1.4.1. PLANAR VIBRATION

For planar vibrations, eqs. (1.94) become ($q_1 \equiv 0$)

$$\begin{bmatrix} 1 & 0 \\ 0 & 1 \end{bmatrix} \begin{bmatrix} \delta\ddot{p}_1 \\ \delta\ddot{q}_1 \end{bmatrix} + \begin{bmatrix} \ell_x \left(\frac{k_x}{\ell_x} + 3p_1^2 \right) & 0 \\ 0 & \ell_y \left(\frac{k_y}{\ell_y} + p_1^2 \right) \end{bmatrix} \begin{bmatrix} \delta p_1 \\ \delta q_1 \end{bmatrix} = \begin{bmatrix} 0 \\ 0 \end{bmatrix} \tag{1.95}$$

Substituting the steady state solution $p_1 = A\cos\omega\tau + \bar{c}_1$ with A and ω related by eq. (1.65) into eqs. (1.95) gives uncoupled Hill's equations (which have been receiving more attention recently*).

*See works by E. K. H. Hoehn [16] and W. Magnus and S. Winkler [17].

$$\begin{bmatrix} 1 & 0 \\ 0 & 1 \end{bmatrix} \begin{bmatrix} \delta\ddot{p}_1 \\ \delta\ddot{q}_1 \end{bmatrix} + \begin{bmatrix} 6\bar{c}_1 \ell_x A\cos\omega\tau + 3A^2 \ell_x \cos^2\omega\tau + k_x + 3\bar{c}_1^2 \ell_x & 0 \\ 0 & 2\ell_y \bar{c}_1 A\cos\omega\tau + \ell_y A^2 \cos^2\omega\tau + k_y + \bar{c}_1^2 \ell_y \end{bmatrix} \begin{bmatrix} \delta p_1 \\ \delta q_1 \end{bmatrix}$$

$$= \begin{bmatrix} 0 \\ 0 \end{bmatrix} \qquad (1.96)$$

Eqs. (1.96) can be rewritten

$$\begin{bmatrix} 1 & 0 \\ 0 & 1 \end{bmatrix} \begin{bmatrix} \delta\ddot{p}_1 \\ \delta\ddot{q}_1 \end{bmatrix} + \begin{bmatrix} (\alpha_x + \epsilon_{1x}\cos\omega\tau + \epsilon_{2x}\cos 2\omega\tau) & 0 \\ 0 & (\alpha_y + \epsilon_{1y}\cos\omega\tau + \epsilon_{2y}\cos 2\omega\tau) \end{bmatrix} \begin{bmatrix} \delta p_1 \\ \delta q_1 \end{bmatrix} = \begin{bmatrix} 0 \\ 0 \end{bmatrix} \qquad (1.97)$$

where

$$\begin{aligned} \alpha_x &= 3\ell_x \bar{c}_1^2 + k_x + \epsilon_{2x} \\ \alpha_y &= \ell_y \bar{c}_1^2 + k_y + \epsilon_{2y} \\ \epsilon_{2x} &= (3/2)\, A^2 \ell_x \\ \epsilon_{2y} &= (1/2)\, A^2 \ell_y \\ \epsilon_{1x} &= 6\,\bar{c}_1 A \ell_x \\ \epsilon_{1y} &= 2\bar{c}_1 A \ell_y \end{aligned} \qquad (1.98)$$

From the Floquet theory if σ is a characteristic exponent, then Hill's eqs. (1.97) have solutions in the form of:

$$\begin{bmatrix} \delta p_1 \\ \delta q_1 \end{bmatrix} = e^{\sigma\omega\tau} \begin{bmatrix} Q_1 \\ Q_2 \end{bmatrix} \qquad (1.99)$$

where Q_1 and Q_2 are periodic functions. An approximate scheme will now be used (see Ho, Scott, and Eisley [11, 12], Williams and Tobias [18] and Efstathiades and Williams [19]). Q_1 and Q_2 are taken to have the forms

$$\begin{bmatrix} Q_1 \\ Q_2 \end{bmatrix} = \begin{bmatrix} a_1 & a_3 & a_5 \\ a_2 & a_4 & a_6 \end{bmatrix} \begin{bmatrix} \cos\omega\tau \\ \sin\omega\tau \\ 1 \end{bmatrix} \tag{1.100}$$

where the a_i's are constants.

Eqs. (1.99) with eqs. (1.100) can be rewritten:

$$\begin{bmatrix} \delta p_1 \\ \delta q_1 \end{bmatrix} = e^{\sigma\omega\tau} \begin{bmatrix} a_1 & a_3 & a_5 \\ a_2 & a_4 & a_6 \end{bmatrix} \begin{bmatrix} \cos\omega\tau \\ \sin\omega\tau \\ 1 \end{bmatrix} \tag{1.101}$$

Substituting δp_1 in eqs. (1.101) into the first equation of (1.97) and balancing the coefficients of the same harmonics and neglecting the higher powers* of σ gives

$$\left(\begin{bmatrix} -\omega^2+\alpha_x+\frac{1}{2}\epsilon_{2x} & 0 & \epsilon_{1x} \\ 0 & (-\omega^2+\alpha_y-\frac{1}{2}\epsilon_{2x}) & 0 \\ \epsilon_{1x} & 0 & 2\alpha_x \end{bmatrix} + 2\sigma\omega^2 \begin{bmatrix} 0 & 1 & 0 \\ -1 & 0 & 0 \\ 0 & 0 & 0 \end{bmatrix} \right) \begin{bmatrix} a_1 \\ a_3 \\ a_5 \end{bmatrix} = \begin{bmatrix} 0 \\ 0 \\ 0 \end{bmatrix} \tag{1.102}$$

* The reader should recall that in the undamped case, the stability boundaries emanate from the ϵ-axis in the σ-ϵ plane. Hence in the vicinity of this axis σ may be taken to be small.

Note that one equation above has been multiplied by 2 to preserve the symmetry. In order to have nontrivial solutions for the a_i's, the determinant of the coefficients must be equal to zero, which gives,

$$\begin{vmatrix} (-\omega^2 + \alpha_x + \frac{1}{2}\epsilon_{2x}) & 2\sigma\omega^2 & \epsilon_{1x} \\ -2\sigma\omega^2 & (-\omega^2+\alpha_x - \frac{1}{2}\epsilon_{2x}) & 0 \\ \epsilon_{1x} & 0 & 2\alpha_x \end{vmatrix} = 0 \qquad (1.103)$$

Expansion of this determinant yields the characteristic equation:

$$(-\omega^2+\alpha_x)^2 - \frac{1}{4}\epsilon_{2x}^2 + 4\sigma^2\omega^4 - \frac{1}{2}\frac{\epsilon_{1x}^2}{\alpha_x}(-\omega^2+\alpha_x - \frac{1}{2}\epsilon_{2x}) = 0 \qquad (1.104)$$

(The last term in eq. (1.104) is of higher order*, and therefore neglected). In order for the system to be stable, the values of the σ's must have negative real parts or be pure imaginary. Eq. (1.104) gives

$$\sigma_{1,2} = \mp \left[-(-\omega^2+\alpha_x)^2 + \frac{1}{4}\epsilon_{2x}^2\right]^{1/2} / 2\omega^2 \qquad (1.105)$$

Hence stability requires

$$(-\omega^2+\alpha_x)^2 > \frac{1}{4}\epsilon_{2x}^2 \qquad (1.106)$$

Expression (1.106) with eqs. (1.98) gives the stability boundaries

$$C_4 A^4 + C_2 A^2 + C_o = 0 \qquad (1.107)$$

where

---

* The term is of $O(A^6)$ which is negligible compared to the other terms which are $O(A^4)$.

$$C_o = (-\omega^2 - 2k_x)^2$$
$$C_2 = 3(-\omega^2 - 2k_x)\ell_x \qquad (1.108)$$
$$C_4 = (27/16)\,\ell_x$$

Similarly, substituting δq_1 in eqs. (1.101) into the second equation of (1.97) and balancing the coefficients of the same harmonics and neglecting the higher powers of σ gives

$$\left(\begin{bmatrix} -\omega^2+\alpha_y+\frac{1}{2}\epsilon_{2y} & 0 & \epsilon_{1y} \\ 0 & (-\omega^2+\alpha_y-\frac{1}{2}\epsilon_{2y}) & 0 \\ \epsilon_{1y} & 0 & 2\alpha_y \end{bmatrix} + 2\sigma\omega^2 \begin{bmatrix} 0 & 1 & 0 \\ -1 & 0 & 0 \\ 0 & 0 & 0 \end{bmatrix} \right) \begin{bmatrix} a_2 \\ a_4 \\ a_6 \end{bmatrix} = \begin{bmatrix} 0 \\ 0 \\ 0 \end{bmatrix} \qquad (1.109)$$

In order to have nontrivial solutions for the a_i's, the determinant of the coefficients must be equal to zero, which gives

$$\begin{vmatrix} (-\omega^2 + \alpha_y + \frac{1}{2}\epsilon_{2y}) & 2\sigma\omega^2 & \epsilon_{1y} \\ -2\sigma\omega^2 & (-\omega^2 + \alpha_y - \frac{1}{2}\epsilon_{2y}) & 0 \\ \epsilon_{1y} & 0 & 2\alpha_y \end{vmatrix} = 0 \qquad (1.110)$$

Expansion of this determinant yields the characteristic equation:

$$(-\omega^2 + \alpha_y)^2 - \frac{1}{4}\epsilon_{2y}^2 + 4\sigma^2\omega^4 - \frac{1}{2}\frac{\epsilon_{1y}^2}{\alpha_y}(-\omega^2+\alpha_y-\frac{1}{2}\epsilon_{2y}) = 0 \qquad (1.111)$$

The last term in eq. (1.111) is of higher order and therefore will be neglected. In order for the system to be stable, the values of the σ's must have negative real parts or be pure imaginary:

$$\sigma_{1,2} = \mp \left[-(-\omega^2+\alpha_y)^2 + \frac{1}{4}\epsilon_{2y}^2 \right]^{1/2} / 2\omega^2 \qquad (1.112)$$

Hence stability requires:

$$(-\omega^2 + \alpha_y)^2 > \frac{1}{4}\ \epsilon_{2y}^2 \tag{1.113}$$

Eq. (1.113) with eqs. (1.98) gives the stability boundaries for the y-z plane

$$D_4 A^4 + D_2 A^2 + D_o = 0 \tag{1.114}$$

where

$$\begin{aligned} D_o &= [-\omega^2 + k_y - (\ell_y/\ell_x)\, k_x]^2 \\ D_2 &= [-\omega^2 + k_y - (\ell_y/\ell_x) k_x]\ \ell_y \\ D_4 &= (3/16)\, \ell_y^2 \end{aligned} \tag{1.115}$$

Eqs. (1.107) and (1.114) define the stability regions for planar response. Both eqs. (1.107) and (1.114) will be solved numerically later.

Eqs. (1.107) with $\bar{c}_1 = 0$ gives the in-plane stability boundaries for symmetric vibration (snap-through):

$$\bar{C}_4 A^4 + \bar{C}_2 A^2 + \bar{C}_o = 0 \tag{1.116}$$

where

$$\begin{aligned} \bar{C}_o &= (-\omega^2 + k_x)^2 \\ \bar{C}_2 &= 3(-\omega^2 + k_x)\ell_x \\ \bar{C}_4 &= (27/16)\, \ell_x^2 \end{aligned} \tag{1.117}$$

Eq. (1.114) with $\bar{c}_1 = 0$ gives the out-of-plane stability boundaries for symmetric vibration (snap-through):

$$\bar{D}_4 A^4 + \bar{D}_2 A^2 + \bar{D}_o = 0 \tag{1.118}$$

where

$$\begin{aligned} \bar{D}_o &= (-\omega^2 + k_y)^2 \\ \bar{D}_2 &= (-\omega^2 + k_y)\ell_y \\ \bar{D}_4 &= (3/16)\,\ell_y^2 \end{aligned} \tag{1.119}$$

Eq. (1.116) and (1.118) will be solved numerically later.

1.4.2. NONPLANAR VIBRATION

Consider now the stability of the nonplanar response. Substituting eqs. (1.69) and (1.70), with $\phi = S\frac{\pi}{2}$, S = 1, 3, 5, into eqs. (1.94) gives the coupled Hill's equations

$$\begin{bmatrix} 1 & 0 \\ 0 & 1 \end{bmatrix} \begin{bmatrix} \delta\ddot{p}_1 \\ \delta\ddot{q}_1 \end{bmatrix} + \begin{bmatrix} (\bar{\alpha}_x+\bar{\epsilon}_{2x}\cos 2\omega\tau + \bar{\epsilon}_{1x}\cos\omega\tau) & (\beta_{2x}\sin 2\omega\tau+\beta_{1x}\sin\omega\tau) \\ (\beta_{2y}\sin 2\omega\tau+\beta_{1y}\sin\omega\tau) & (\bar{\alpha}_y+\bar{\epsilon}_{2y}\cos 2\omega\tau+\bar{\epsilon}_{1y}\sin\omega\tau) \end{bmatrix} \begin{bmatrix} \delta p_1 \\ \delta q_1 \end{bmatrix} = \begin{bmatrix} 0 \\ 0 \end{bmatrix} \tag{1.120}$$

where

$$\begin{aligned}
\bar{\alpha}_x &= (3A^2/2 + 3\bar{c}_1^2 + \frac{B^2}{2})\,\ell_x + k_x \\
\bar{\epsilon}_{1x} &= 6\,\bar{c}_1 A \ell_x \\
\bar{\epsilon}_{2x} &= (3A^2/2 - \frac{B^2}{2})\,\ell_x \\
\bar{\alpha}_y &= (\frac{3B^2}{2} + \bar{c}_1^2 + \frac{A^2}{2})\,\ell_y + k_y \\
\bar{\epsilon}_{1y} &= 2\,\bar{c}_1\,\ell_y A \\
\bar{\epsilon}_{2y} &= (\frac{A^2}{2} - \frac{3B^2}{2})\,\ell_y \\
\beta_{1x} &= -2\,\bar{c}_1\,\ell_x B \\
\beta_{2x} &= -AB\ell_x \\
\beta_{1y} &= -2\,\bar{c}_1\,\ell_y B \\
\beta_{2y} &= -AB\,\ell_y
\end{aligned} \tag{1.121}$$

Assume the solutions of eqs. (1.120) in the form of

$$\begin{bmatrix} \delta p_1 \\ \\ \delta q_1 \end{bmatrix} = e^{\sigma\omega\tau} \begin{bmatrix} Q_{11} \\ \\ Q_{22} \end{bmatrix} \tag{1.122}$$

where Q_{11} and Q_{22} are periodic functions. An approximate scheme will be used (see Ho, Scott, and Eisley [11, 12]). Q_{11} and Q_{22} are taken to have the form

$$\begin{bmatrix} Q_{11} \\ \\ Q_{22} \end{bmatrix} = e^{\sigma\omega\tau} \begin{bmatrix} a_{11} & a_{33} & a_{55} \\ & & \\ a_{22} & a_{44} & a_{66} \end{bmatrix} \begin{bmatrix} \cos\omega\tau \\ \sin\omega\tau \\ 1 \end{bmatrix} \tag{1.123}$$

Eqs. (1.122) with eqs. (1.123) can then be rewritten

$$\begin{bmatrix} \delta p_1 \\ \\ \delta q_1 \end{bmatrix} = e^{\sigma\omega\tau} \begin{bmatrix} a_{11} & a_{33} & a_{55} \\ & & \\ a_{22} & a_{44} & a_{66} \end{bmatrix} \begin{bmatrix} \cos\omega\tau \\ \sin\omega\tau \\ 1 \end{bmatrix} \tag{1.124}$$

Substituting δp_1 and δq_1 in eqs. (1.124) into eqs. (1.120) and balancing the coefficients of the same harmonics and neglecting the higher powers of σ gives

$$\left(\begin{bmatrix} (-\omega^2 + \bar{\alpha}_x + \frac{1}{2}\bar{\epsilon}_{2x}) & 0 & 0 & \frac{1}{2}\beta_{2x} \\ 0 & (-\omega^2 + \bar{\alpha}_y + \frac{1}{2}\bar{\epsilon}_{2y}) & \frac{1}{2}\beta_{2y} & 0 \\ 0 & \frac{1}{2}\beta_{2x} & (-\omega^2 + \bar{\alpha}_x - \frac{1}{2}\bar{\epsilon}_{2x}) & 0 \\ \frac{1}{2}\beta_{2y} & 0 & 0 & (-\omega^2 + \bar{\alpha}_y - \frac{1}{2}\bar{\epsilon}_{2y}) \end{bmatrix} + \right.$$

$$+ \quad 2\sigma\omega^2 \left[\begin{bmatrix} 0 & 0 & 1 & 0 \\ 0 & 0 & 0 & 1 \\ -1 & 0 & 0 & 0 \\ 0 & -1 & 0 & 0 \end{bmatrix} \right) \begin{bmatrix} a_{11} \\ a_{22} \\ a_{33} \\ a_{44} \end{bmatrix} = 0 \tag{1.125}$$

In order to have nontrivial solutions for the aij's, the determinant of the coefficients must be equal to zero, which gives

$$\begin{vmatrix} -g_1\sigma & g_2 & h_1 & 0 \\ g_2 & -g_1\sigma & 0 & h_2 \\ h_3 & 0 & g_1\sigma & g_2 \\ 0 & h_4 & g_2 & g_1\sigma \end{vmatrix} = 0 \tag{1.126}$$

where

$$\begin{aligned} g_1 &= 2\omega \\ g_2 &= \frac{1}{2}\beta_{2x} = \frac{1}{2}\beta_{2y} \\ h_1 &= (-\omega^2 + \bar{\alpha}_x - \frac{1}{2}\bar{\epsilon}_{2x}) \\ h_2 &= (-\omega^2 + \bar{\alpha}_y - \frac{1}{2}\bar{\epsilon}_{2y}) \\ h_3 &= (-\omega^2 + \bar{\alpha}_x + \frac{1}{2}\bar{\epsilon}_{2x}) \\ h_4 &= (-\omega^2 + \bar{\alpha}_y + \frac{1}{2}\bar{\epsilon}_{2y}) \end{aligned} \tag{1.127}$$

Expansion of this determinant yields the characteristic equation

$$(g_1\sigma)^4 + R(g_1\sigma)^2 + S = 0 \tag{1.128}$$

where

$$R = h_2 h_4 + h_1 h_3 - 2g_2^2$$
$$S = (h_1 h_4 - g_2^2)\ (h_2 h_3 - g_2^2) \qquad (1.129)$$

Stability requires that the roots of eq. (1.128) must be imaginary.

$$\sigma_{1,2} = \mp \frac{1}{g_1\sqrt{2}} \sqrt{-R \mp \sqrt{R^2 - 4S}} \qquad (1.130)$$

The roots are imaginary if

i) $S > 0$

ii) $R > 0$ (1.131)

iii) $R^2 > 4S$

Setting S to zero yields stability boundaries. Consider nonsymmetric vibration, i.e., $\bar{c}_1 \neq 0$. Then the coefficients h_1, h_2, h_3, h_4 and g_2 are determined from eqs. (1.127) with (1.121, with $\bar{c}_1 \neq 0$) and (1.81). They are as follows:

$$h_1 = \frac{1}{2} A^2 \ell_x + (-k_x - k_y)$$
$$h_2 = -\frac{1}{2} A^2 \ell_y + 2(\omega^2 - k_y + k_x)$$
$$h_3 = (-\frac{2}{3}\omega^2 + \frac{13}{6} A^2 \ell_x - \frac{5}{3} k_x - \frac{1}{3} k_y) \qquad (1.132)$$
$$h_4 = \frac{1}{2} A^2 \ell_y$$
$$g_2^2 = \frac{1}{4} A^2 \ell_x \left[-\frac{4}{3} (-\omega^2 + k_y - k_x) - \frac{1}{3} A^2 \ell_x \right]$$

Setting S = 0 then gives

$$\left(\frac{1}{2}A^2\ell_x\right)\left[\frac{2}{3}A^2\ell_x - \frac{2}{3}\omega^2 - \frac{1}{3}k_y - \frac{5}{3}k_x\right]\left[4(\omega^2+k_x-k_y) - A^2\ell_y\right] \cdot$$

$$\left[\frac{1}{2}\left(-\frac{2}{3}\omega^2 - \frac{5}{3}k_x - \frac{1}{3}k_y\right) + A^2\ell_x\right] = 0 \qquad (1.133)$$

Equation (1.133) gives three stability boundaries. Note that the first factor is the same as the nonsymmetric nonplanar free vibration response expression (1.82) and the third factor is a derivative of this expression with respect to amplitude A and is a locus of vertical tangents. The second factor yields 1.113 again, that is, a factor determining the stability of plane motion to out-of-plane perturbations.

Similarly, for symmetric vibration, i.e., $\bar{c}_1 = 0$, the stability condition from expression (1.131) can be written

$$\bar{S} > 0 \qquad (1.134)$$

where

$$\bar{S} = (\bar{h}_1\bar{h}_4 - \bar{g}_2^2)\ (\bar{h}_2\bar{h}_3 - \bar{g}_2^2) \qquad (1.135)$$

The coefficients $\bar{h}_1$, $\bar{h}_2$, $\bar{h}_3$, $\bar{h}_4$ and $\bar{g}_2$ are determined from eqs. (1.127) with (1.121, with $\bar{c}_1 = 0$) and (1.88), and are as follows:

$$\bar{h}_1 = \frac{1}{2}A^2\ell_x + (k_x - k_y)$$

$$\bar{h}_2 = -\frac{1}{2}A^2\ell_y + 2(\omega^2 - k_y)$$

$$\bar{h}_3 = -\frac{2}{3}\omega^2 + k_x - \frac{1}{3}k_y + \frac{13}{6}A^2\ell_x \qquad (1.136)$$

$$\bar{h}_4 = \frac{1}{2}A^2\ell_y$$

$$\bar{g}_2^2 = \frac{1}{4}A^2\ell_x\left[-\frac{4}{3}(-\omega^2 + k_y) - \frac{1}{3}A^2\ell_x\right]$$

The expressions for $\bar{R}$ and $\bar{R}^2-4\bar{S}$ can be found from eqs. (1.129), replacing h_1 by $\bar{h}_1$, h_2 by $\bar{h}_2$, etc. Substituting expression (1.135) into (1.134) gives the stability boundaries for symmetric vibration

$$\left(\frac{1}{2}A^2\ell_x\right)\left(\frac{2}{3}A^2\ell_x-\frac{2}{3}\omega^2-\frac{1}{3}k_y+k_x\right)\left[4\left(\omega^2-k_y\right)-A^2\ell_y\right]\cdot$$

$$\left[\frac{1}{2}\left(-\frac{2}{3}\omega^2+k_x-\frac{1}{3}k_y\right)+A^2\ell_x\right]=0 \qquad (1.137)$$

Again eq. (1.137) gives three stability boundaries. Note that the first factor is the same as the symmetric free vibration response expression (1.89) and the third factor is the derivative of this expression with respect to amplitude A. Again the second factor is the out-of-plane stability equation for the planar vibration. It appears that no general statements can be made regarding $R>0$ and $R^2>4S$ in expression (1.131) and they must be treated numerically.

Similar conclusions apply to $\bar{R}$, $\bar{S}$ and $\bar{R}^2-4\bar{S}$ for the case of snap-through vibrations $\bar{c}_1=0$.

1.5. NUMERICAL RESULTS AND CONCLUSIONS

In this section, fairly detailed numerical exploration of the response and stability eqs. (1.65), (1.66), (1.81), (1.82), (1.88), (1.89), (1.107), (1.114), (1.116), (1.118), (1.131), and (1.134) will be given. All of these equations are nonlinear algebraic equations, and they were solved numerically using a program termed "POLRT" provided in the Scientific Subroutine Package. In all cases viscous damping is taken to be zero.

Shown in Figures 1.7 through 1.10 are unsymmetric ($\bar{c}_1 \neq 0$, that is to say, local motion about the buckled position) plane response curves for various force levels $F(\equiv 4LF_{ox}/A_o\pi E)$, $= 10\times10^{-6}, 50\times10^{-6}$, beam geometries $\alpha = .005, .01$ and $\beta = .01, .02$, initial buckling states $\lambda = 2, 4$, and linear mode shapes (i.e., $\eta = 1, 2$)*.

The unprimed letters designate plane stability zones with points inside corresponding to instabilities in that plane perturbations grow there. That is to say, perturbations corresponding to these points cause the initially plane forced motion to change to a different plane motion.

Region ABC comes from expression (1.107) with $m = 1$. It illustrates the well-known planar jump phenomena. As the frequency decreases, the amplitude of the lowest branch slowly increases until the point of vertical tangency is reached. Then the motion abruptly

* The previous analysis was for $m = n = 1$. However, it can be extended in a straight forward manner to the case $n = 2$.

jumps to one of larger amplitude. The region where this larger amplitude ends up dictates the nature of the ensuing motion, depending on the type of instability zone encountered. As will be seen, this depends in a complicated manner on the force level F, the beam geometry (α, β) and the initial buckled state (λ).

Regions E'F'G' and I'J'K' stem from expression (1.114) and the analogous expression for n = 2. The primed letters designate out-of-plane stability zones with points inside corresponding to instabilities in that plane perturbations grow there. That is to say, perturbations corresponding to these points cause the initially plane forced motion to become a nonplanar one. Whether these are steady-state or not depends on an examination of the stability of whirling motions. In fact at this point a central issue of the work has been answered, namely, whirling motion can occur even in the presence of an initial buckled state, as the presence of these zones show.

One important general remark regarding the out-of-plane instability zones can be made here. Using eqs. (1.55) and (1.98) the equation for the out-of-plane stability zone, eq. (1.113) can be written

$$\left[-\omega^2 + \frac{\pi^4}{12} \left\{ n^4 \beta^2 - \frac{\ell_y}{\ell_x} m^4 \alpha^2 - \lambda (\beta^2 n^2 \gamma^2 - \alpha^2 m^2) \right\} \right] = -\frac{1}{2} \epsilon_{2y}$$

On noting $\gamma = \frac{b}{a}$, $\alpha = \frac{2b}{L}$, $\beta = \frac{2a}{L}$, it is seen from the above equation that the out-of-plane instability zones are independent of the initial buckled state, i.e., λ, when m = n. In particular this is true for the

primary case under study here, namely, first mode interactions. This may not be too surprising in that an effect of buckling is to "stiffen" the beam in the x-z plane.

Before proceeding, in order to give the reader a feeling for the magnitudes involved in the sequel, the choice of parameters will now be illustrated. Consider, for example, $\alpha \left(= \frac{2a}{L} \right) = .005$, $\beta \left(= \frac{2b}{L} \right) = .01$ for a 100" long beam. The cross-section would have area ($\frac{1}{2}$" x 1"). For such a beam, expression (1.63) with $\lambda = 2$ gives $\bar{c}_1 = (-k_x / \ell_x)^{1/2}$ with $k_x = 8.11 \alpha^2 (1-\lambda) = -2.02 \times 10^{-4}$ and $\ell_x = 24.35$, i.e., $\bar{c}_1 = .00288$. But $\bar{c}_1$ is the dimensionless amplitude of $\bar{u} \left(= \frac{u}{L} \right)$ in the buckled state. Thus for this beam, $\lambda = 2$ corresponds to an initial buckled amplitude of .29". Changing λ from 2 to 4 changes this amplitude to .50". Note that $\alpha = .01$, $\beta = .02$ corresponds to (1" x 2") cross-section for a 100" long beam. The initial buckled amplitude for this beam, with $\lambda = 4$, is approximately 1".

The curves for $F = 10 \times 10^{-6}$ will first be examined. For the beam with $\alpha = .005$ and $\beta = .01$, Figures 1.7 and 1.8 show that for both $\lambda = 2$ and $\lambda = 4$, the amplitudes (after the jumps) end up inside of the out-of-plane instability zones so that whirling motions do occur. This new type of jump phenomena was also found by Ho, Scott, and Eisley [11]. It is interesting to note that an increase in λ moves the terminal point away from these instability zones. Thus it appears that increasing the initial buckling state makes whirling motion less likely. This trend

is also evident in Figures 1.9 and 1.10 which are for a beam with a larger cross-section, i. e., $\alpha = .01$, $\beta = .02$. In fact the jump for $\lambda = 4$ ends up out of the non-planar instability zone.

The figures also show that the same pattern can be seen for the larger force level $F = 50 \times 10^{-6}$, that is, an increase in λ tends to decrease the possibility of whirling motion. Up to now the discussion has focused on the phenomena encountered in a hypothetical experiment as the frequency is decreased from large values. It should be noted that on increasing the frequency from zero, whirling motions also occur, but are not generated by jumps. As soon as the boundary E'F' is met, the initially plane motion slowly changes to a nonplanar one.

Shown isolated in Figures 1.11 and 1.12 are the stability zones for various values of the parameters. It is seen that increasing λ causes the planar instability regions to move to higher frequencies. Thus buckling the beam results in jump phenomena occurring at higher frequencies. It is also seen, as noted in general, that changing λ does not alter the out-of-plane instability zones. Further, it is seen that making the beam thicker, i.e., increasing α and β, though it has relatively little effect on the width of the zones, moves them to higher frequencies.

Shown in Figures 1.13 through 1.14 are plane response curves for the symmetric vibrations ($\bar{c}_1 = 0$, that is snap-through motions)

involving the first modes, i.e. m = n = 1. The same cross-sections as before are treated, namely, $\alpha = .005$, $\beta = .01$ and $\alpha = .01$, $\beta = .02$. However, now only $\lambda = 1.1$ is studied, this value close to 1 being in deference to the fact that the approximate analytic scheme is likely to be accurate only for mild snap-through motions. Superimposed on the figures are the stability zones $\bar{A}\bar{B}\bar{C}\bar{D}$ for plane perturbations, as calculated from eqs. (1.116) and for out-of-plane perturbations $\bar{E}'\bar{F}'\bar{G}'$, as calculated from eqs. (1.118). It is interesting to note that the free vibration curve F = 0, which is a stability boundary for $\bar{A}\bar{B}\bar{C}\bar{D}$, intersects, in general, the $|A|$ -axis at a non-zero value. This shows, not too surprisingly, that free, snap-through vibration below a certain amplitude cannot occur. It should be stated here that another central issue of the work has been answered at this stage. The presence of the zone $\bar{E}'\bar{F}'\bar{G}'$ shows <u>whirling snap-through motion can also occur for symmetric motion</u>.

The figures show that for the thin beam ($\alpha = .005$, $\beta = .01$), the jumps at the vertical tangents end up in the zone $\bar{E}'\bar{F}'\bar{G}'$ for both force levels, so that whirling motions develop. However, for the thick beam ($\alpha = .01$, $\beta = .02$), the jump for the low force level $F = 10 \times 10^{-6}$ ends up out of this zone, so that the resulting motion is <u>planar.</u>

To close the comments on plane response, it should be noted that the current analysis indicates the possibility of both snap-through

and non-snap-through vibrations. However, it does not involve a criterion as to which will occur for a given force level (though it seems clear that a certain maximum force level would be required for snap-through). In fact, criteria for dynamic snap-through of the allied problem of arches are a topic of current research in mechanics. Shown in Figures 1.15 through 1.22 are nonplanar response curves for the nonsymmetric local vibrations ($\bar{c}_1 \neq 0$) involving the first modes (i.e., $m = n = 1$) and for two force levels, namely $F = 10 \times 10^{-6}$ and $F = 50 \times 10^{-6}$, the same beam geometries $\alpha = .005, .01$ and $\beta = .01, .02$, and initial buckling states $\lambda = 2, 4$ as treated before. Superimposed on the figures are the stability zones for nonplanar perturbations. The stability zones in this case are quite complicated. Consider first "local" vibration (i.e., $\bar{c}_1 \neq 0$). Recall from expression (1.131) that three conditions must be simultaneously satisfied in order for the nonplanar motions to be stable, i.e.,

$$S > 0 \tag{1.138}$$

$$R > 0 \tag{1.139}$$

$$R^2 > 4S \tag{1.140}$$

It turns out that the situation for $\lambda = 2$ differs somewhat from that for $\lambda = 4$ and the former will be described first. For $\lambda = 2$, the inequality (1.139) is always satisfied. Examining expression (1.138), it is found that S changes from positive to negative to positive to negative, as the curves A"B", A"C" and A"E" respectively are crossed. Examination of expression (1.140) shows that $R^2 - 4S$ changes from positive

to negative to positive as the curves Q''H'' and Q''B'' are respectively crossed. Hence the only regions in which all the inequalities are satisfied are the zone E''T''C'' an d F''Q''H'' indicated by cross-hatching on the figures. Inside these zones is the only place where the non-planar motions are stable.

Since A''B'' is the locus of vertical tangents and response curves must pass through this locus, it appears that the only region in which out-of-phase* (i.e., after resonance or, equivalently, below the back bone curve A''C'') motions can occur is in the vicinity of the point Q''. This region is so small that for all practical purposes, such motions can be regarded as unlikely to occur. As Figures 1.15 an d 1.17 show, this conclusion is valid for both the "thin" ($\alpha = .005$, $\beta = .01$) and "thick" ($\alpha = .01$, $\beta = .02$) cross-sections and both force levels (the out-of-phase response curves for $F = 50 \times 10^{-6}$ are off scale in Figure 1.15).

Consider now the higher initial buckling state, $\lambda = 4$. The inequalities (1.138) and (1.140) give the same results as discussed for the $\lambda = 2$ case. However expression (1.139) differs in that R changes from negative to positive as the curve A''P'' is crossed. The only region in which all the inequalities are satisfied is the zone F''E''A''C'', indicated by cross-hatching on the figures. Inside this zone is the only place where the non-planar motions are stable. This gives the same result as for $\lambda = 2$, i.e., no out-of phase nonplanar motions are feasible. It should

* This refers to the phase between the vibrations in the xz-plane and the forcing function.

be noted that these conclusions differ from these of Ho, Scott and Eisley [11, 12] who found a very narrow region of stability in the out-of-phase region in their work on unbuckled beams.

Consider the case of frequency increasing from zero. For the thin beam and $\lambda = 2$ and 4, no nonplanar motions are possible until the boundary T"E" is met. Thereafter, the planar motion changes continuously with frequency to a whirling motion. This is further attested to by the corresponding growth of the B curves, as seen in Figures 1.18 and 1.20. For both beam geometries one effect of changing λ from 2 to 4 can be seen. Figures 1.19 and 1.21 show that for $\lambda = 4$ low-frequency, low-force-level whirling motions are possible. Thus increasing λ appears in this case to make whirling motions more likely.

Response and stability curves for the snap-through vibrations, $\bar{c}_1 = 0$, are shown in Figures (1.23) through (1.26).

Stability involves consideration of $\bar{R} > \bar{S}$ and $\bar{R}^2 - 4\bar{S}$ (see eq. (1.134)) and the same general characteristics emerge, i.e., for all practical purposes, out-of-phase nonplanar motions are impossible for both thin and thick beams and for both force levels. Note that thickening the beam drives the zone in which nonplanar motions are possible toward higher frequencies.

In summary of the results, it is seen that for various beam geometries and force levels, whirling motions of both snap-through and non-snap-through type can occur even in the presence of initial buckling.

PART TWO

STEADY-STATE NONLINEAR VIBRATION OF VISCOELASTIC, LAYERED BEAMS

2.1. INTRODUCTION

Due to engine excitation or environmental disturbances, flexural vibration control of structures, such as aircraft and missile frames, automobile components, etc., has received considerable attention in the literature in recent years. Principal goals of researchers in this field were the construction of viable approximate theories and the assessment of various families of viscoelastic materials used in controlling vibration for constrained and unconstrained layers.

Linear and nonlinear flexural vibration of damped sandwich beams and plates has been discussed by several authors. An extensive review of this work can be found in the paper of Hyer, Scott and Anderson [20]. One important item that has not received attention though is the use of unconstrained tapes in nonlinear vibrations.

The present study concerns the theoretical and experimental investigations of forced, nonlinear, damped vibration of a sandwich beam (i.e., steel elastic core coated with thin viscoelastic layers) with fixed end conditions. Due to axial stretching of the elastic core, nonlinearity is introduced into the problem. Damping effect of the system is considered due to viscoelastic coatings. A set of three coupled nonlinear partial differential equations is derived. Galerkin's

method is used to eliminate the spatial variable. Then the frequency-amplitude relation for a harmonic excitation force is obtained using the harmonic balance procedure. The nonlinear frequency-amplitude relation is explored numerically. The experimental results are compared to analytical predictions in terms of resonant amplitude of the frequency-response of the system.

2.2. DERIVATION OF THE EQUATIONS OF MOTION

In this chapter, a theory based upon assumptions similar to those used by Kovac, Anderson, and Scott [21], and others, will be developed. It is assumed that the elastic core experiences axial stretching, bending, and shear deformation and that only planar motions occur. The viscoelastic face layers are very thin, and their flexural rigidities are negligible. This fact allows the face sheets to be treated as membranes, an approximation used by Yu [22] and Hertelendy and Goldsmith [23]. The resultant forces and moment acting on a differential beam element are shown in Figure 2.2. Modelled on Timoshenko beam theory, the shear and bending deformations of an infinitesimal beam element are illustrated in Figure 2.1:

a) The beam element before deformation, where h is the thickness of the elastic core, τ is the thickness of the viscoelastic layers.

b) The beam element under shear deformation (i.e., ϕ is the shear deformation). This figure assumes that the viscoelastic face layers experience no shear deformation.

c) The beam element under shear and bending deformation, i.e., $\frac{\partial w}{\partial x} = \phi + \theta$ where $\frac{\partial w}{\partial x}$ is the slope of the deflection curve, $\theta(x, t)$ is the slope due to bending only, and $w(x, t)$ is the transverse displacement of the middle surface.

A set of three equations of motion (Figure 2. 2) is obtained by considering y-axis moments and summing forces in the x and z-directions:

$$\left[N^{\tau}(x+\Delta x, t)+N^{b}(x+\Delta x, t)\right]\cos(\theta+\phi+\frac{\Delta\theta+\Delta\phi}{2})+N^{c}(x+\Delta x, t)\cos(\theta+\frac{\Delta\theta}{2})$$

$$-\left[N^{\tau}(x, t)+N^{b}(x, t)\right]\cos(\theta+\phi-\frac{\Delta\theta+\Delta\phi}{2})-N^{c}(x, t)\cos(\theta-\frac{\Delta\theta}{2})$$

$$-Q^{c}(x+\Delta x, t)\sin(\theta+\frac{\Delta\theta}{2})+Q^{c}(x, t)\sin(\theta-\frac{\Delta\theta}{2})$$

$$=\Delta x\left[\rho^{c}A^{c}\ddot{u}^{c}+\rho^{\tau}A^{\tau}\ddot{u}^{\tau}+\rho^{b}A^{b}\ddot{u}^{b}\right] \qquad (2.5)$$

Dividing both sides by Δx and taking the limit as $\Delta x \to 0$ and using

$$\cos\theta = 1 \quad , \qquad \sin\theta = \theta$$

gives on noting $\rho^{\tau} = \rho^{b}$, $A^{\tau} = A^{b}$

$$\frac{\partial}{\partial x}\left[(N^{\tau}+N^{b}+N^{c})-Q^{c}\theta\right] = \rho^{c}A^{c}\ddot{u}^{c}+\rho^{\tau}A^{\tau}(\ddot{u}^{\tau}+\ddot{u}^{b}) \qquad (2.6)$$

Note that in the inertia terms, u^{c} is to be interpreted as a centerline quantity. Similarly, summing forces in the z-direction gives

$$\frac{\partial}{\partial x}\left[(N^{\tau}+N^{b})(\phi+\theta)+N^{c}\theta-Q^{c}\right]+a(x)q(t) = (\rho^{c}A^{c}+2\rho^{\tau}A^{\tau})\ddot{w} \qquad (2.7)$$

Taking y-axis moments and assuming no rotatory inertia due to shear gives

$$-\frac{\partial M^{c}}{\partial x}+Q^{c}=\rho^{c}I^{c}\ddot{\theta}+\frac{1}{2}\rho^{\tau}A^{\tau}(\tau+h)(\ddot{u}^{\tau}-\ddot{u}^{b}) \qquad (2.8)$$

In these equations, I^{c}, ρ^{c}, and A^{c} are moment of inertia, density and cross-sectional area of the elastic core; ρ^{τ}, ρ^{b}, A^{τ}, and A^{b} are the density and cross-sectional areas of the face layers, respectively; q(t) stands for the time dependency of the exciting force, and a(x) its

spatial dependency. The superscripts τ. b, and c stand for top, bottom, and core, respectively. A dot stands for the time derivative.

To proceed further, relations between the stress resultants and the displacements must be obtained. The damping effect of the viscoelastic face sheets is taken into account by modeling the viscoelastic layers as a Kelvin solid*

$$\sigma_{xx}^{\tau} = E^{\tau} E_{xx}^{\tau} + \zeta^{\tau} \dot{E}_{xx}^{\tau} \tag{2.9}$$

where E^{τ} and ζ^{τ} are material parameters, and E_{xx}^{τ} is Green's strain measure. A similar expression exists for σ^{b}.

Displacements are assumed of the form (see Figure 2.1), on taking the top and bottom layers to be the same so that the neutral axis is at the geometric center,

$$\begin{aligned} u^{c} &= u(x, t) - z\theta \\ u^{\tau} &= u(x, t) + \frac{h}{2}\theta + \tau(\phi + \theta) \\ u^{b} &= u(x, t) - \frac{h}{2}\theta - \tau(\phi + \theta) \end{aligned} \tag{2.10}$$

Since $\tau << h$, the last terms of u^{τ}, u^{b} are neglected. Under this assumption, the simplified displacement expressions are:

$$\begin{aligned} u^{c} &= u(x, t) - z\theta \\ u^{\tau} &= u(x, t) + \frac{h}{2}\theta \\ u^{b} &= u(x, t) - \frac{h}{2}\theta \end{aligned} \tag{2.11}$$

---

* This terminology, though common, is not strictly accurate in that the material parameters are allowed to be frequency dependent later. The procedure is adequate since only harmonic motions are considered here. A sound general procedure is given in Hyer, Scott and Anderson [20].

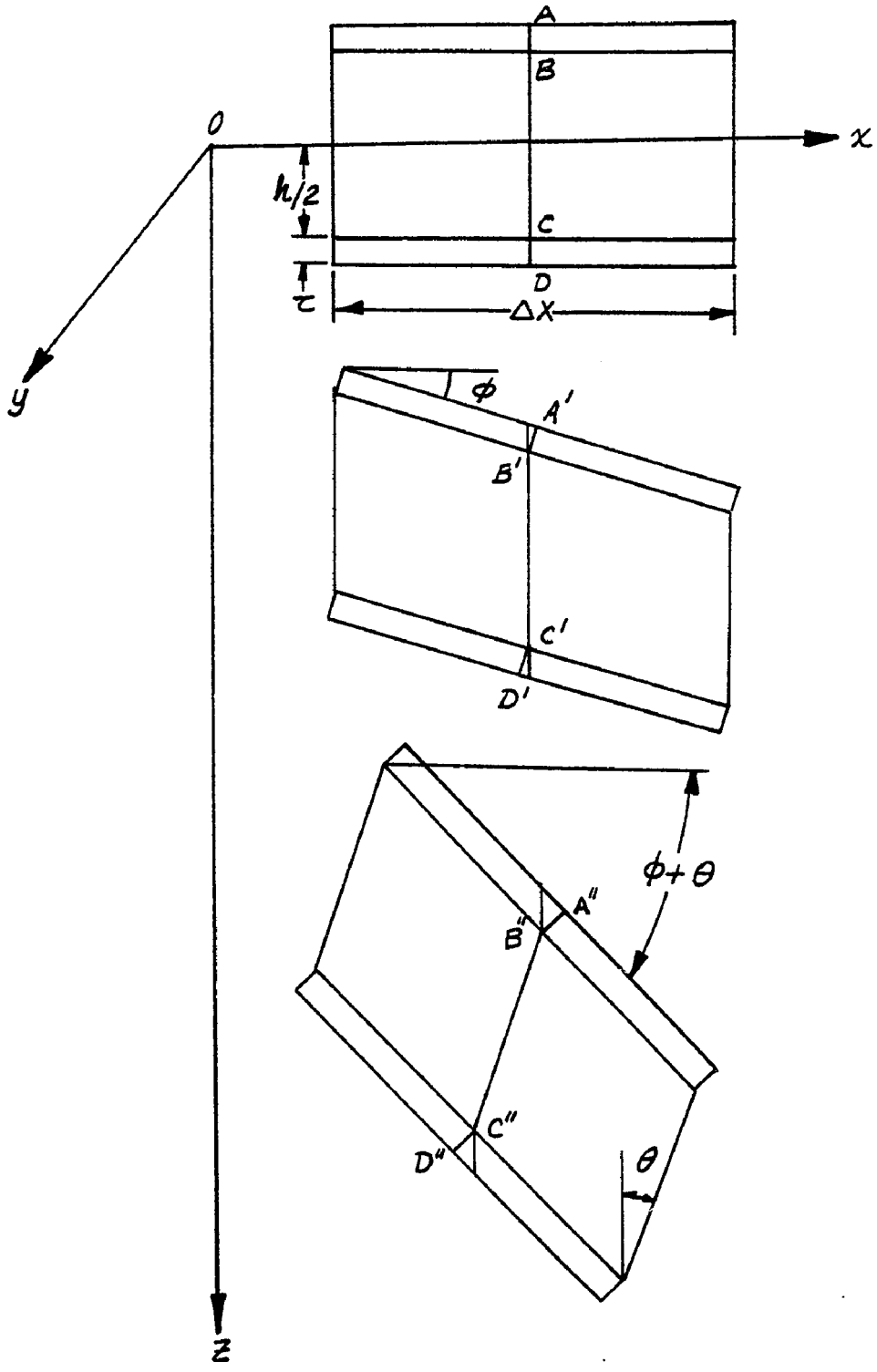


Figure 2.1. Shear and bending deformations of an infinitesimal beam element.

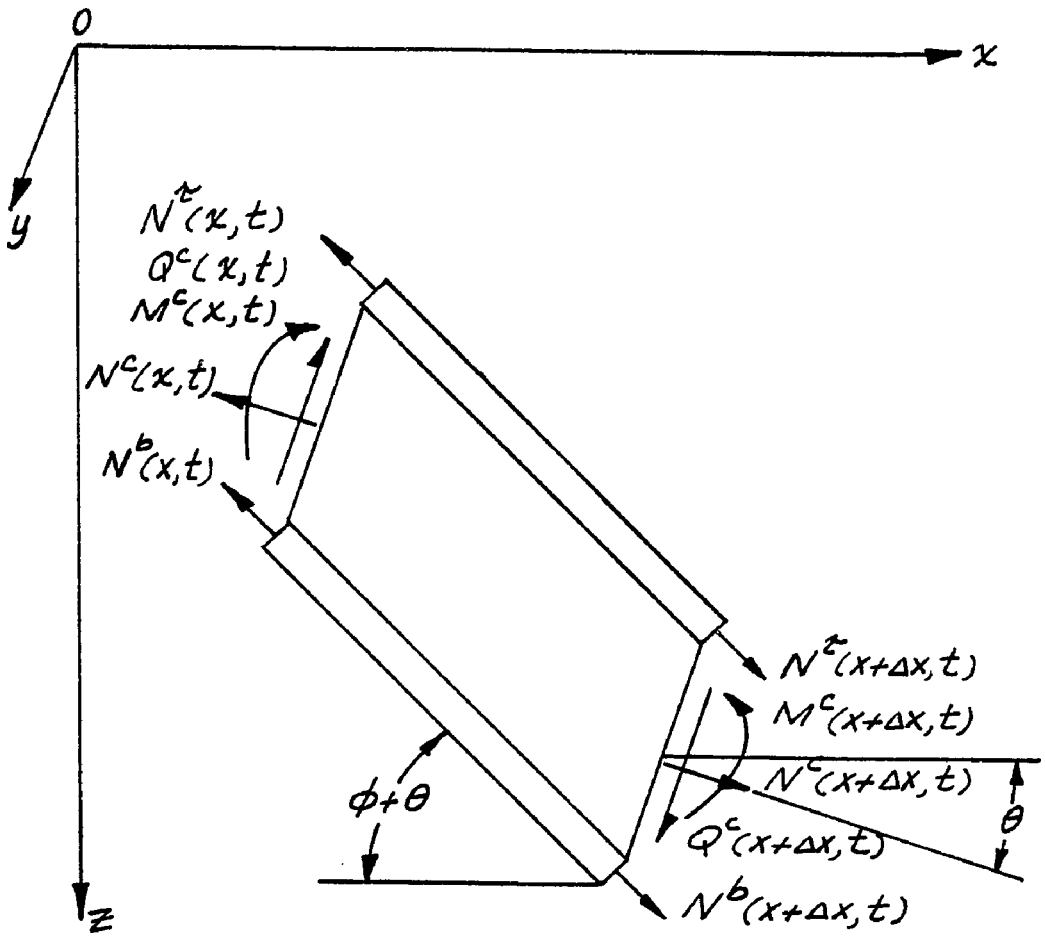


Figure 2.2. Force resultants and moments acting on an infinitesimal beam element.

In these expressions, it is assumed that the displacements are continuous across the elastic-viscoelastic layers and the displacement of face layers due to shear deformation of the elastic core is neglected.

The strain displacement relations are taken as (based on Green's strain measure in the x-direction):

$$E_{xx} = \frac{\partial u}{\partial x} + \frac{1}{2}\left(\frac{\partial w}{\partial x}\right)^2$$

and

$$E_{yy} = E_{zz} = E_{xy} = E_{yz} = 0 \qquad (2.12)$$

$$E_{xz} = \frac{1}{2}\phi = \frac{1}{2}\left(\frac{\partial w}{\partial x} - \theta\right)$$

Eqs. (2.12) are based on the assumption that the dominant nonlinear term is $\left(\frac{\partial w}{\partial x}\right)^2$. All other nonlinear terms are taken to be negligible. Substituting the assumed displacements, eqs. (2.11), into the strain displacement relation, eqs. (2.12) yields

$$E^c_{xx} = \frac{\partial u}{\partial x} + \frac{1}{2}\left(\frac{\partial w}{\partial x}\right)^2 - z\frac{\partial \theta}{\partial x}$$

$$E^\tau_{xx} = \frac{\partial u}{\partial x} + \frac{1}{2}\left(\frac{\partial w}{\partial x}\right)^2 + \frac{h}{2}\frac{\partial \theta}{\partial x} \qquad (2.13)$$

$$E^b_{xx} = \frac{\partial u}{\partial x} + \frac{1}{2}\left(\frac{\partial w}{\partial x}\right)^2 - \frac{h}{2}\frac{\partial \theta}{\partial x}$$

$$E^c_{xz} = \frac{1}{2}\left(\frac{\partial w}{\partial x} - \theta\right)$$

The nonlinearity in the above equations is needed to describe the axial stretching of the beam. During large amplitude lateral displacements, the ends of the beam are restrained so that they remain a

fixed distance apart and this induces axial stretching.

The stress-displacement relations are obtained from eqs. (2.9) and (2.12)

$$\sigma_{xx}^{c} = E^{c}\left[\frac{\partial u}{\partial x} - z\left(\frac{\partial \theta}{\partial x}\right) + \frac{1}{2}\left(\frac{\partial w}{\partial x}\right)^{2}\right]$$

$$\sigma_{xx}^{\tau} = E^{\tau}\left[\frac{\partial u}{\partial x} + \frac{h}{2}\left(\frac{\partial \theta}{\partial x}\right) + \frac{1}{2}\left(\frac{\partial w}{\partial x}\right)^{2}\right] + \zeta^{\tau}\left[\frac{\partial \dot{u}}{\partial x} + \frac{h}{2}\frac{\partial \dot{\theta}}{\partial x} + \frac{1}{2}\left(\frac{\partial \dot{w}}{\partial x}\right)^{2}\right]$$

$$\sigma_{xx}^{b} = E^{b}\left[\frac{\partial u}{\partial x} - \frac{h}{2}\left(\frac{\partial \theta}{\partial x}\right) + \frac{1}{2}\left(\frac{\partial w}{\partial x}\right)^{2}\right] + \zeta^{\tau}\left[\frac{\partial \dot{u}}{\partial x} - \frac{h}{2}\frac{\partial \dot{\theta}}{\partial x} + \frac{1}{2}\left(\frac{\partial \dot{w}}{\partial x}\right)^{2}\right]$$

$$\sigma_{xz}^{c} = G_{c}\left(\frac{\partial w}{\partial x} - \theta\right) \qquad (2.14)$$

The stress-resultants are defined by

$$N^{c} = \int_{c} \sigma_{xx}^{c}\, dz$$

$$N^{\tau} = \int_{\tau} \sigma_{xx}^{\tau}\, dz$$

$$N^{b} = \int_{b} \sigma_{xx}^{b}\, dz \qquad (2.15)$$

$$M^{c} = \int_{c} \sigma_{xx}^{c}\, z\, dz$$

$$Q^{c} = \int_{c} \sigma_{xz}^{c}\, dz$$

The integrations are over the thicknesses of the face layers; the thickness of the core refers to the deformed configuration. Here it is

assumed that for the relatively small deformation at hand, the deformed configuration can be replaced by the initial configuration. Here, and throughout all this work, the width of the beam is taken as unity.

Substitution of eqs. (2.14) into eqs. (2.15) yields, introducing the Timoshenko shear coefficient k ($k^2 = 2/3$ for rectangular cross-section),

$$N^c = E^c A^c \left[\frac{\partial u}{\partial x} + \frac{1}{2} \left(\frac{\partial w}{\partial x} \right)^2 \right]$$

$$N^\tau = E^\tau A^\tau \left[\frac{\partial u}{\partial x} + \frac{h}{2} \left(\frac{\partial \theta}{\partial x} \right) + \frac{1}{2} \left(\frac{\partial w}{\partial x} \right)^2 \right] + \zeta^\tau A^\tau \left[\frac{\partial \dot{u}}{\partial x} + \frac{h}{2} \left(\frac{\partial \dot{\theta}}{\partial x} \right) + \frac{1}{2} \left(\frac{\partial \dot{w}}{\partial x} \right)^2 \right]$$

$$N^b = E^b A^b \left[\frac{\partial u}{\partial x} - \frac{h}{2} \left(\frac{\partial \theta}{\partial x} \right) + \frac{1}{2} \left(\frac{\partial w}{\partial x} \right)^2 \right] + \zeta^b A^b \left[\frac{\partial \dot{u}}{\partial x} - \frac{h}{2} \left(\frac{\partial \dot{\theta}}{\partial x} \right) + \frac{1}{2} \left(\frac{\partial \dot{w}}{\partial x} \right)^2 \right]$$

$$M^c = E^c I^c \left(\frac{\partial \theta}{\partial x} \right) \qquad (2.16)$$

$$Q^c = k^2 bhG_c \left(\frac{\partial w}{\partial x} - \theta \right)$$

The nonlinear stretching force in the top and bottom viscoelastic layers is small compared to that in the core, since $E^\tau = E^b << E^c$; therefore, the last term in the 2nd and 3rd equations may be deleted, and this is done in the sequel.

Substitution of eqs. (2.16) into eqs. (2.6), (2.7), and (2.8) yields

$$\frac{\partial}{\partial x}\left[\left(2A^{T}E^{T}+A^{c}E^{c}\right)\frac{\partial u}{\partial x}+\frac{E^{c}A^{c}}{2}\left(\frac{\partial w}{\partial x}\right)^{2}-K\left(\frac{\partial w}{\partial x}-\theta\right)\theta+2A^{T}\zeta^{T}\frac{\partial \dot{u}}{\partial x}\right] = m\ddot{u}$$

$$\frac{\partial}{\partial x}\left[\left\{2E^{T}A^{T}\frac{\partial u}{\partial x}+2A^{T}\zeta^{T}\frac{\partial \dot{u}}{\partial x}\right\}\left(\phi+\theta\right)+E^{c}A^{c}\left\{\frac{\partial u}{\partial x}+\frac{1}{2}\left(\frac{\partial w}{\partial x}\right)^{2}\right\}\theta - K\left(\frac{\partial w}{\partial x}-\theta\right)\right]+a(x)\,q(t) = m\ddot{w}$$

$$-\frac{\partial}{\partial x}\left[E^{c}I^{c}\frac{\partial \theta}{\partial x}\right]+K\left(\frac{\partial w}{\partial x}-\theta\right) = I\ddot{\theta} \qquad (2.17)$$

or

$$\frac{\partial}{\partial x}\left[B_{c}\frac{\partial u}{\partial x}+\frac{E^{c}A^{c}}{2}\left(\frac{\partial w}{\partial x}\right)^{2}-K\left(\frac{\partial w}{\partial x}-\theta\right)\theta+2\zeta^{T}A^{T}\frac{\partial \dot{u}}{\partial x}\right] = m\ddot{u}$$

$$\frac{\partial}{\partial x}\left[\left\{2E^{T}A^{T}\frac{\partial u}{\partial x}+2\zeta^{T}A^{T}\frac{\partial \dot{u}}{\partial x}\right\}\frac{\partial w}{\partial x}+E^{c}A^{c}\left\{\frac{\partial u}{\partial x}+\frac{1}{2}\left(\frac{\partial w}{\partial x}\right)^{2}\right\}\theta - K\left(\frac{\partial w}{\partial x}-\theta\right)\right]+a(x)q(t) = m\ddot{w} \qquad (2.18)$$

$$-\frac{\partial}{\partial x}\left[D_{c}\frac{\partial \theta}{\partial x}\right]+K\left(\frac{\partial w}{\partial x}-\theta\right) = I\ddot{\theta}$$

where

$$\begin{aligned} D_{c} &= E^{c}I^{c} \\ K &= k^{2}bh\,G_{c} \\ m &= \rho^{c}A^{c}+2\rho^{T}A^{T} \\ I &= \rho^{c}I^{c}+\frac{1}{2}\rho^{T}A^{T}h\,(h+\tau) \\ B_{c} &= 2A^{T}E^{T}+E^{c}A^{c} \end{aligned} \qquad (2.19)$$

Now as explained by Yu [22] , the nonlinear term $K\left(\frac{\partial w}{\partial x}-\theta\right)\theta$ in the 1st equation of eqs. (2.18) is less important than the other nonlinear term in that equation. He has shown that this nonlinear term

is the horizontal component of the resultant shear force Q^c. On the other hand, the nonlinear terms in the 2nd equation of eqs. (2.18) are the vertical component of the normal resultant force N^c which contributes directly to the transverse flexural motion of the beam. Hence the nonlinear term in the 1st equation of eqs. (2.18) will be omitted, resulting in the equations*

$$\frac{\partial}{\partial x}\left[B_c \frac{\partial u}{\partial x} + \frac{E^c A^c}{2}\left(\frac{\partial w}{\partial x}\right)^2 + 2A^T\zeta^T \frac{\partial \dot{u}}{\partial x}\right] = m\ddot{u}$$

$$\frac{\partial}{\partial x}\left[\left\{2E^T A^T \frac{\partial u}{\partial x} + 2A^T\zeta^T \frac{\partial \dot{u}}{\partial x}\right\}\frac{\partial w}{\partial x} + E^c A^c\left\{\frac{\partial u}{\partial x} + \frac{1}{2}\left(\frac{\partial w}{\partial x}\right)^2\right\}\theta - K\left(\frac{\partial w}{\partial x} - \theta\right)\right] + a(x)q(t) = m\ddot{w}$$

$$-\frac{\partial}{\partial x}\left[D_c \frac{\partial \theta}{\partial x}\right] + K\left(\frac{\partial w}{\partial x} - \theta\right) = I\ddot{\theta} \qquad (2.20)$$

When damping and nonlinear terms are neglected in the 1st equation of eqs. (2.20), it becomes a simple linear extensional equation of motion for a sandwich beam:

$$\frac{\partial}{\partial x}\left(B_c \frac{\partial u}{\partial x}\right) = m\ddot{u} \qquad (2.21)$$

Then the 2nd and 3rd equations reduce to

---

* The reader should note, in contrast to the equation of Part One, that no integrals from 0 to L arise in the present formulation. Such a simplification is not made here because of complexities introduced by shear deformation.

$$- \frac{\partial}{\partial x} \left(D_c \frac{\partial \theta}{\partial x} \right) + K \left(\frac{\partial w}{\partial x} - \theta \right) = I\ddot{\theta}$$

$$\frac{\partial}{\partial x} \left[K \left(\frac{\partial w}{\partial x} - \theta \right) \right] + a(x)q(t) = m\ddot{w} \qquad (2.22)$$

Furthermore, if the rotatory inertia and shear deformation are neglected, i.e. $\ddot{\theta} = 0$, $\zeta = 0$, eqs. (2.22) reduce to

$$\frac{\partial^2}{\partial x^2} \left(D_c \frac{\partial^2 w}{\partial x^2} \right) + a(x)\, q(t) = m\ddot{w} \qquad (2.23)$$

This is a simple equation of motion for transverse vibration of a sandwich beam.

2. 3. FREQUENCY-AMPLITUDE RELATION

Eqs. (2. 20) are nonlinear partial differential equations. It is unlikely that exact solutions of these equations can be obtained and so approximate methods are used. The governing equations are first reduced to ordinary differential equations using Galerkin's method.

Assume the dependencies:

$$\begin{aligned} w(x, t) &= \tau(t)\, \xi(x) \\ u(x, t) &= \eta(t)\, \gamma(x) \\ \phi(x, t) &= T(t)\mu(x) \end{aligned} \tag{2. 24}$$

where ξ, γ, μ are trial functions which should satisfy the boundary conditions for a clamped-clamped beam, namely

$$\begin{aligned} w(o, t) &= w(L, t) = 0 \\ u(o, t) &= u(L, t) = 0 \\ \theta(o, t) &= \theta(L, t) = 0 \end{aligned} \tag{2. 25}$$

where $\theta = \frac{\partial w}{\partial x} - \phi$. An alternative form of the last eq. in (2. 24) is

$$\theta = T(t)\, g(x) \tag{2. 26}$$

Substituting eqs. (2. 24) into the first equation of (2. 20), multiplying the first resulting equation of eq. (2. 20) by $\gamma(x)$ and integrating from 0 to L yield an equation of the form

$$A_2 \tau^2 + A_3 \eta + A_4 \dot{\eta} + A_5 \ddot{\eta} = 0 \tag{2. 27}$$

where

$$A_2 = \int_o^L E^c A^c \xi' \xi'' \gamma \, dx$$

$$A_3 = \int_o^L B_c \gamma \gamma'' \, dx \qquad (2.28)$$

$$A_4 = \int_o^L 2 \zeta^T A^T \gamma \gamma'' \, dx$$

$$A_5 = - m \int_o^L \gamma^2 \, dx$$

Values can be found for A_2, A_3, A_4 and A_5 once the form of the trial functions has been specified.

Multiplying the second equation of the modified eqs. (2.20) by $\xi(x)$ and integrating from zero to L yields an equation of the form

$$F_1 T + F_2 \eta T + F_3 \eta \tau + F_4 \tau^3 + F_5 \tau \dot{\eta} + F_6 q(t) + F_7 \ddot{\tau} + F_8 T \tau^2 = 0 \qquad (2.29)$$

where

$$F_1 = - K \int_o^L \mu' \xi \, dx \quad , \text{ or } F_1 = K \int_o^L g \xi \, dx$$

$$F_2 = - E^c A^c \int_o^L (\gamma'' \mu \xi + \gamma' \mu' \xi) \, dx \text{ or } F_2 = E^c A^c \int_o^L (\gamma'' g - \gamma' g') \xi \, dx$$

$$F_3 = (2E^T A^T + E^c A^c) \int_o^L (\gamma'' \xi' \xi + \gamma' \xi'' \xi) \, dx \qquad (2.30)$$

$$F_4 = \frac{3}{2} E^c A^c \int_o^L (\xi'' \xi'^2 \xi) \, dx$$

$$F_5 = 2 \zeta^T A^T \int_o^L (\gamma'' \xi' \xi + \gamma' \xi'' \xi) \, dx$$

$$F_6 = \int_o^L a \xi \, dx$$

$$F_7 = -m\int_o^L \xi^2\,dx$$

$$F_8 = -E^cA^c\int_o^L (\xi'\xi''\mu + \tfrac{1}{2}\xi'^2\mu')\xi\,dx, \text{ or } F_8 = E^cA^c\int_o^L (\xi'\xi''g + \tfrac{1}{2}\xi'^2 g')\xi\,dx$$

Again, F_1 through F_8 can be evaluated once the trial functions are specified.

Multiplying the third equation of the modified eqs. (2.20) by $\mu(x)$ (or $g(x)$, if the alternate form eq. (2.26) is used) and integrating from zero to L yields

$$B_1T + B_3\tau + B_2\ddot{\tau} + B_4\ddot{T} = 0 \tag{2.31}$$

where

$$B_1 = \int_o^L (D_c\mu\mu'' + K\mu^2)dx \text{ or } B_1 = -\int_o^L (D_c g''g + Kg^2)\,dx$$

$$B_2 = -I\int_o^{L'} \xi\mu\,dx \text{ or } B_2 = \int_o^{L'} \xi g\,dx$$

$$B_3 = -D_c\int_o^L \mu\xi'''\,dx \text{ or } B_3 = K\int_o^{L'} \xi g\,dx$$

$$B_4 = I\int_o^L \mu^2\,dx \text{ or } B_4 = -I\int_o^L g^2\,dx \tag{2.32}$$

A discussion of the choice of the trial functions will now be given. One set that was tried was

$$\xi(x) = \sin\frac{\pi x}{L}$$

$$\gamma(x) = \sin\frac{2\pi x}{L} \tag{2.33}$$

$$g(x) = \sin\frac{2\pi x}{L}$$

These satisfy the boundary conditions of the problem, eqs. (2.25).

Moreover, they have the feature that the shear deformation angle ϕ is not zero at the boundary, which is physically reasonable. However, severe problems arise in connection with eqs. (2.33). These trial functions lead to $B_2 = 0$, $B_3 = 0$ in eq. (2.32). Now $B_2 = 0$ is a very poor feature since it involves the bending effect of the core. Another bad aspect is that $F_1 = 0$ in eq. (2.29), so that the linear term would be absent. Still another poor feature is that the choice does not lead smoothly to the recovery of Euler-Bernoulli-Kirchhoff beam theory in the limit as shearing deformation vanishes. The problem is singular in the sense that the zero slope condition on θ is maintained by a non-vanishing ϕ as shearing effects vanish. These considerations lead to abandoning the choice in eq. (2.33). Another possible approach is to modify Galerkin's procedure by taking weight functions different from trial functions. (For references, see Crouch, Anderson and Greenwood [14]). However, it was felt that sufficient accuracy could be obtained on taking

$$\xi(x) = 1 - \cos\frac{2\pi x}{L}$$

$$\mu(x) = \sin\frac{2\pi x}{L} \qquad (2.34)$$

$$\gamma(x) = \sin\frac{4\pi x}{L}$$

Note that the same choice of ξ was taken by Eisley [11] and [12], by Yu [22] and Tseng and Dugundji [4]. These functions are such that the boundary conditions in eqs. (2.25) are satisfied. However,

they have the somewhat unsatisfactory feature that the shear deformation angle ϕ is zero at the boundary. It was felt that this unphysical feature was acceptable since shear effects in the core are likely to be small compared to bending effects. The factor 4 in the last of eqs. (2. 34) is introduced since it is a form suggested by the differential equation resulting from the first equation of (2. 20), on neglecting damping.

For the choice of trial functions (2. 34), the various constants are

$$A_2 = \frac{2E^cA^c\pi^3}{L^2} \quad , \qquad A_3 = -\frac{8\pi^2 B_c}{L}$$

$$A_4 = -\frac{16\zeta^T A^T \pi^2}{L} \quad , \qquad A_5 = -\frac{mL}{2}$$

$$B_1 = \left(K - \frac{4\pi^2 D_c}{L^2}\right)\frac{L}{2} \quad , \qquad B_2 = -I\pi \qquad (2.35)$$

$$B_3 = 4D_c\pi^3/L^2 \quad , \qquad B_4 = IL/2$$

$$F_1 = K\pi \quad , \qquad F_2 = -\frac{2E^cA^c\pi^2}{L}$$

$$F_3 = -(2E^TA^T + E^cA^c)\frac{\pi^3}{L^2} \quad , \quad F_4 = -\frac{3}{2}E^cA^c(\pi^4/L^3)$$

$$F_5 = -2\zeta^T A^T \pi^3/L^2 \quad , \quad F_6 = aL^*$$

$$F_7 = -\frac{3}{2}mL \quad , \quad F_8 = \frac{3}{2}E^cA^c\pi^3/L^2$$

Approximate solutions to the eqs. (2. 27), (2. 29) and (2. 31) under conditions of harmonic forcing will be sought as follows: a simple

* This assumes that the spatial dependency of the external force is a constant. In the sequel a is set equal to one.

approximate solution* of eq. (2.29) is

$$\tau(t) = W(\omega)\cos\omega t \tag{2.36}$$

Substituting eq. (2.36) into eq. (2.31) gives

$$B_4\ddot{T} + B_1 T = (B_2\omega^2 W\cos\omega t - B_3 W\cos\omega t) \tag{2.37}$$

The steady-state solution of eq. (2.37) is

$$T_{ss}(t) = \bar{A}_1\cos\omega t = \gamma_1 W\cos\omega t \tag{2.38}$$

where

$$\bar{A}_1 = \left(\frac{B_2\omega^2 - B_3}{B_1 - B_4\omega^2}\right) W \equiv \gamma_1 W \tag{2.39}$$

Substituting eq. (2.36) into eq. (2.27) gives

$$A_3\eta + A_4\dot{\eta} + A_5\ddot{\eta} = -\frac{1}{2}A_2 W^2(1+\cos 2\omega t) \tag{2.40}$$

The steady-state solution of eq. (2.40) is

$$\eta_{ss}(t) = \bar{A}_2\cos(2\omega t - \alpha_2) + \bar{A}_3 \tag{2.41}$$

where

$$\bar{A}_3 = -\frac{A_2}{2A_3} W^2 \equiv \bar{\gamma}_3 W^2$$

$$\bar{A}_2 = \left(D_1^2 + D_2^2\right) W^2 \equiv \beta_2^2 W^2$$

$$D_1 = -\frac{\omega A_2 A_4}{\Delta} \tag{2.42}$$

$$D_2 = -\frac{(A_3 - 4\omega^2 A_5)}{\Delta} A_2$$

$$\Delta = (A_3 - 4\omega^2 A_5)^2 + 4\omega^2 A_4^2$$

---

* It is assumed that no super or subharmonics arise in the response.

$$\alpha_2 = \tan^{-1}(D_1/D_2)$$

In summary:

$$\tau(t) = W(\omega)\cos\omega t \tag{2.43}$$

$$T(t) = \bar{A}_1\cos\omega t \tag{2.44}$$

$$\eta(t) = \bar{A}_2\cos(2\omega t - \alpha_2) + \bar{A}_3 \tag{2.45}$$

Note that the coefficients $\bar{A}_1$, $\bar{A}_2$, and $\bar{A}_3$ are frequency dependent.

Explicitly, suppose the forcing function is given by

$$q(t) = H\cos\omega t + G\sin\omega t \tag{2.46}$$

Substituting eqs. (2.43), (2.44), (2.45) and (2.46) into eq. (2.29) yields, noting the trigonometric identities,

$$\begin{aligned}\cos\omega t\cos(2\omega t - \alpha_2) &= \tfrac{1}{2}\cos\alpha_2(\cos\omega t + \cos 3\omega t)\\ &\quad + \tfrac{1}{2}\sin\alpha_2(\sin\omega t + \sin 3\omega t)\\ \cos\omega t\sin(2\omega t - \alpha_2) &= -\tfrac{1}{2}\sin\alpha_2(\cos\omega t + \cos 3\omega t)\\ &\quad + \tfrac{1}{2}\cos\alpha_2(\sin\omega t + \sin 3\omega t)\end{aligned} \tag{2.47}$$

$$\begin{aligned}&F_1\bar{A}_1\cos\omega t + F_2\bar{A}_2\bar{A}_1\left[\tfrac{1}{2}\cos\alpha_2(\cos\omega t+\cos 3\omega t)+\tfrac{1}{2}\sin\alpha_2(\sin\omega t+\sin 3\omega t)\right]\\ &+ F_2\bar{A}_1\bar{A}_3\cos\omega t + F_3\bar{A}_2 W\left[\tfrac{1}{2}\cos\alpha_2(\cos\omega t+\cos 3\omega t)+\tfrac{1}{2}\sin\alpha_2(\sin\omega t+\sin 3\omega t)\right]\\ &+ F_3 W\bar{A}_3\cos\omega t + F_4 W^3\left(\tfrac{3}{4}\cos\omega t+\tfrac{1}{4}\cos 3\omega t\right) - F_7\omega^2 W\cos\omega t\\ &+ F_8 W^2\bar{A}_1\left(\tfrac{3}{4}\cos\omega t+\tfrac{1}{4}\cos 3\omega t\right) + F_6\left|H\cos\omega t + G\sin\omega t\right|\\ &- 2\omega W\bar{A}_2\left[-\tfrac{1}{2}\sin\alpha_2(\cos\omega t+\cos 3\omega t)+\tfrac{1}{2}\cos\alpha_2(\sin\omega t+\sin 3\omega t)\right] = 0\end{aligned} \tag{2.48}$$

The method of harmonic balance will now be employed. Equating the coefficients of $\cos\omega t$ and $\sin\omega t$ to zero and neglecting the higher

order harmonics gives

$$F_1\bar{A}_1+\frac{1}{2}F_2\bar{A}_1\bar{A}_2\cos\alpha_2+F_2\bar{A}_1\bar{A}_3+\frac{1}{2}F_3\bar{A}_2W\cos\alpha_2+F_3W\bar{A}_3$$

$$+ F_5\omega W\bar{A}_2\sin\alpha_2+\frac{3}{4}F_4W^3-F_7\omega^2W+\frac{3}{4}F_8\bar{A}_1W^2 = - F_6H$$

$$\frac{1}{2}F_2\bar{A}_1\bar{A}_2\sin\alpha_2 + \frac{1}{2}F_3\bar{A}_2W\sin\alpha_2 - F_5\omega W\bar{A}_2\cos\alpha_2 = - F_6G \qquad (2.49)$$

Squaring both sides of these two equations and adding them together gives, after some lengthy algebra, the frequency-amplitude relation:

$$C_7W^6+C_5W^4+C_3W^2+C_1 = 0 \qquad (2.50)$$

where

$$C_1 = - F_6^2F^2 \quad \text{where } F^2 = H^2 + G^2 \qquad (2.51)$$

$$C_3 = (F_1\gamma_1-F_7\omega^2)^2$$

$$C_5 = (F_1\gamma_1-F_7\omega^2)\Big[(F_2\gamma_1+F_3)(\beta_2\cos\alpha_2+2\bar{\gamma}_3)+\frac{3}{2}(F_4+F_8\gamma_1) +2\omega F_5\beta_2\sin\alpha_2\Big]$$

$$C_7=(9/16)(F_4+F_8\gamma_1)^2+(F_4F_8\gamma_1)\Big[\frac{3}{4}(F_3+F_2\gamma_1)(\beta_2\cos\alpha_2+2\bar{\gamma}_3) + \frac{3}{2}F_5\omega\beta_2\sin\alpha_2\Big]+(F_2\gamma_1+F_3)^2+(\frac{1}{4}\beta_2^2+\cos\alpha_2\beta_2\bar{\gamma}_3+\bar{\gamma}_3^2)+(F_2\gamma_1+$$

$$+ F_3)2\omega\beta_2\bar{\gamma}_3F_5\sin\alpha_2+\omega^2F_5^2\beta_2^2$$

If the damping term is deleted in eq. (2.49), then $A_4 \equiv 0$, $F_5 \equiv 0$ which implies $\alpha_2 \equiv 0$, and some simplifications can be achieved, namely:

Let

$$(F_1\gamma_1-F_7\omega^2) = P_1$$

$$(F_2\gamma_1+F_3) = P_2 \qquad (2.52)$$

$$(\beta_2 + 2\bar{\gamma}_3) = P_3$$

$$(F_4+F_8\gamma_1) = P_4$$

Then the coefficients of eq. (2.51) become

$$C_3 = P_1^2$$

$$C_5 = P_1(P_2P_3 + \frac{3}{2} P_4) \tag{2.53}$$

$$C_7 = (\frac{3}{4} P_4 + \frac{1}{2} P_2P_3)^2$$

and eq. (2.50) can be written

$$(\frac{3}{4} P_4 + \frac{1}{2}P_2P_3)^2 W^6 + P_1(P_2P_3+\frac{3}{2}P_4)W^4+P_1^2W^2 = F_6^2 F^2 \tag{2.54}$$

Taking the square root of both sides of eq. (2.54) yields

$$K_4W^3+K_2W+K_o = 0 \tag{2.55}$$

where

$$K_o = F_6F$$

$$K_2 = (F_1\gamma_1 - F_7\omega^2)$$

$$K_4 = \frac{3}{4}(F_4+F_8\gamma_1)+\frac{1}{2}(F_2\gamma_1+F_3)(\beta+2\bar{\gamma}_3) \tag{2.56}$$

The responses for the damped and undamped cases can be obtained from eqs. (2.50) and (2.55), using, for example, the Newton-Raphson iterative technique for nonlinear algebraic equations. Numerical results will be given and analyzed in the next section.

2.4. PARAMETRIC STUDY

One of the major goals of the present study is to assess the effect of unconstrained damping tapes on the amplitudes of nonlinear vibration of beams. A commonly available damping tape is ISPD 111 and this is the one chosen for study here. Its loss tangent δ and shear modulus G as a function of frequency are shown in Figure 2.3*. From such data the damping parameter ζ can be calculated from the relationship provided by the 3M Company

$$\zeta = \frac{G}{\omega} 14.5 \times 10^{-6} \tan \delta$$

where G is measured in psi and ω in Hertz.

Shown in Figure 2.4 are the variations of G and δ at 100 Hz. with temperature. It is seen that δ peaks in the vicinity of normal room temperature.

The elastic core material chosen for the study was a steel with Young's modulus $E=30\times10^6$ psi and shear modulus $G=10\times10$ psi and density $\rho = .283\#/in^3$. The length of the beam L was 12"; its depth b was 1".

The first phase of the parametric study is the effect of one tape of thickness .008" (the thickness supplied) on beams of varying thickness h. Shown in Figures 2.5 through 2.10 are the damped and undamped frequency responses at the force level F = .1 lbs, as computed from

---

* The author is grateful to the 3M Company, Saint Paul, Minnesota, for supplying not only this data, but also actual tape samples.

eqs. (2.50) and (2.55)*. The first feature worthy of notice is the rather pronounced nonlinearities involved. However, the most important feature, as can be seen from a close inspection of the figures, is the fact that one layer of the tape has very little effect on the response. A more thorough assessment of the effect is given in Figure 2.11. Shown there are theoretical plots of the amplitude at 70 Hz. (chosen since the loss tangent is maximum at this frequency) as functions of the tape thickness for F = .1 lbs. These curves were computed using eqs. (2.50).

A somewhat surprising feature of these curves is the nonlinear relationship, to the scale of the figures, between response amplitude and tape thickness. It is seen more graphically that the effect of taping, though present, is quite small. The effects can be seen qualitatively in Table 1. To achieve a reduction in amplitude of just 5%, layers of at least the beam thickness must be applied.

In summary of the study, it is seen that unconstrained damping treatment is not particularly effective, and the design or "fix-it" recommendations are to use constrained layers, if at all possible. These recommendations are known for linear vibrations (see Plunkett [24]) and to the author's knowledge are here confirmed for the first time for nonlinear vibrations.

---

* The heavy points in the figures are experimental points and will be discussed in the next section.

Beam Thickness	Viscoelastic Face Layer-Thickness			
	.008"	.016"	.032"	.064"
	AMPLITUDE % REDUCTION			
.018"	2.18	4.3	8.7	16.8
.022"	2	3.9	6.9	13.9
.035"	.8	1.9	4.1	9.1

TABLE 1

Percentage reduction in amplitudes

2.5. EXPERIMENTAL RESULTS

To lend some further confidence to the theoretical model and to test if indeed the effects of damping are small, an experiment was performed. During the experiment, .018", .022" and .035" thick and 12" long, 1" wide steel beam samples were used. Each test sample was coated on both sides with .008" thick self-adhesive viscoelastic tape ISPD 111. The bonding between viscoelastic faces and elastic core faces and elastic core looked very good, and it was felt that the zero relative displacement assumption used in the theory was justified.

The experimental facility originally was developed by Bennett [25] for an experimental study of nonlinear mode coupling in homogeneous beams with clamped-clamped boundary conditions. Kovac, Anderson, and Scott [21] used the same facility for their experimental study of forced, nonlinear damped vibration of a symmetric, three-layer composite beam. Although the main ideas are the same, a new test fixture was designed to overcome some shortcomings of the previous set-up.

Each beam sample was clamped between L-shaped steel blocks, which were bolted together rigidly to control the axial tension in the specimen (see Figure 2.12). A yoke was then placed on these support blocks to prevent the ends of the beam from moving towards each other. This test assembly rested on the bed of a tensile machine. A compressive load was applied to the yoke to keep the support blocks at a fixed distance from each other. The distance between the support

blocks was fixed at a 12" span using adjustment of the steel rods.

During the experiment, it was observed that the axial load, clamped support condition, and the length of the beams had significant effect on the response characteristics of the beam. An inexactness of the boundary condition (namely, not perfectly clamped), small preload, and a slight increase or decrease in the beam length from the desired 12" test length resulted in a substantial difference in the fundamental frequency, nonlinear hardening, and amplitude.

In order to eliminate these undesirable effects, the following procedure was adopted. During mounting of the specimen into the support blocks, the induced axial tensile and compressive load was maintained at zero by adjusting the span between support blocks with the steel rod screw arrangement. This condition of zero load was monitored by two symmetric foil-type strain gages placed on opposite sides of the beam.

A C-type 3" x 5" x 1" electromagnet was designed to excite the beam. The magnet had no mechanical contact with the beam sample, thus eliminating extraneous inertia effects on the system. The fundamental mechanical frequency of the magnet assembly was lower than 5 Hz. The lowest frequency at which response measurements were made was higher than 20 Hz. Therefore, there was no mechanical interference between the magnet and the response of the beam.*

* In situations where superharmonics are likely to occur, considerably more care has to be taken. See Hyer, Anderson, and Scott [20] for a description of a device involving feedback control.

The force generated by the magnet was measured by an Endevco Model 3300A accelerometer. However, the acceleration level was low so the signal was amplified using an amplifier (Dana Model 3530). Force calibration was achieved as follows. Since the magnet is suspended by a frictionless pin as indicated in Figure 2.12, it is free to oscillate in response to the reaction force exerted on it by the beam. The measured acceleration "a" at the accelerometer mount on the magnet is converted to the excitation force by means of the relation $F = (I+m\ell^2)a/\ell_1^2$ where ℓ_1 is the distance from the accelerometer to the pin, and ℓ is the distance from the center of mass of the magnet assembly to the pin. The quantity ℓ was measured by hanging the magnet assembly from two different attachment points, with the intersection of the vertical lines determining the center of mass. The moment of inertia I was also determined experimentally; the magnet assembly was suspended as a pendulum by a 50" long weightless string and the period of oscillation determined.

One problem that arises in connection with electromagnetic forcing, as Kung and Pao [26] point out in connection with their experimental work on circular plates, is that the magnitude of the forcing function changes with frequency. A constant force level, as indicated by a display on an oscilloscope (see Figure 2.13), was maintained by adjusting the gain on an amplifier in the oscillator circuit for the various frequency settings involved in the experiment.

The responses which were relatively free of distortion (see Figure 2. 14) were measured by a Bently-Nevada proximeter (Probe Type Proximeter 308). This is an inductive proximity device which did not come in contact with the beam. Before commencement of the experiment, an accurate proximeter calibration was conducted. A calibration plot of voltage versus distance curve was generated by measuring the distance to a beam sample attached to the micrometer spindle. Micrometer readings were compared to the proximeter output signal read on a DC voltmeter. The calibration curve and device are shown in Figure 2. 15. As can be seen, the response curve of the proximeter was linear between . 05" and . 1" distance from the beam sample. During the experiment, the proximeter was placed approximately . 08" from the beam sample (i. e., in the linear range). The response data, i. e., the RMS value of amplitude, were determined by means of an RMS voltmeter.

Shown as heavy points on Figures 2. 5 through 2. 10 are the values determined experimentally. As the curves for undamped response show, excellent agreement is found between the theory and experiment, which supports the plausibility of the theory. The curves for the damped response verify that the effects of damping by one layer are indeed small as predicted by theory. Finally it is interesting to note that, as found also by Kung and Pao [26], jumps from both low to high and high to low amplitudes involve intervals in which the motion

is not sinusoidal but the beating type (see Figures 2. 16a and b).

LIST OF REFERENCES

[1] Ho, C.-H., "Nonlinear Beam Vibrations," Ph. D. dissertation, University of Michigan, 1973.

[2] Eisley, J. G., "Nonlinear Vibrations of Beams and Rectangular Plates," ZAMP, Vol. 15, 1964, pp. 167-174.

[3] Min, G.-B. and Eisley, J. G., "Nonlinear Vibration of Buckled Beams," J. Engr. Ind., Vol. 94, 1972, pp. 637-646.

[4] Tseng, W.-Y. and Dugundji, J., "Nonlinear Vibrations of a Buckled Beam under Harmonic Excitation," J. Appl. Mech., Vol. 38, 1971, pp. 467-476.

[5] Ames, W. F., Lee, S. Y., Zaiser, J. N., "Non-linear Vibration of a Traveling Threadline," Int. J. Nonlinear Mech., Vol. 3, 1968, pp. 449-469.

[6] Ames, W. F. and Vicario, A. A., Jr., "Longitudinal Wave Propagation on a Traveling Threadline-I," Devl. in Mech., Vol. 5, 1969, p. 733.

[7] Ames, W. F., Lee, S. Y., Vicario, A. A., Jr., "Longitudinal Wave Propagation on a Traveline Threadline-II," Int. J. Nonlinear Mech., Vol. 5, 1970, pp. 413-426.

[8] Shih, L. Y., "Three-dimensional Non-linear Vibration of a Traveling String," Int. J. Nonlinear Mech., Vol. 6, 1971, pp. 427-434.

[9] Haight, E. C. and King, W. W., "Stability of Nonlinear Oscillations of an Elastic Rod," J. Acoust. Soc. Amer., Vol. 52, 1972, pp. 899-911.

[10] Rodgers, L. C. and Warner, W. H., "Dynamic Stability of Out-of-Plane Motion of Curved Elastic Rods," SIAM J. Appl. Math., Vol. 24, 1973, pp. 36-43.

[11] Ho, C.-H, Scott, R. A., Eisley, J. G., "Nonplanar, Nonlinear Oscillations of a Beam: Part 1, Forced Motions," Int. J. Nonlinear Mech., Vol. 10, 1975, pp. 113-127.

[12] Ho, C.-H., Scott, R. A., Eisley, J. G., "Non-planar, Nonlinear Oscillations of a Beam: Part 2, Free Motions," J. Sound Vib., Vol. 47, 1976, pp. 333-339.

[13] Herrmann, G., "Influence of Large Amplitudes on Flexural Motions of Elastic Plates," NACA TN 3578.

[14] Crouch, J. G., Anderson, W. J., Greenwood, D. T., "Eigenvalue Errors in the Method of Weighted Residuals," AIAA J., Vol. 8, 1970, pp. 2048-2054.

[15] Hayashi, C., Nonlinear Oscillations in Physical Systems, McGraw-Hill, Inc., New York, 1964.

[16] Hoehn, E. K. H., "Properties of Stability Diagrams for Hill's Equation," ZAMM, Vol. 54, 1974, pp. 734-737.

[17] Magnus, W. and Winkler, S., Hill's Equations, Interscience Publishers, New York, 1966.

[18] Williams, C. J. H. and Tobias, S. A., "Forced Undamped Non-Linear Vibrations of Imperfect Circular Discs," J. Mech. Eng. Sci, Vol. 5, 1963, pp. 325-335.

[19] Efstathiades, G. J. and Williams, C. J. H., "Vibration Isolation Using Non-Linear Springs," Int. J. Mech. Sci., Vol. 9, 1967, pp. 27-44.

[20] Hyer, M. W., Anderson, W. J., and Scott, R. A., "Non-linear Vibrations of Three Layer Beams with Viscoelastic Cores: I, Theory," J. Sound Vib., Vol. 46, 1976, pp. 121-136.

[21] Kovac, E. J., Jr., Anderson, W. J., Scott, R. A., "Forced Non-Linear Vibrations of a Damped Sandwich Beam," J. Sound Vib., Vol. 17, 1971, pp. 25-39.

[22] Yu, Y.-Y., "Nonlinear Flexural Vibrations of Sandwich Plates," J. Acoust. Soc. Amer., Vol. 34, 1962, pp. 1176-1183.

[23] Hertelendy, P. and Goldsmith, W., "Flexural Vibrations of an Elastic Plate with Two Symmetric Viscoelastic Coatings," J. Appl. Mech., Vol. 34, 1967, pp. 187-194.

[24] Plunkett, Robert, "Design for Vibration Control by Damping," ASME Paper 74-DE-10, Presented at the Design Engineering Conference and Show, Chicago, Illinois, April 1-4, 1974.

[25] Bennett, J. A., "A Multiple Degree of Freedom Approach to Nonlinear Beam Vibrations," Ph. D. dissertation, University

of Michigan, 1969.

[26] Kung, C. C. and Pao, Y.-H., "Nonlinear Flexural Vibrations of a Clamped Circular Plate," J. Appl. Mech., Vol. 39, 1972, pp. 1050-1054.

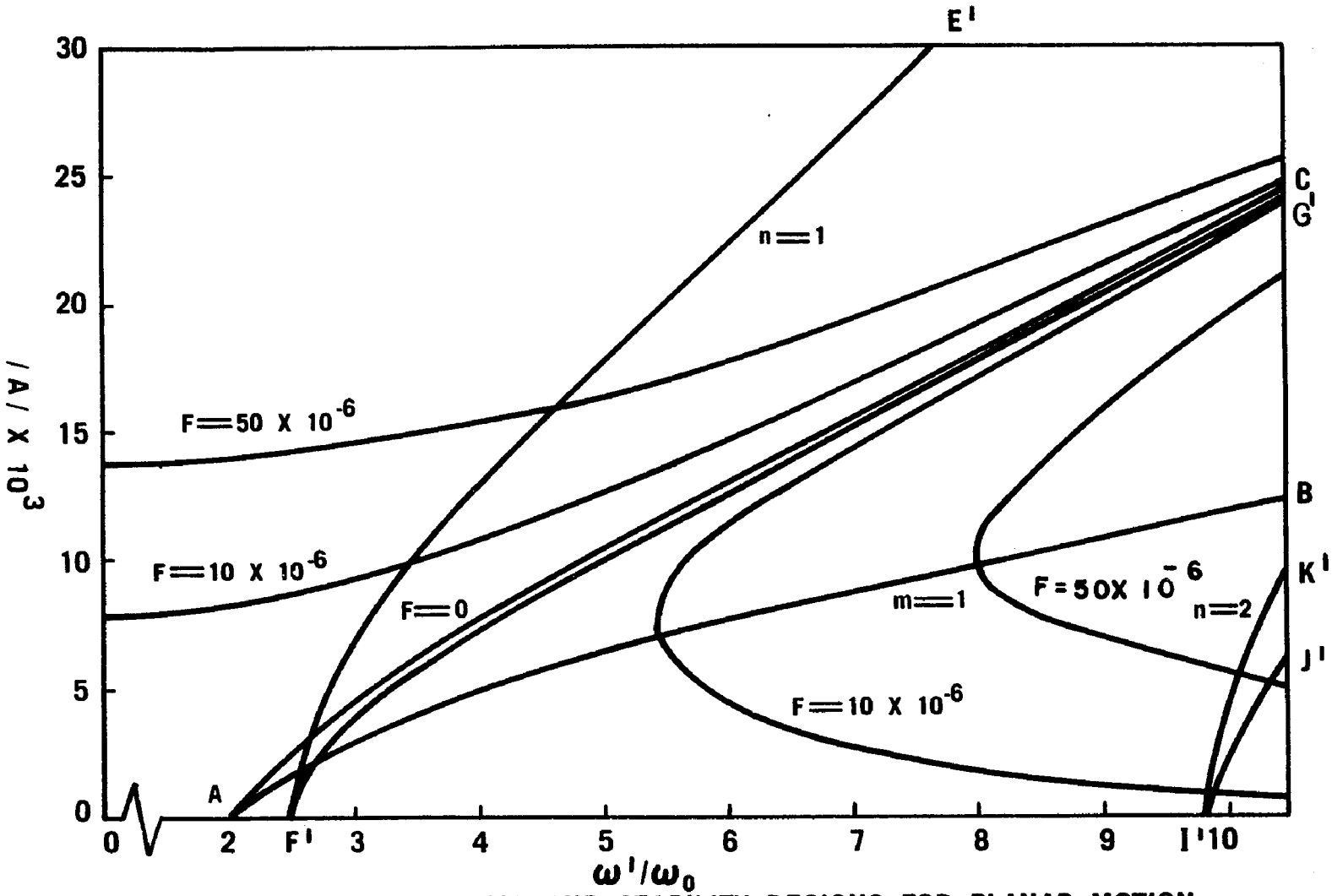


FIGURE 1.7 RESPONSE AND STABILITY REGIONS FOR PLANAR MOTION
$m=1, n=1,2, \alpha=.005, \beta=.01, \lambda=2, \bar{c}_1 \neq 0.$

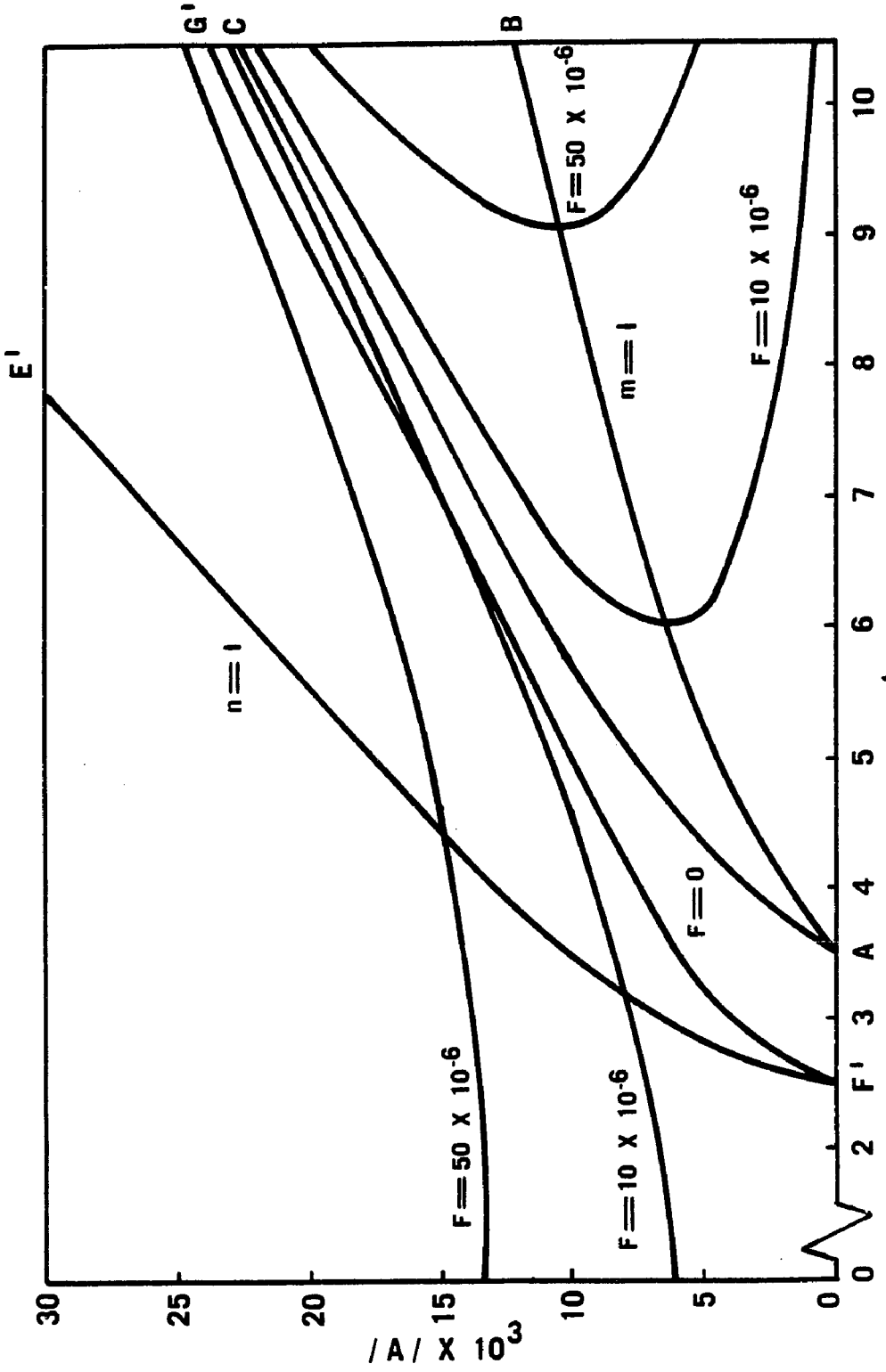


FIGURE 1.8 RESPONSE AND STABILITY REGIONS FOR PLANAR MOTION
$m = 1,\ n = 1,\quad \alpha = .005, \beta = .01, \lambda = 4,\ \bar{c}_1 \neq 0.$

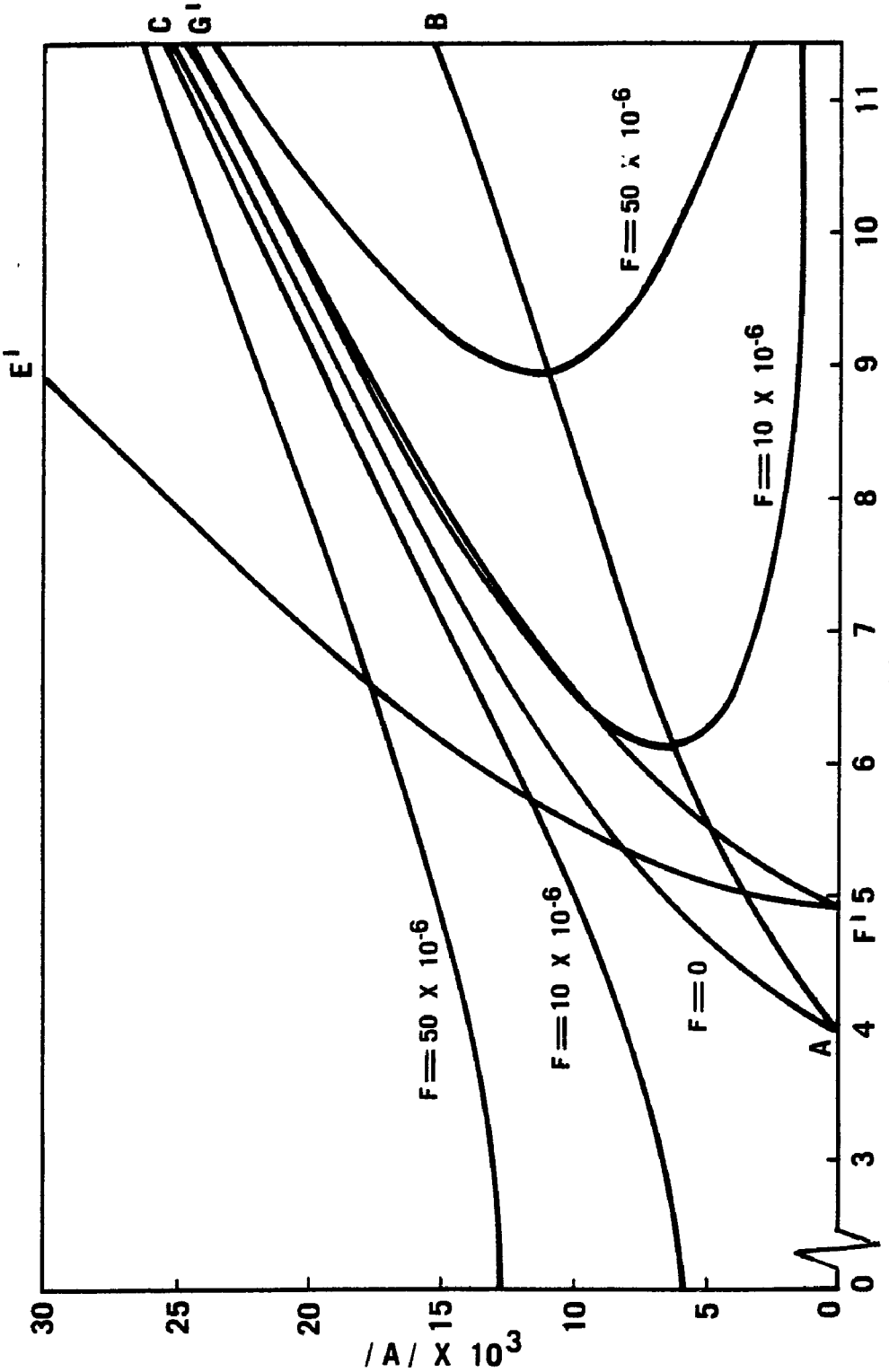


FIGURE 1.9 RESPONSE AND STABILITY REGIONS FOR PLANAR MOTION
$m = 1,\ n = 1,\ \alpha = .01,\ \beta = .02,\ \lambda = 2,\ \bar{c}_1 \neq 0$

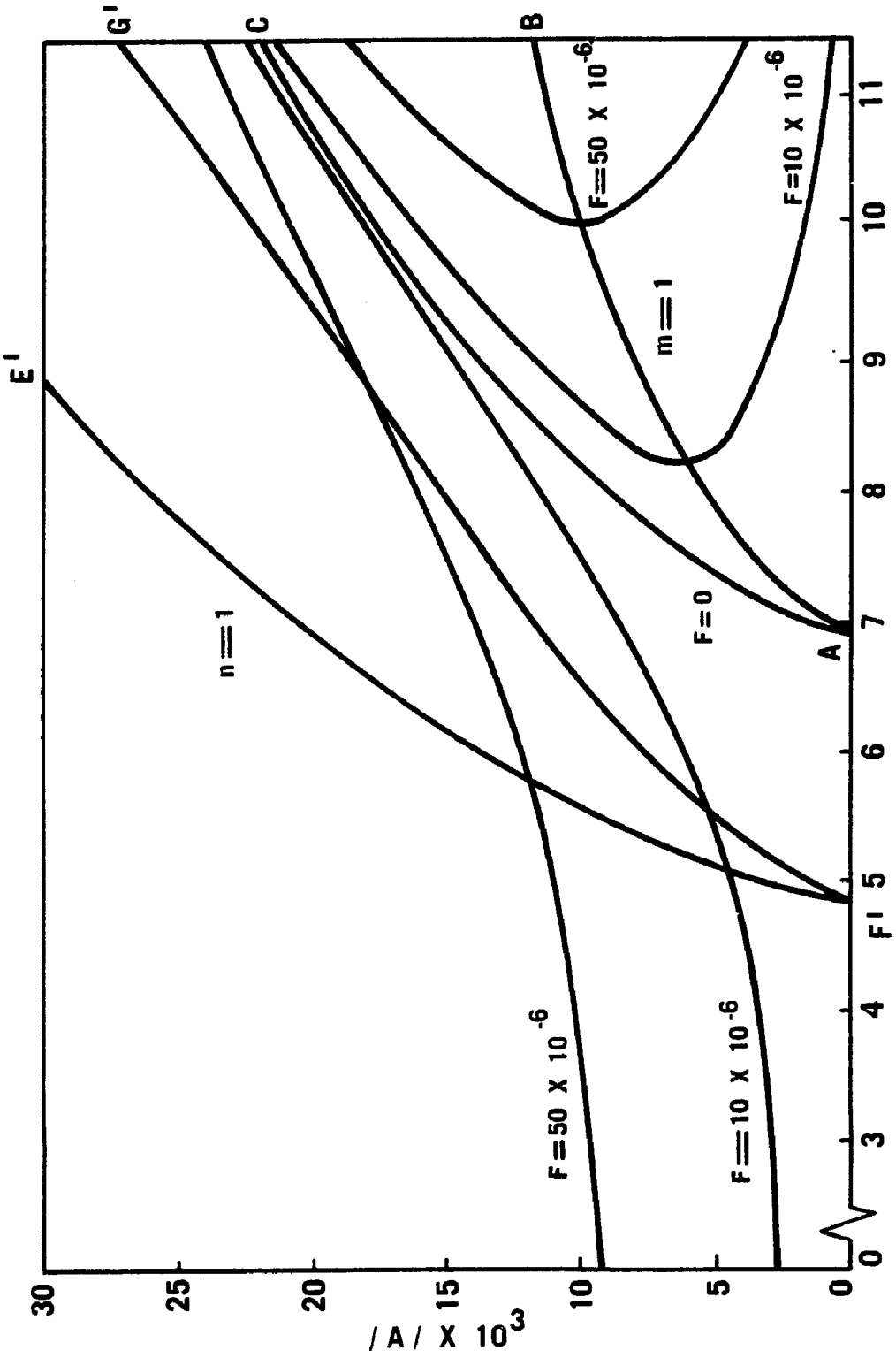


FIGURE 1.10 RESPONSE AND STABILITY REGIONS FOR PLANAR MOTION
m = 1, n = 1, $\alpha = .01$, $\beta = .02$, $\lambda = 4$, $\bar{c}_1 \neq 0$.

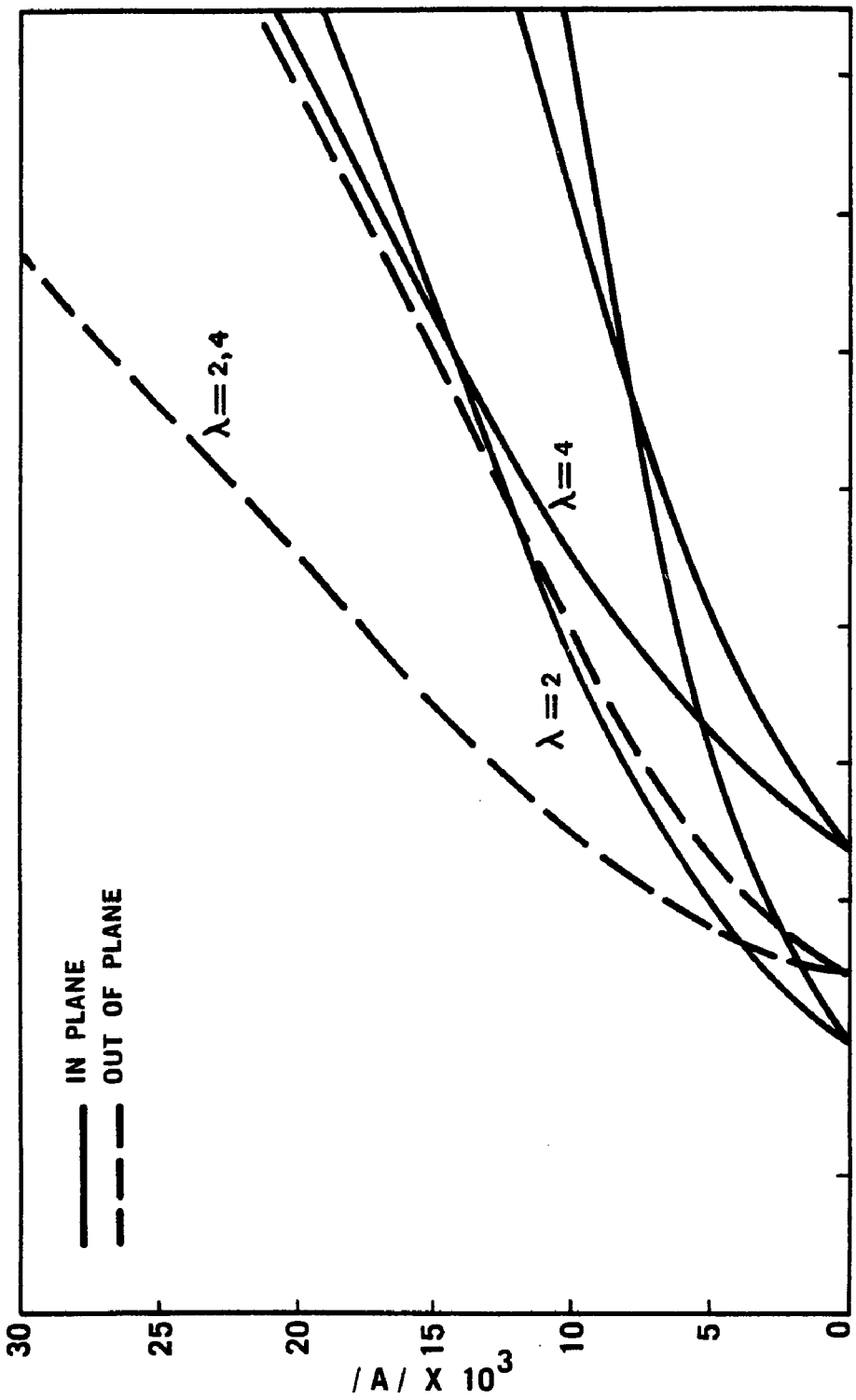


FIGURE 1-11 STABILITY REGIONS FOR PLANAR MOTION
$m = 1$, $n = 1$, $\alpha = .005$, $\beta = .01$ $\lambda = 2,4$, $\bar{c}_1 \neq 0$

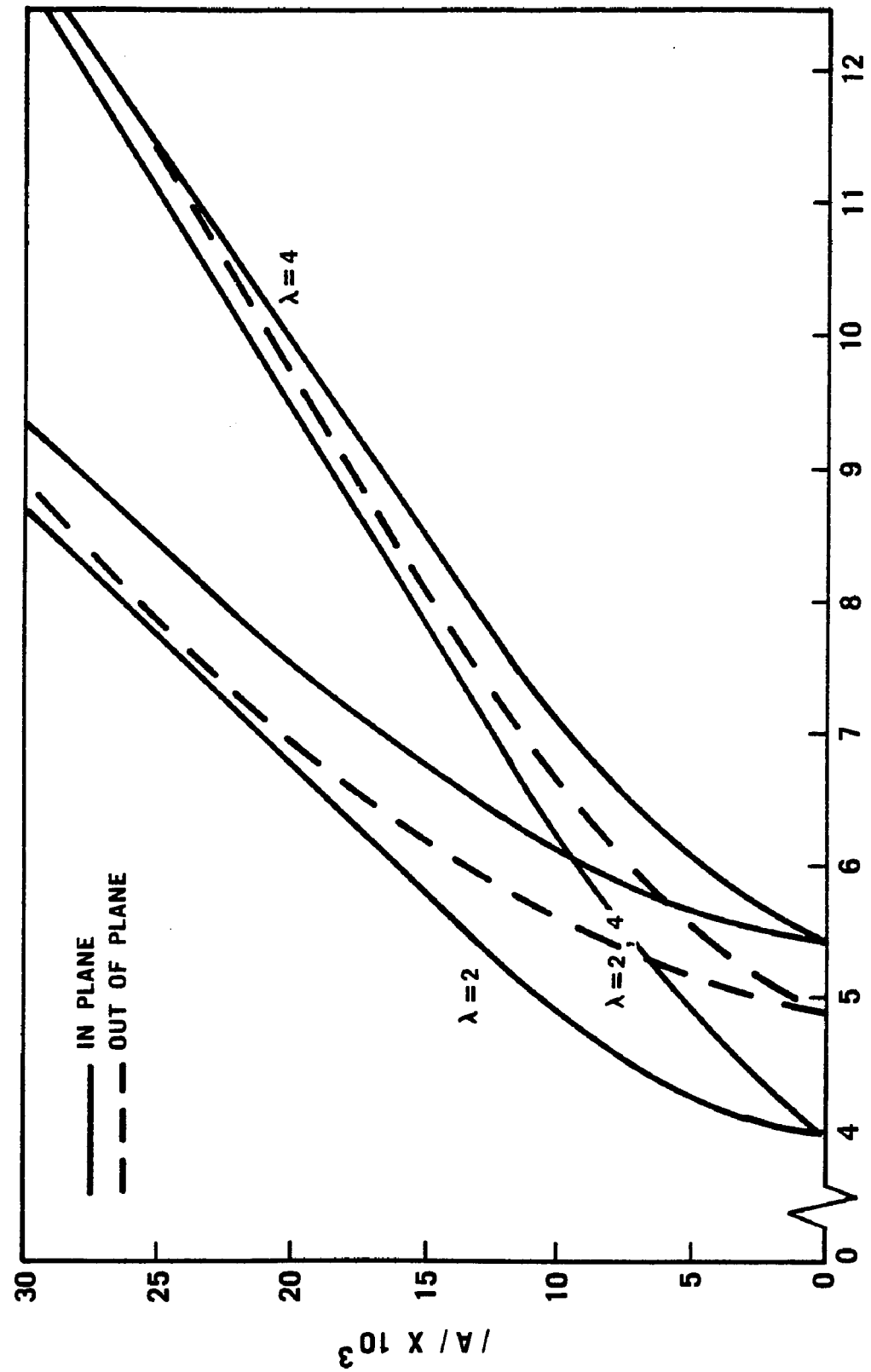


FIGURE 1.12 STABILITY REGIONS FOR PLANAR MOTION
m=1, n=1, α =.01, β =.02, λ =2,4, $\bar{c}_1 \neq 0$

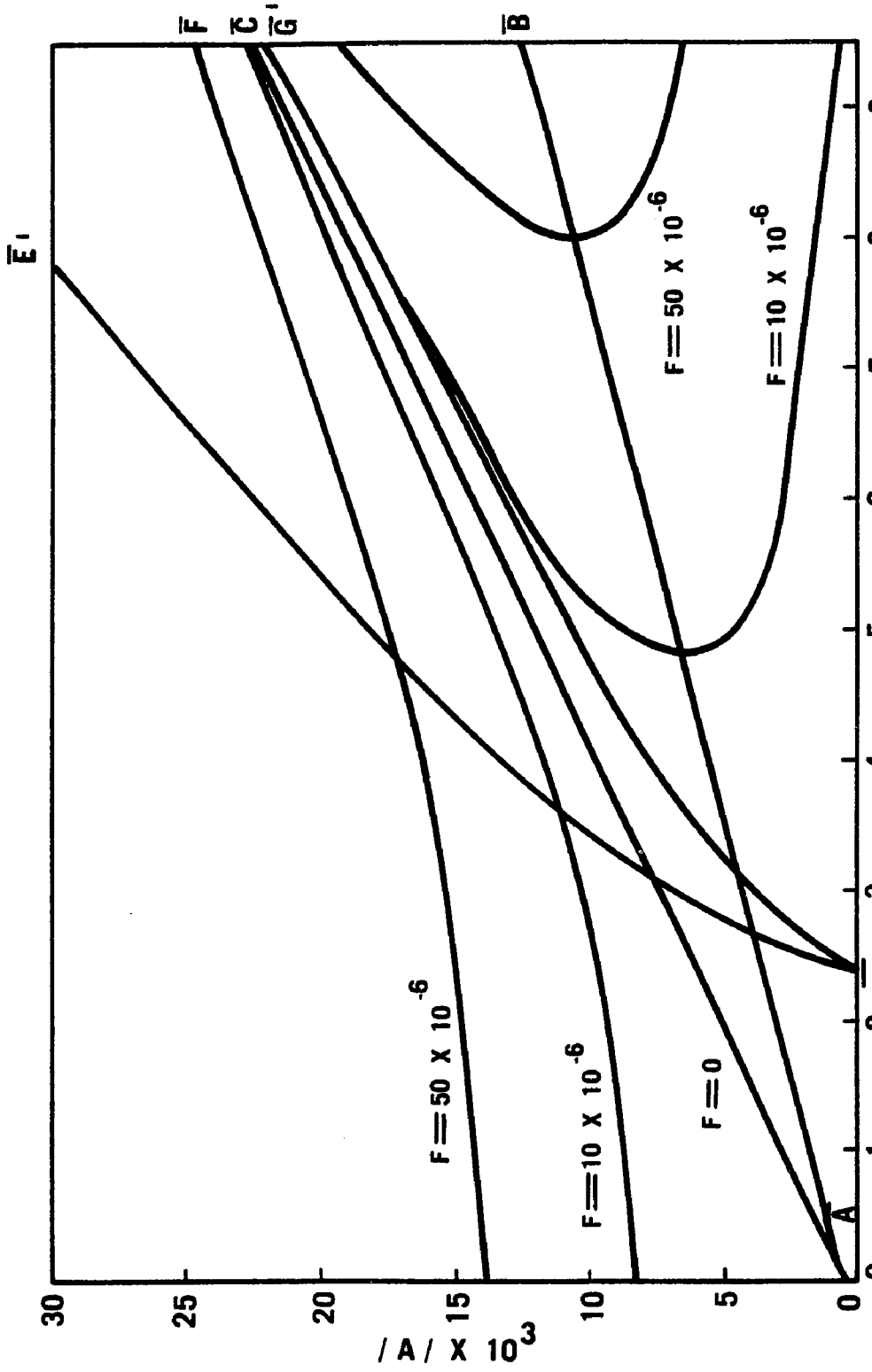


FIGURE 1.13 RESPONSE AND STABILITY REGIONS FOR PLANAR MOTION
$m = 1$, $n = 1$, $\alpha = .005$, $\beta = .01$, $\lambda = 1.1$, $\bar{c}_1 = 0$

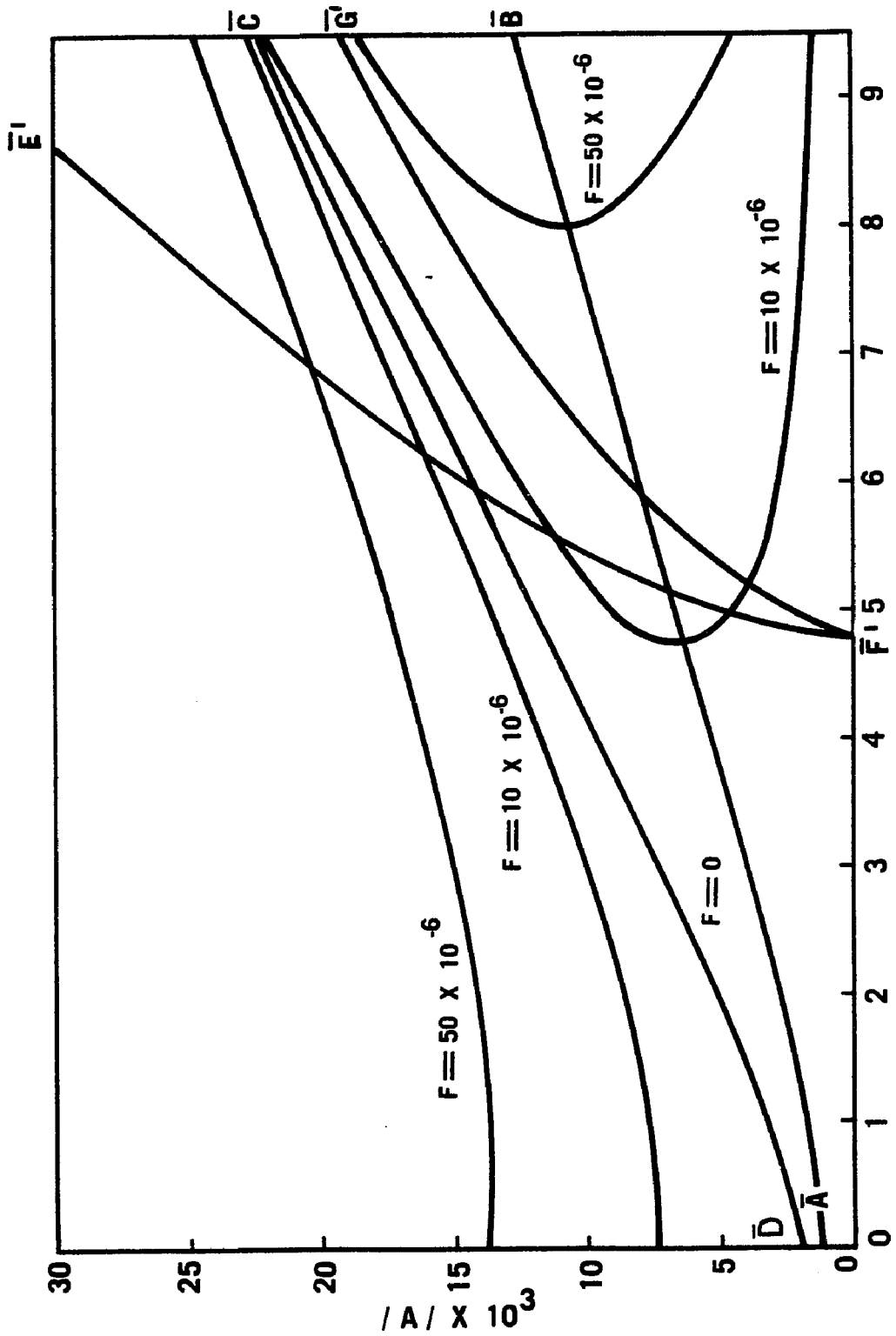


FIGURE 1.14 RESPONSE AND STABILITY REGIONS FOR PLANAR MOTION
$m=1$, $n=1$, $\alpha=.01$, $\beta=.02$, $\lambda=1.1$, $\bar{c}_1=0$

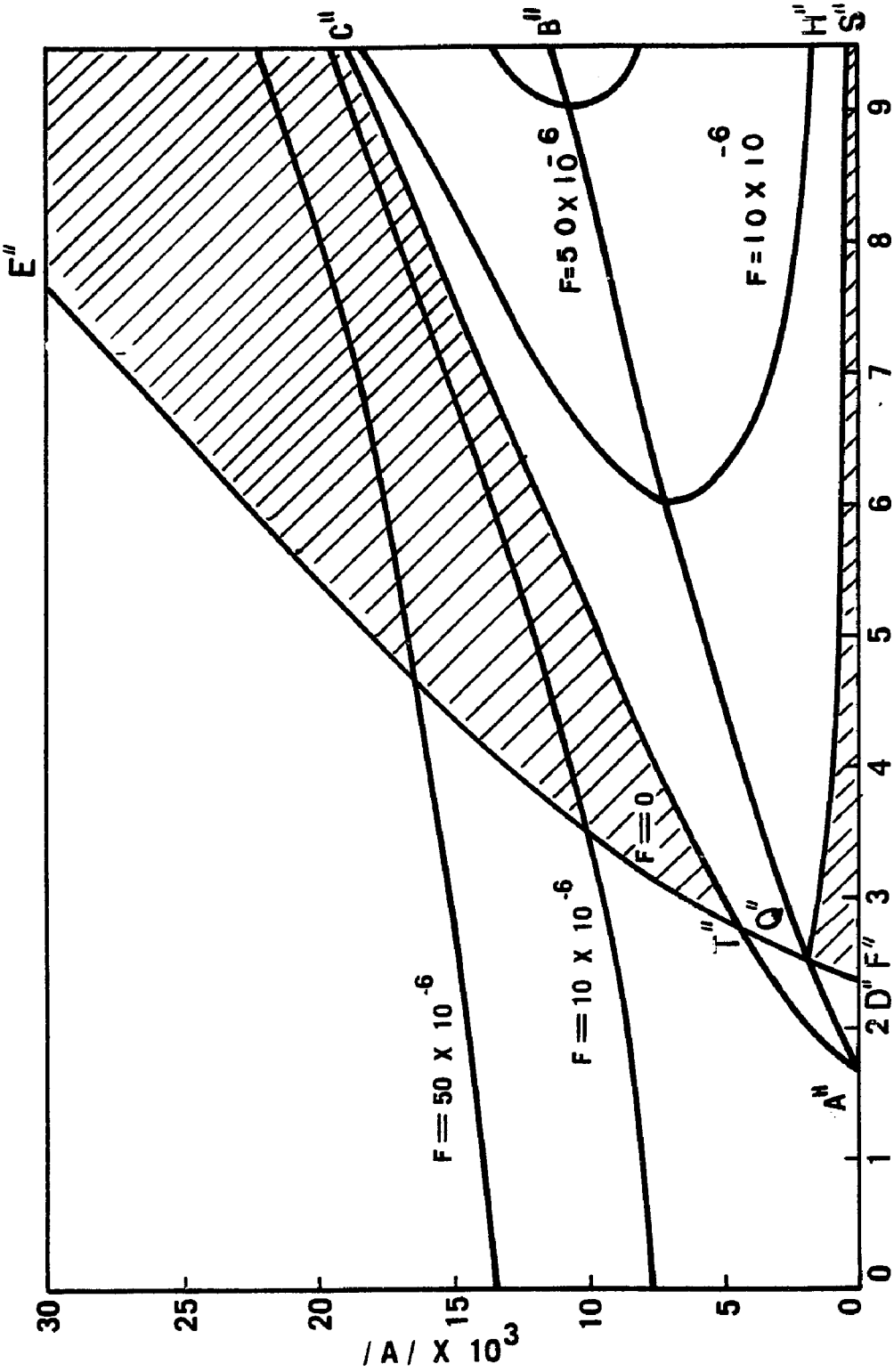


FIGURE 1.15 RESPONSE AND STABILITY REGIONS FOR NONPLANAR MOTION
$m = 1$, $n = 1$, $\alpha = .005$, $\beta = .01$, $\lambda = 2$, $\bar{c}_1 \neq 0$

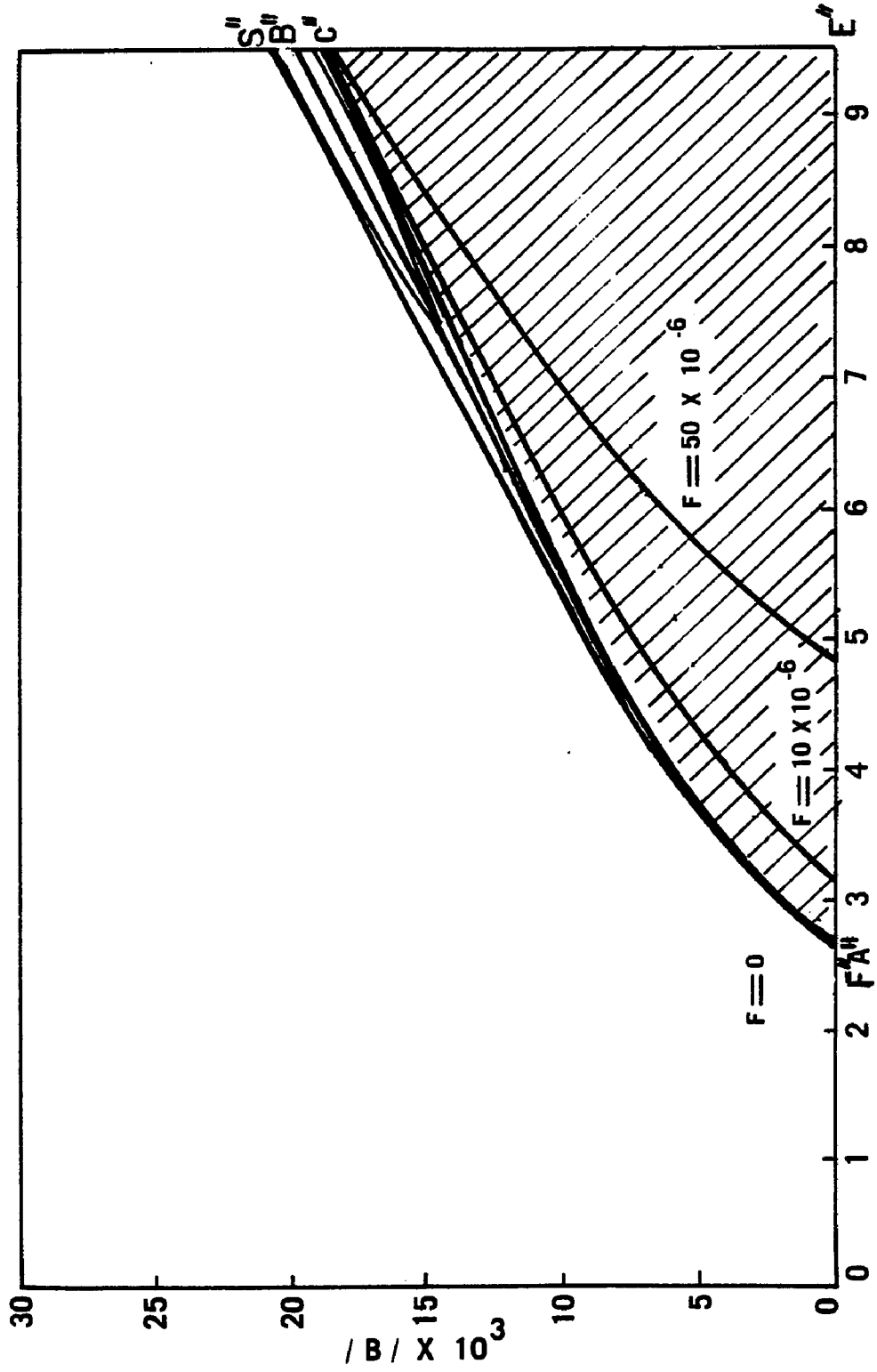


FIGURE 1.16 RESPONSE AND STABILITY REGIONS FOR NONPLANAR MOTION
$m = 1,\ n = 1,\ \alpha = .005, \beta = .01,\ \lambda = 2,\ \bar{c}_1 \neq 0$

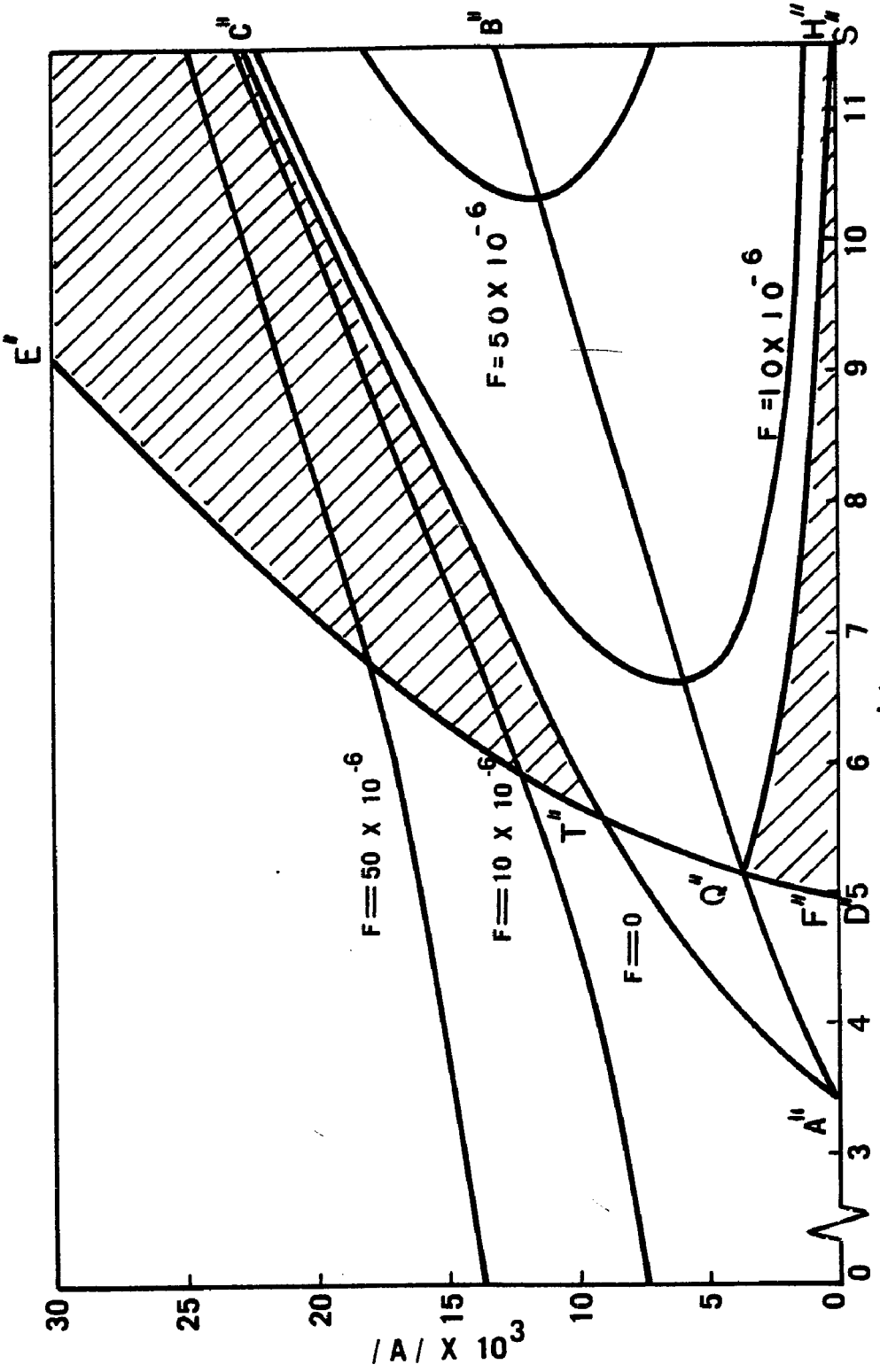


FIGURE 1.17 RESPONSE AND STABILITY REGIONS FOR NONPLANAR MOTION
$m = 1$, $n = 1$, $\alpha = .01$, $\beta = .02$, $\lambda = 2$, $\bar{c}_1 \neq 0$

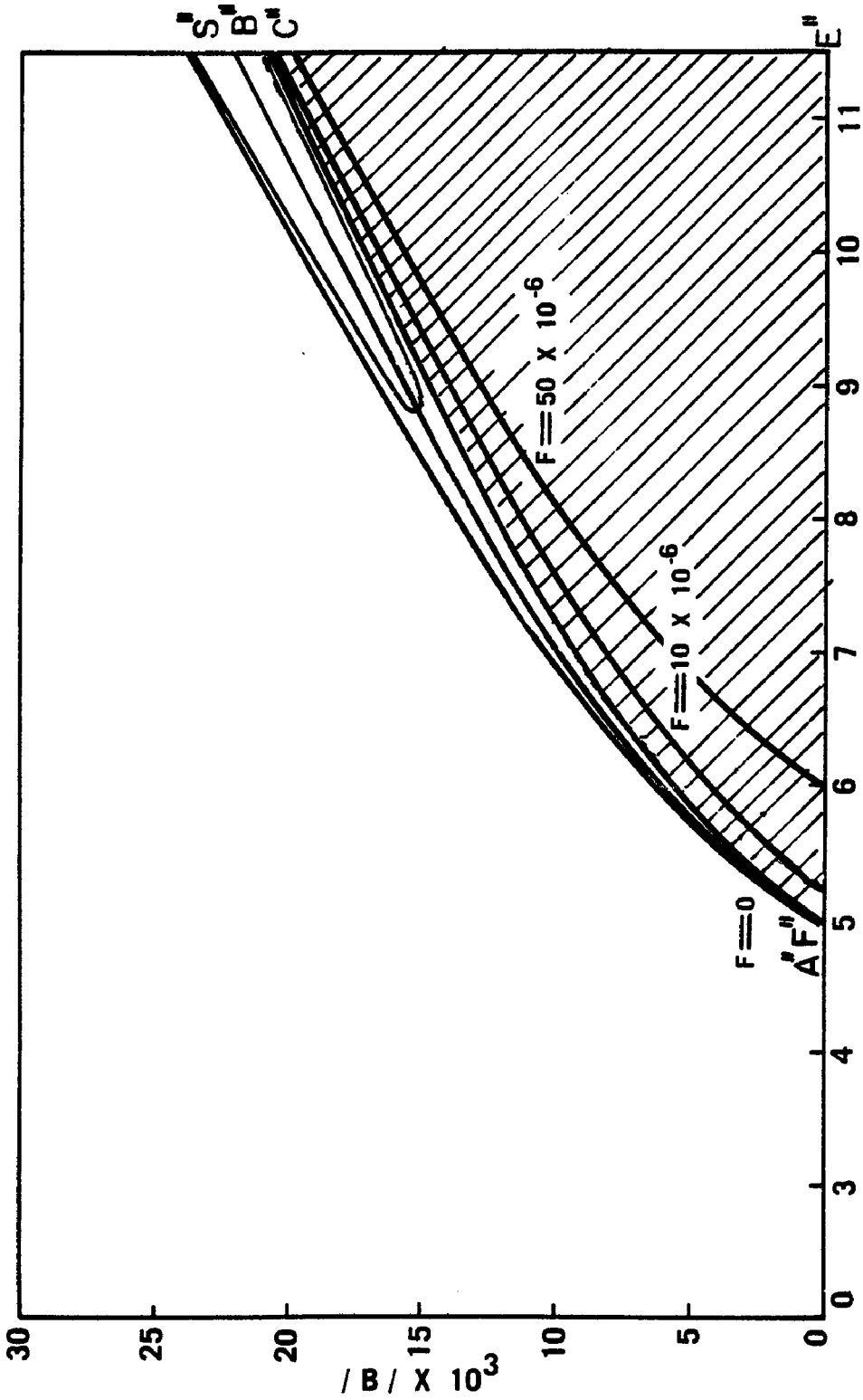


FIGURE 1.18 RESPONSE AND STABILITY REGIONS FOR NONPLANAR MOTION
m=1, n=1, α=.01, β=.02, λ=2, $\bar{c}_1 \neq 0$

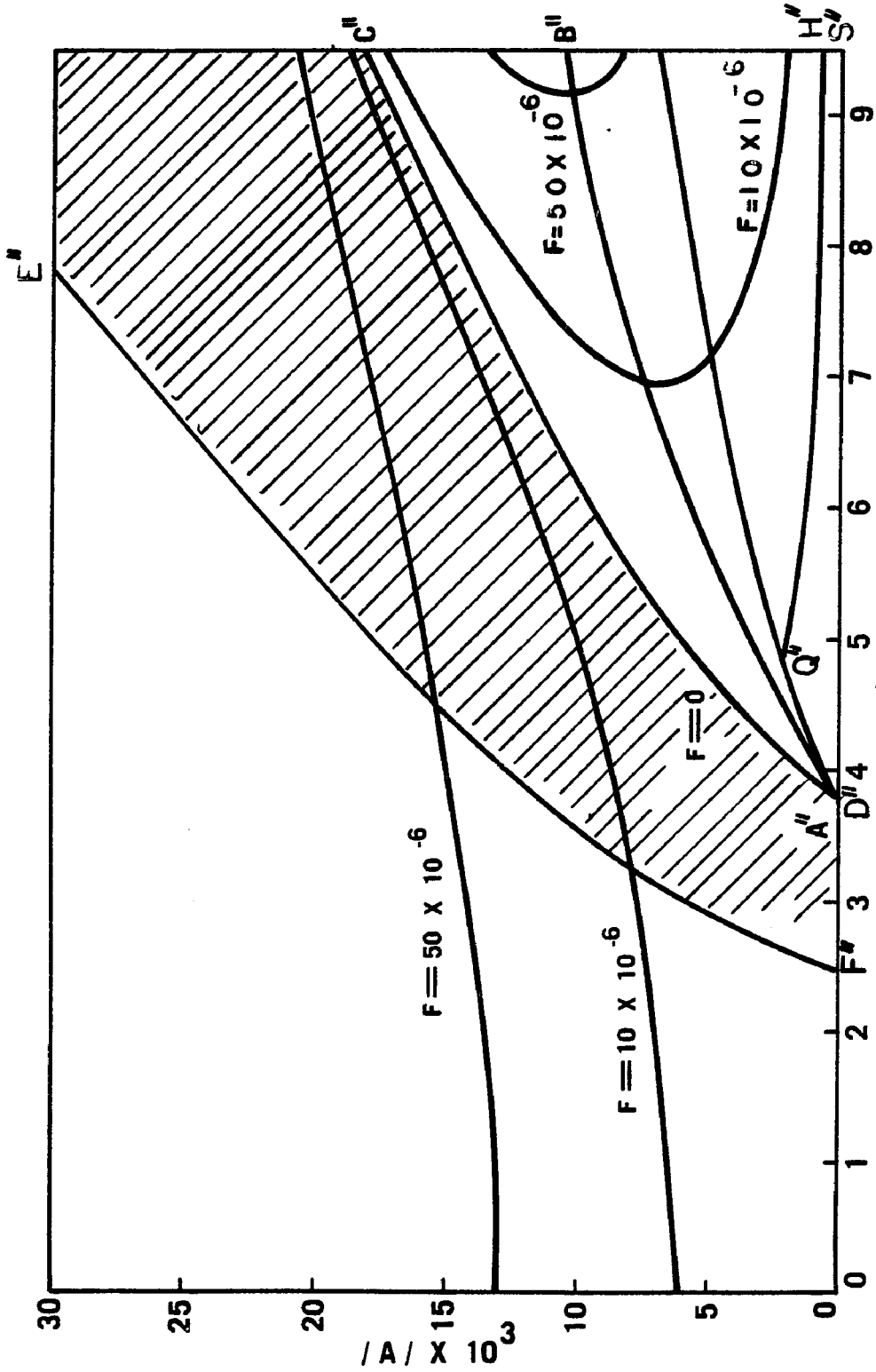


FIGURE 1.19 RESPONSE AND STABILITY REGIONS FOR NONPLANAR MOTION
$m = 1,\ n = 1,\ \alpha = .005, \beta = .01,\ \lambda = 4,\ \bar{c}_1 \neq 0$

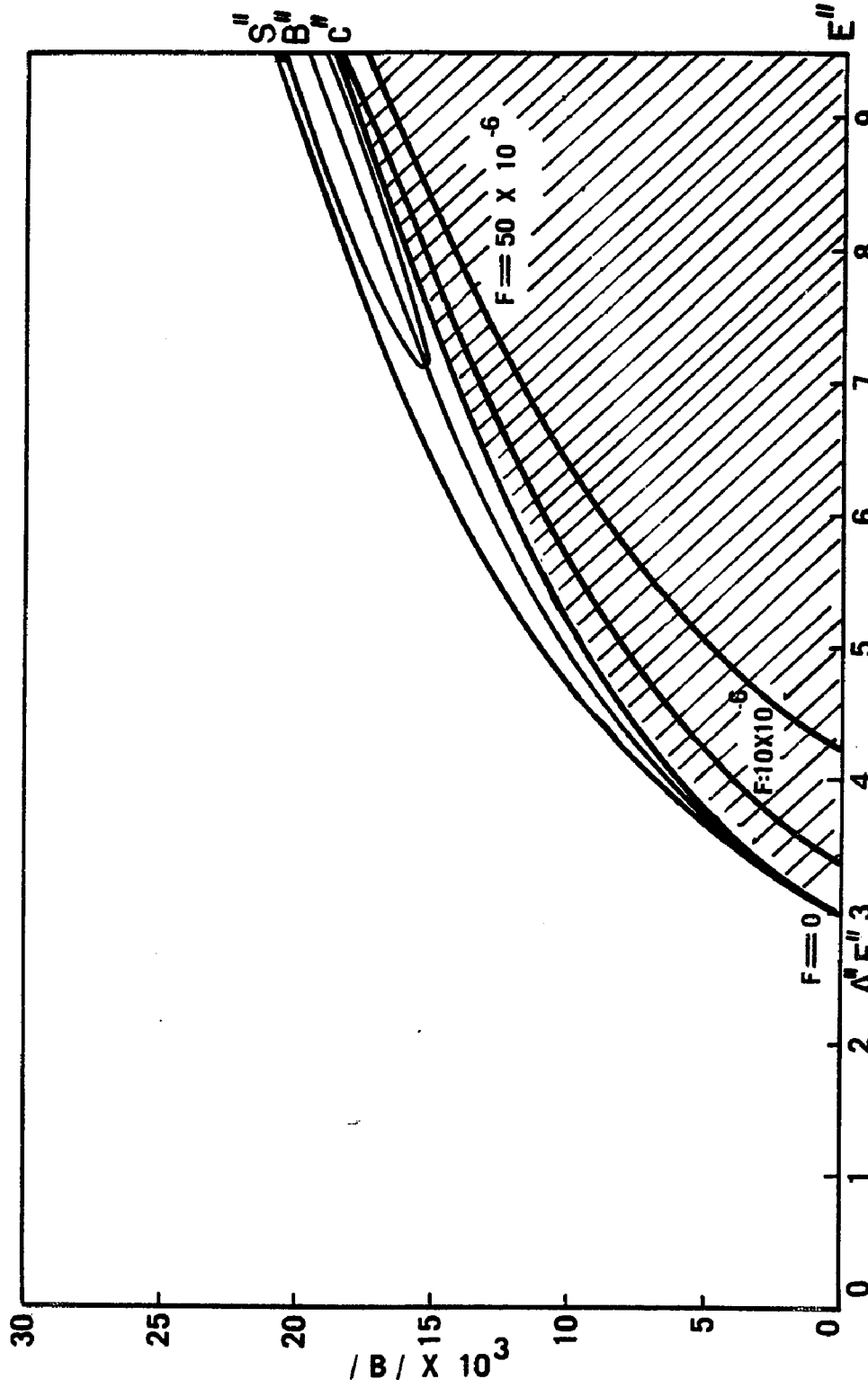


FIGURE 1.20 RESPONSE AND STABILITY REGIONS FOR NONPLANAR MOTION
$m = 1$, $n = 1$, $\alpha = .005$, $\beta = .01$, $\lambda = 4$, $\bar{c}_1 \neq 0$

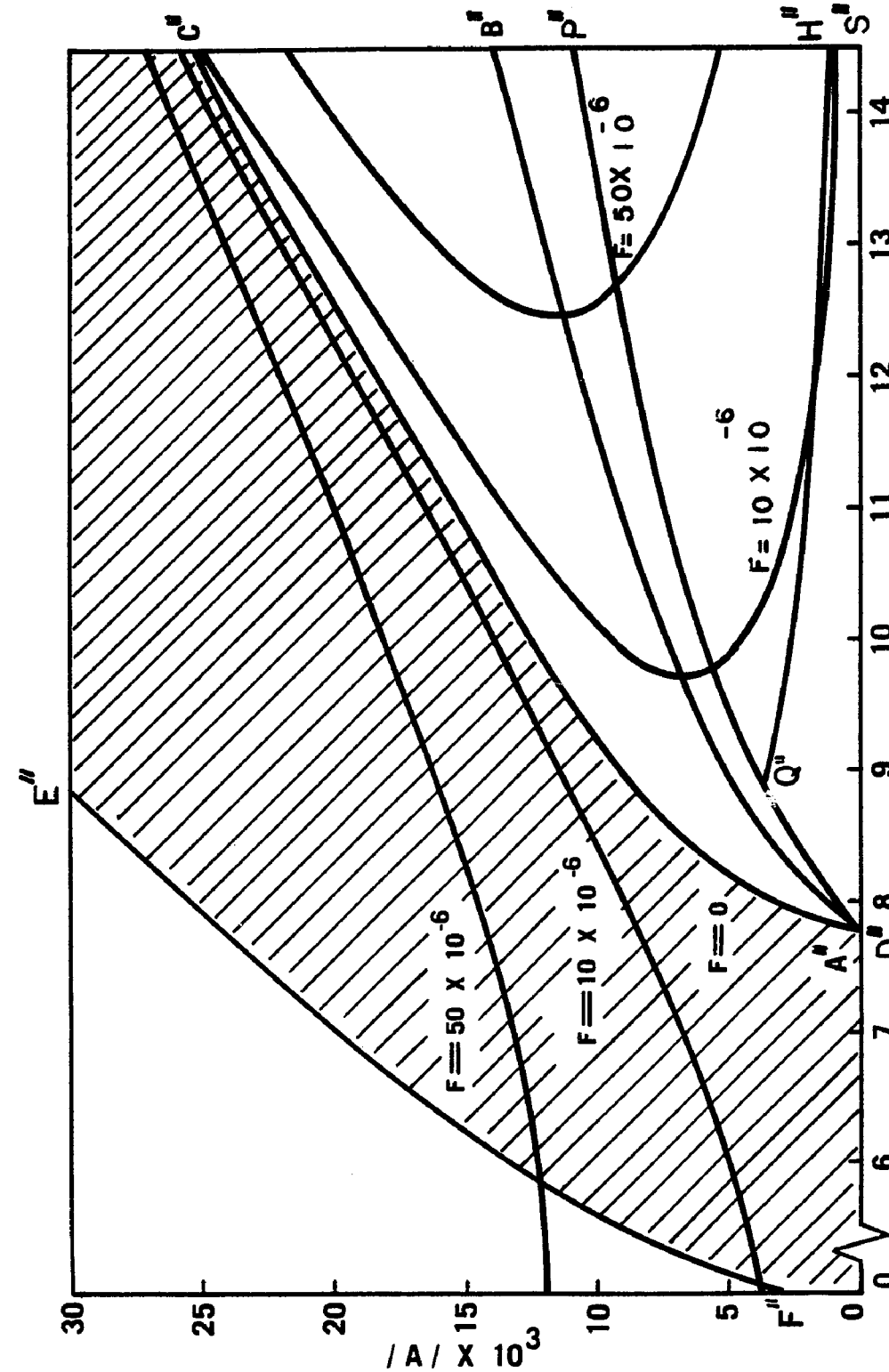


FIGURE 1.21 RESPONSE AND STABILITY REGIONS FOR NONPLANAR MOTION
m=1, n=1, α=.01, β=.02, λ=4, $\bar{c}_1 \neq 0$

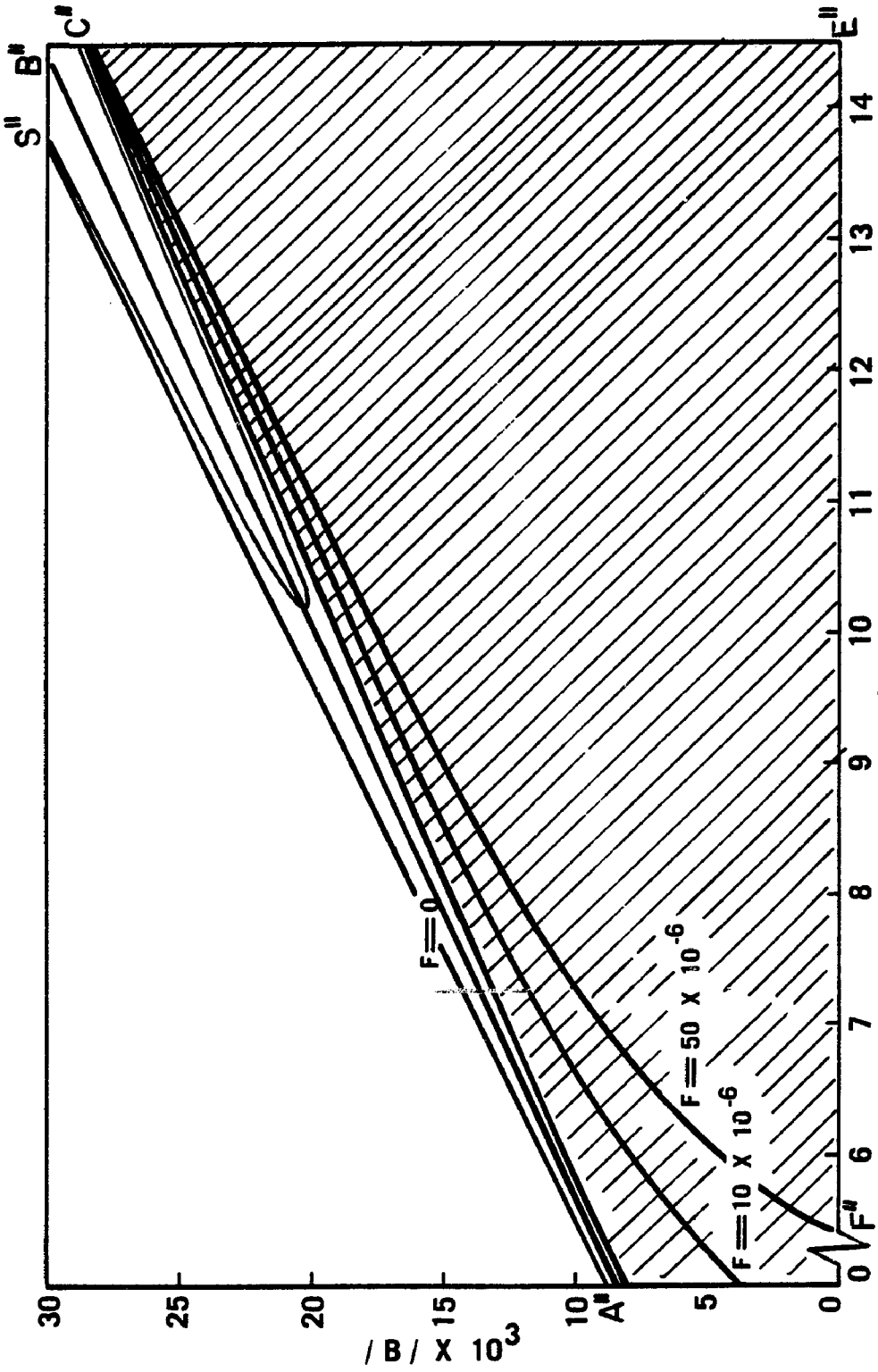


FIGURE 1.2.2 RESPONSE AND STABILITY REGIONS FOR NONPLANAR MOTION
$m=1$, $n=1$, $\alpha=.01$, $\beta=.02$, $\lambda=4$, $\bar{c}_1 \neq 0$

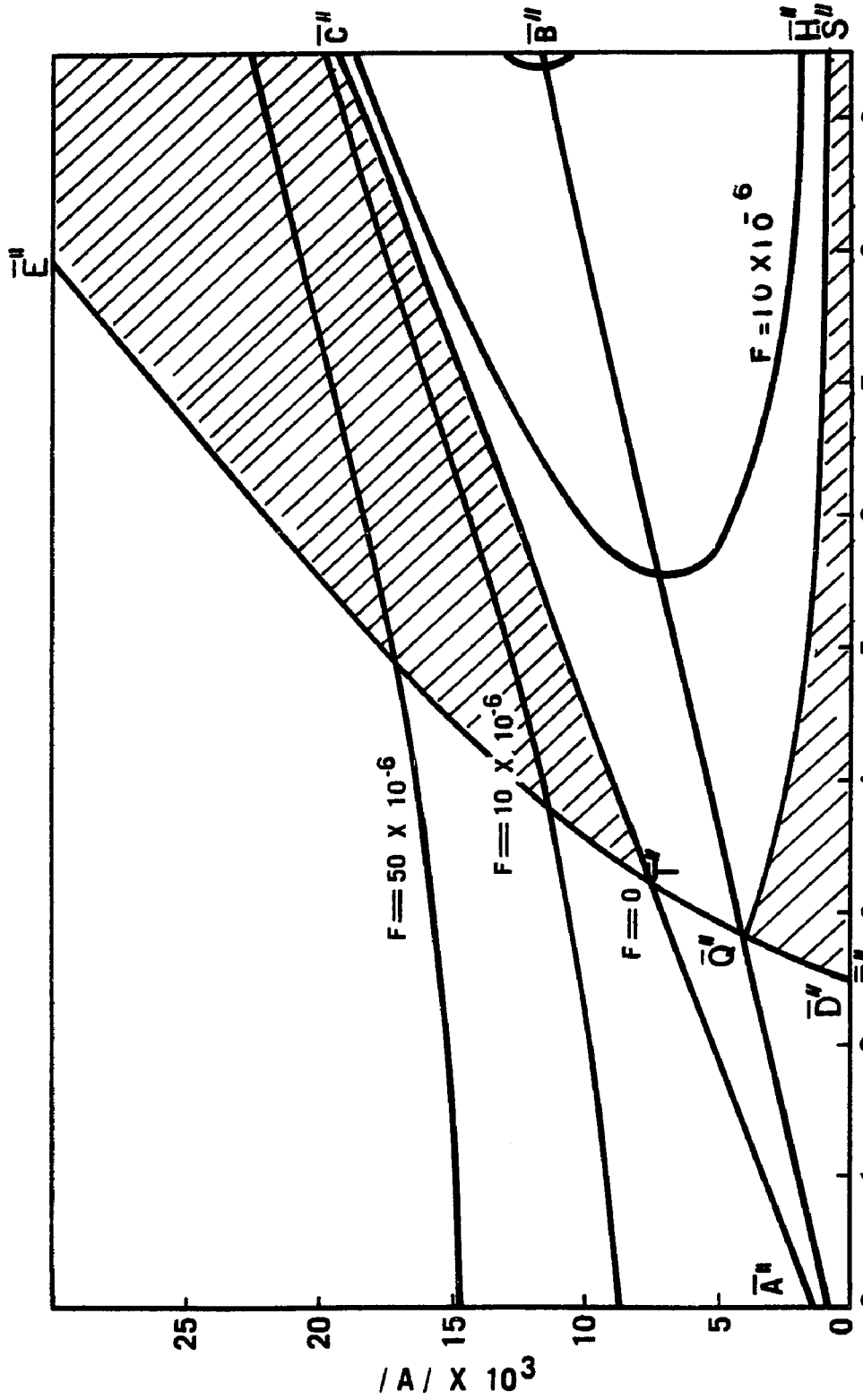


FIGURE 1.23 RESPONSE AND STABILITY REGIONS FOR NONPLANAR MOTION
m = 1, n = 1, α = .005, β = .01, λ = 1.1, $\bar{c}_1$ = 0

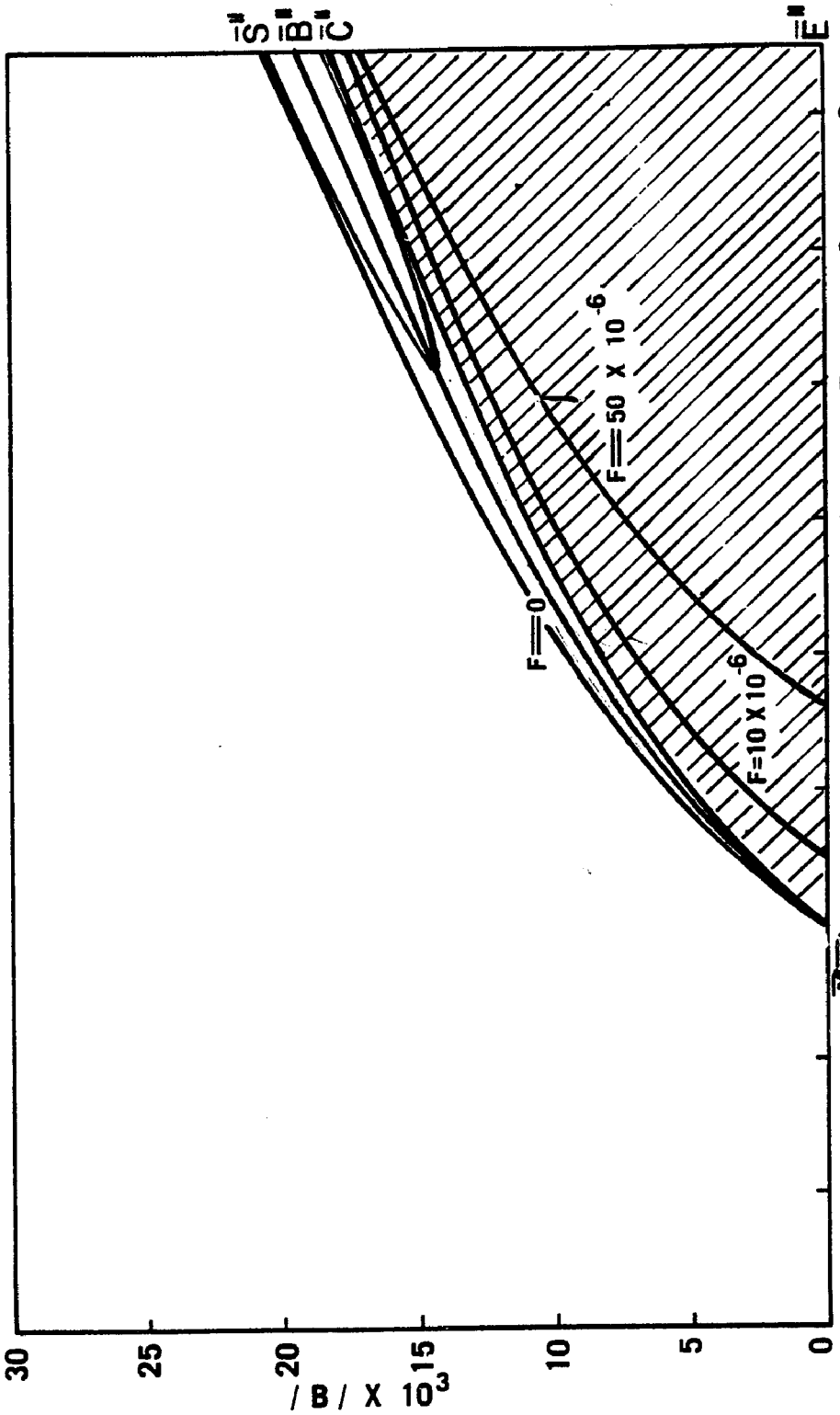


FIGURE 1.24 RESPONSE AND STABILITY REGIONS FOR NONPLANAR MOTION
m = 1, n = 1, α = .005, β = .01, λ = 1.1, $\bar{c}_1$ = 0

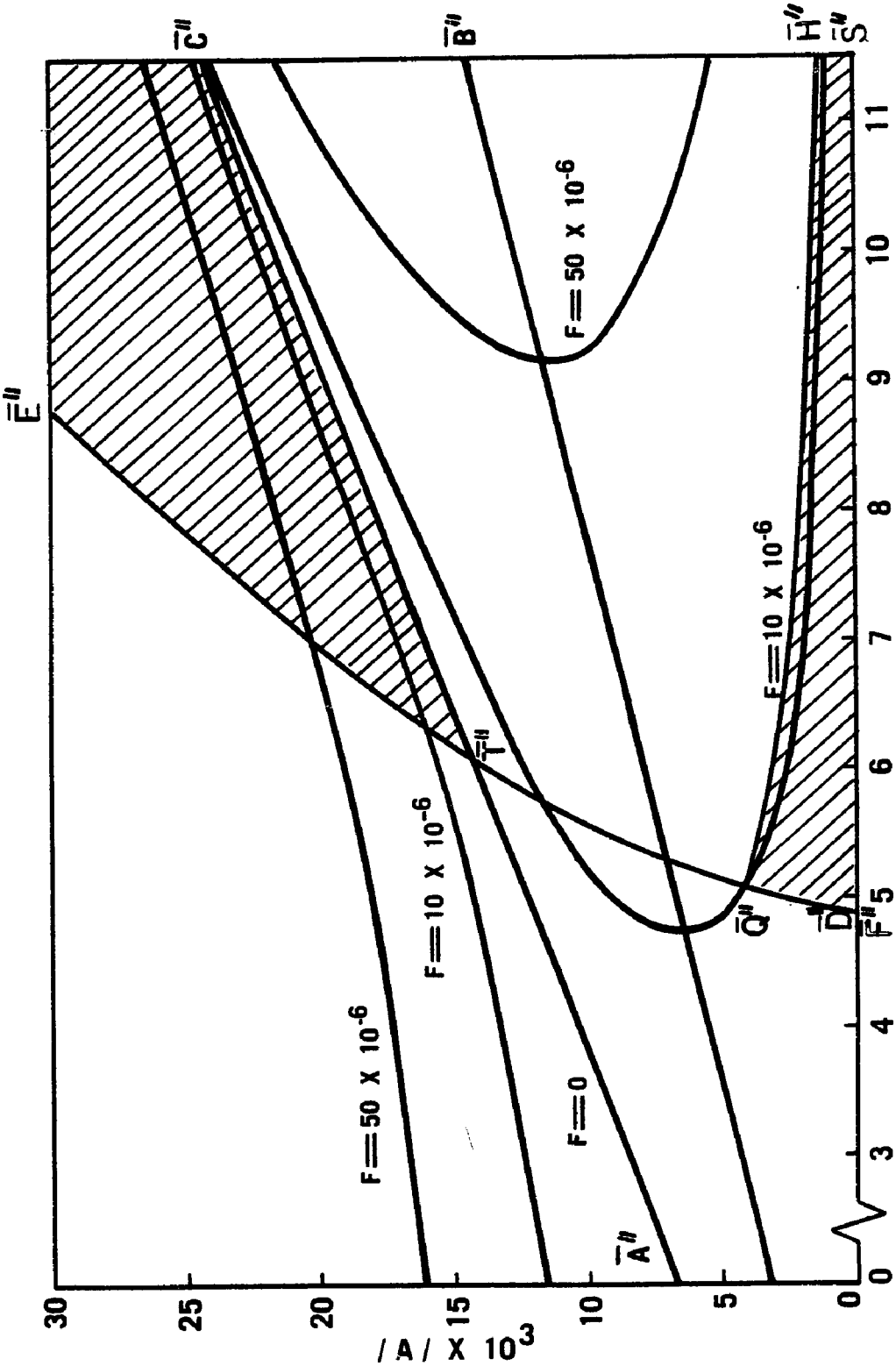


FIGURE 1.25 RESPONSE AND STABILITY REGIONS FOR NONPLANAR MOTION
$m = 1$, $n = 1$, $\alpha = .01$, $\beta = .02$, $\lambda = 1.1$, $\bar{c}_1 = 0$

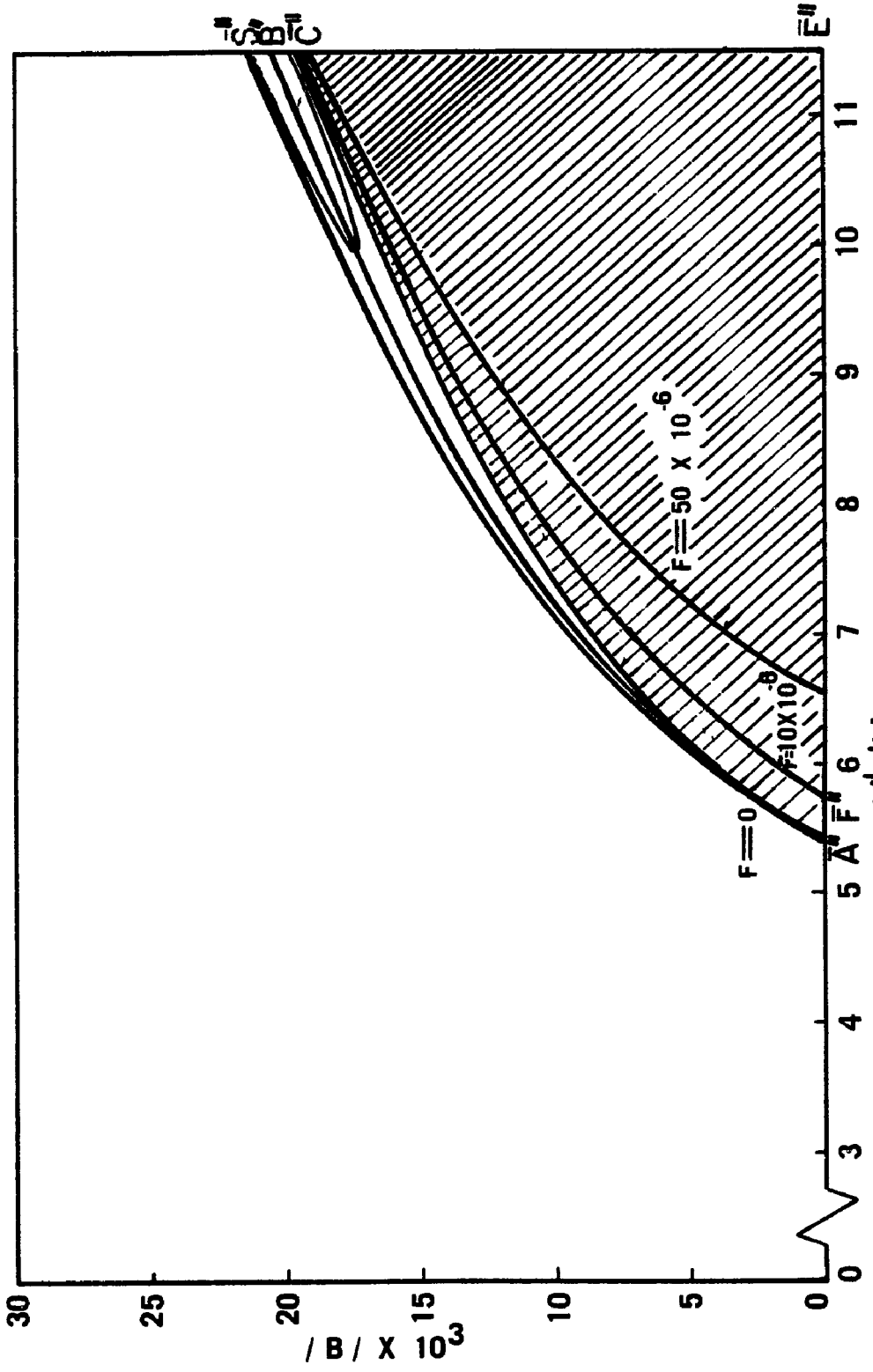


FIGURE 1.26 RESPONSE AND STABILITY REGIONS FOR NONPLANAR MOTION
m = 1, n = 1, α = .01 , β = .02, λ = 1.1, $\bar{c}_1$ = 0

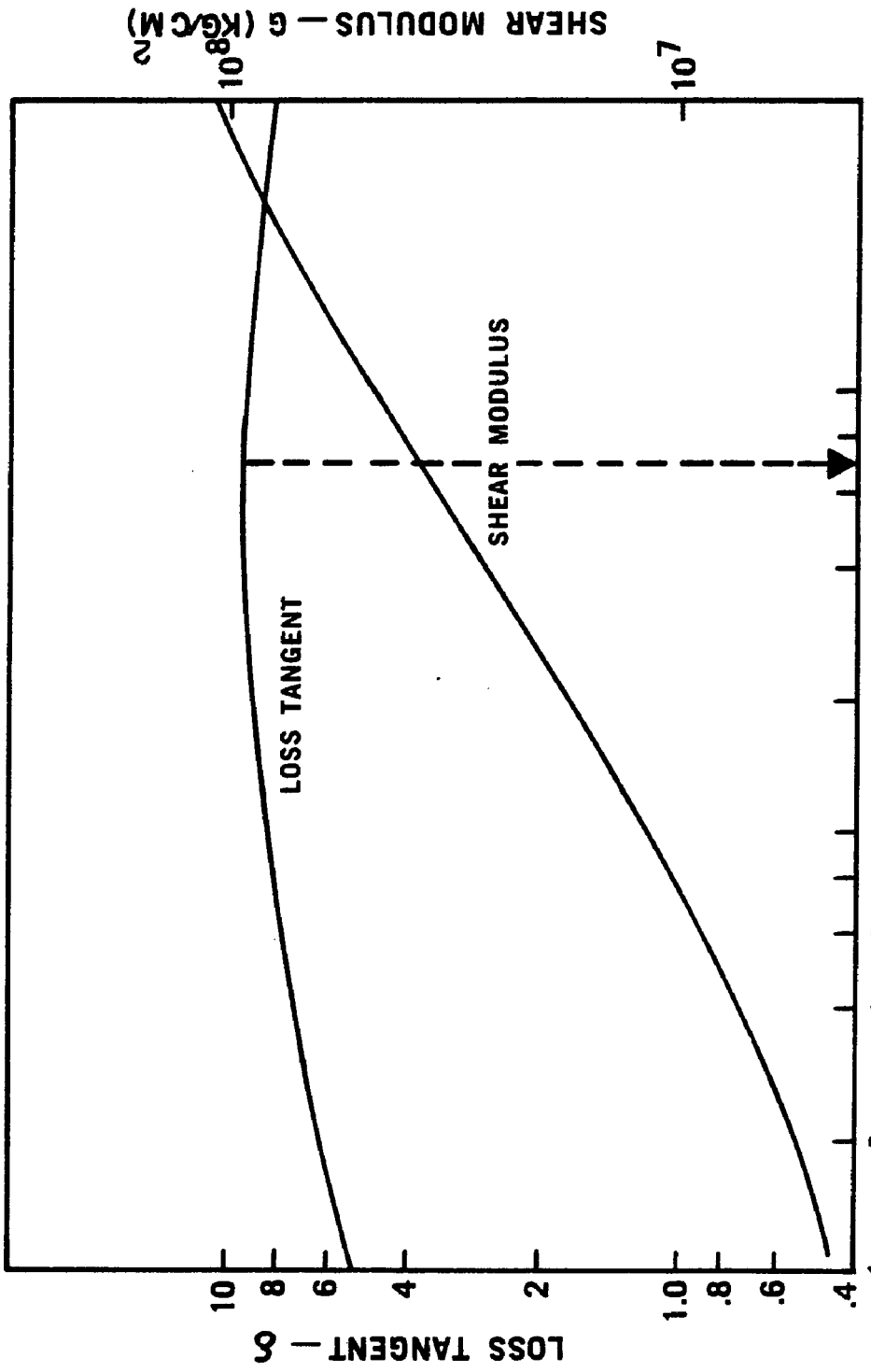


FIGURE 2.3. DYNAMIC MECHANICAL PROPERTIES OF ISPD III.

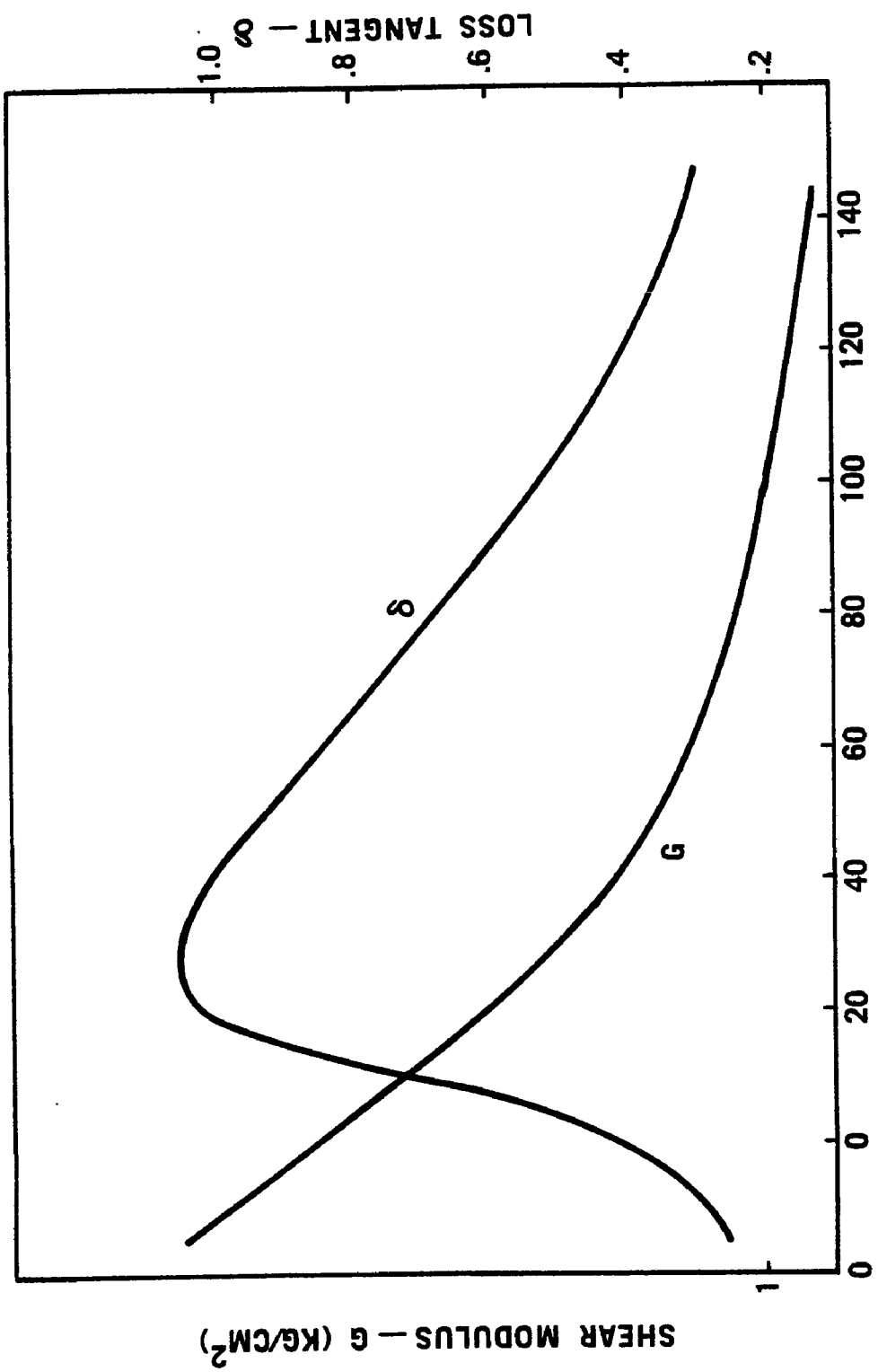


FIGURE 2.4. SHEAR MODULUS AND LOSS TANGENT-TEMPERATURE OF ISPD111@100 HZ.

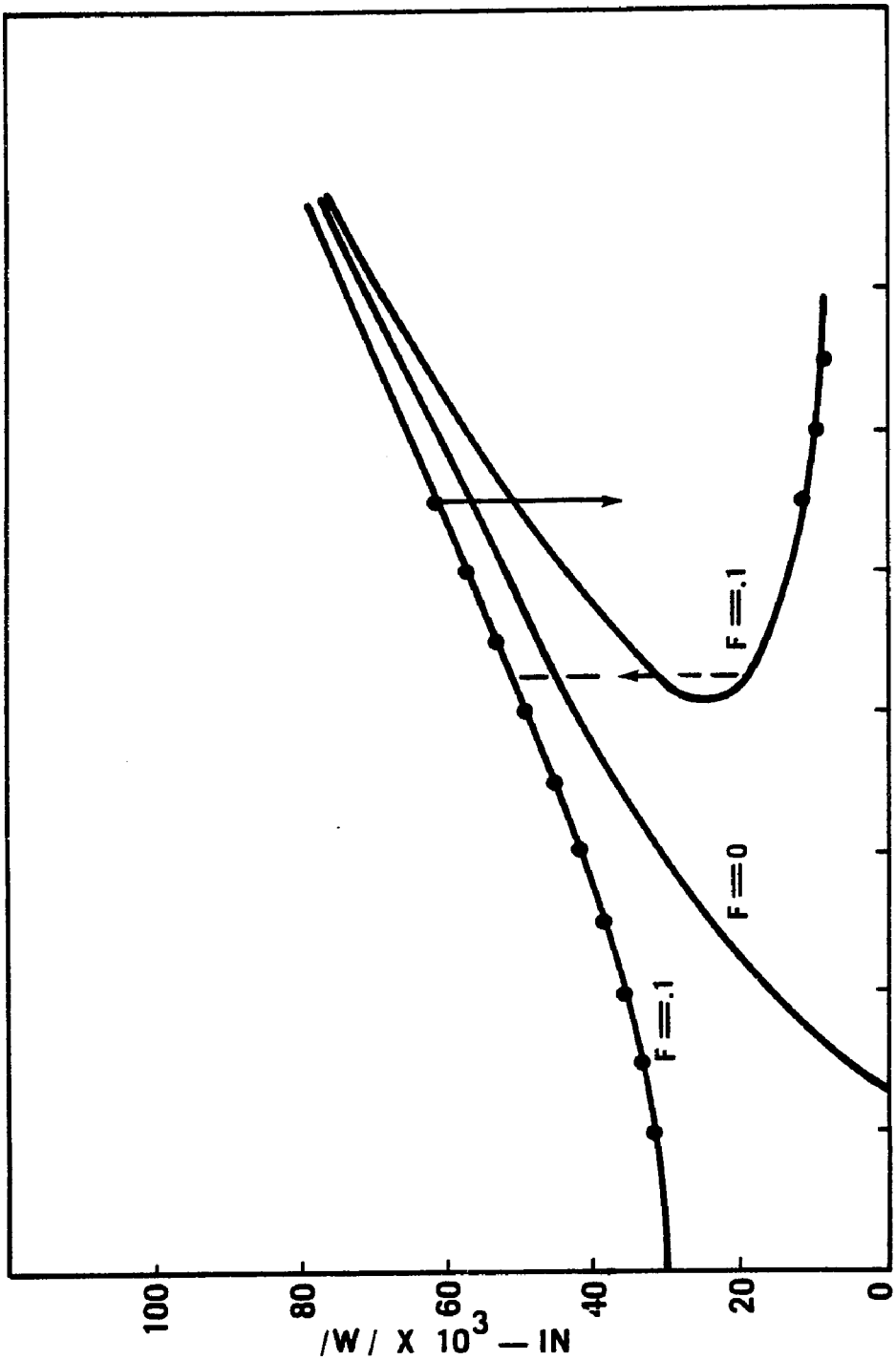


FIGURE 2.5 UNDAMPED RESPONSE. h = .018", b = 1", L = 12".

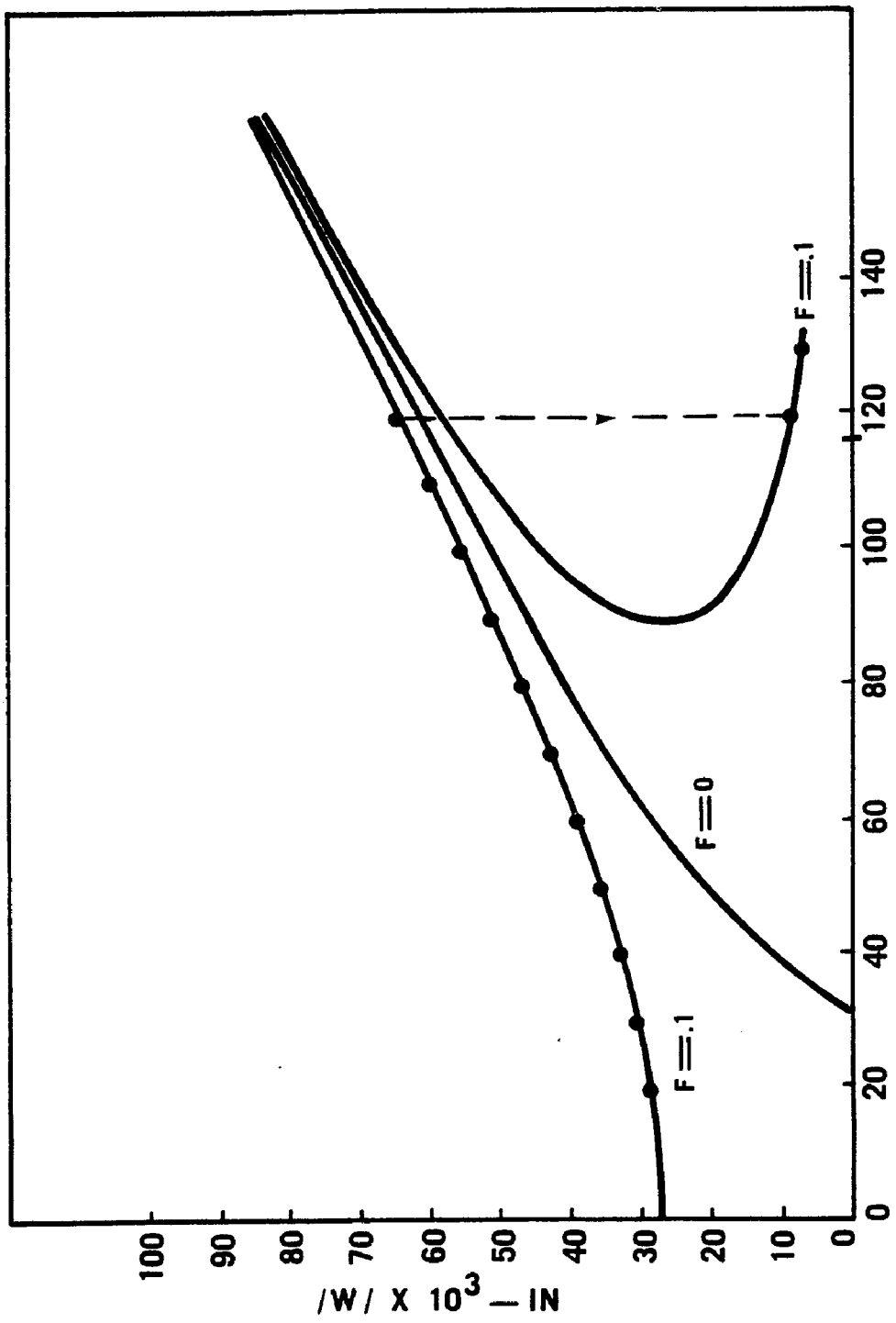


FIGURE 2.6 UNDAMPED RESPONSE. h = 0.22", b = 1", L = 12".

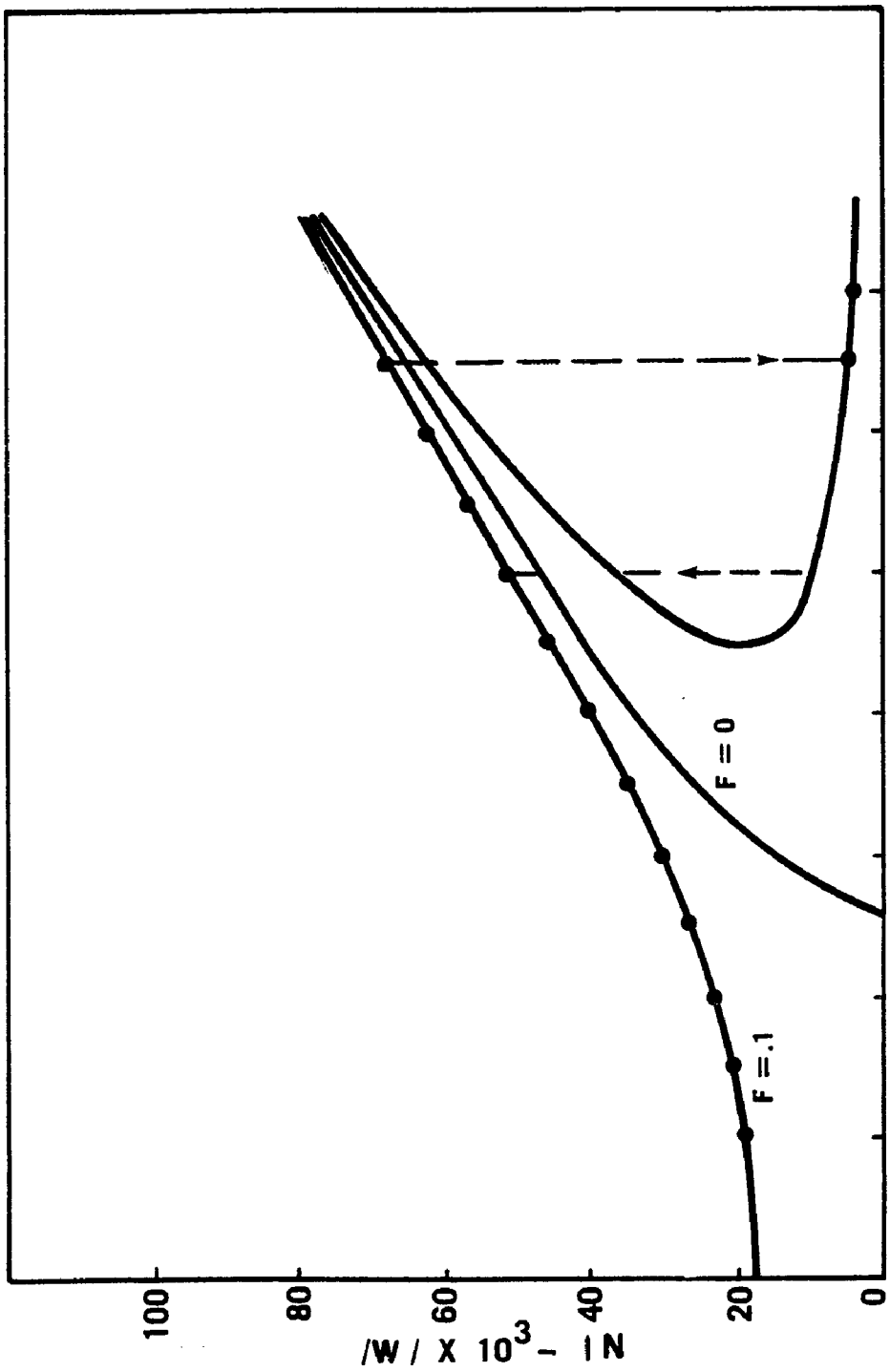


FIGURE 2.7 UNDAMPED RESPONSE. h=.035", b=1", L=12".

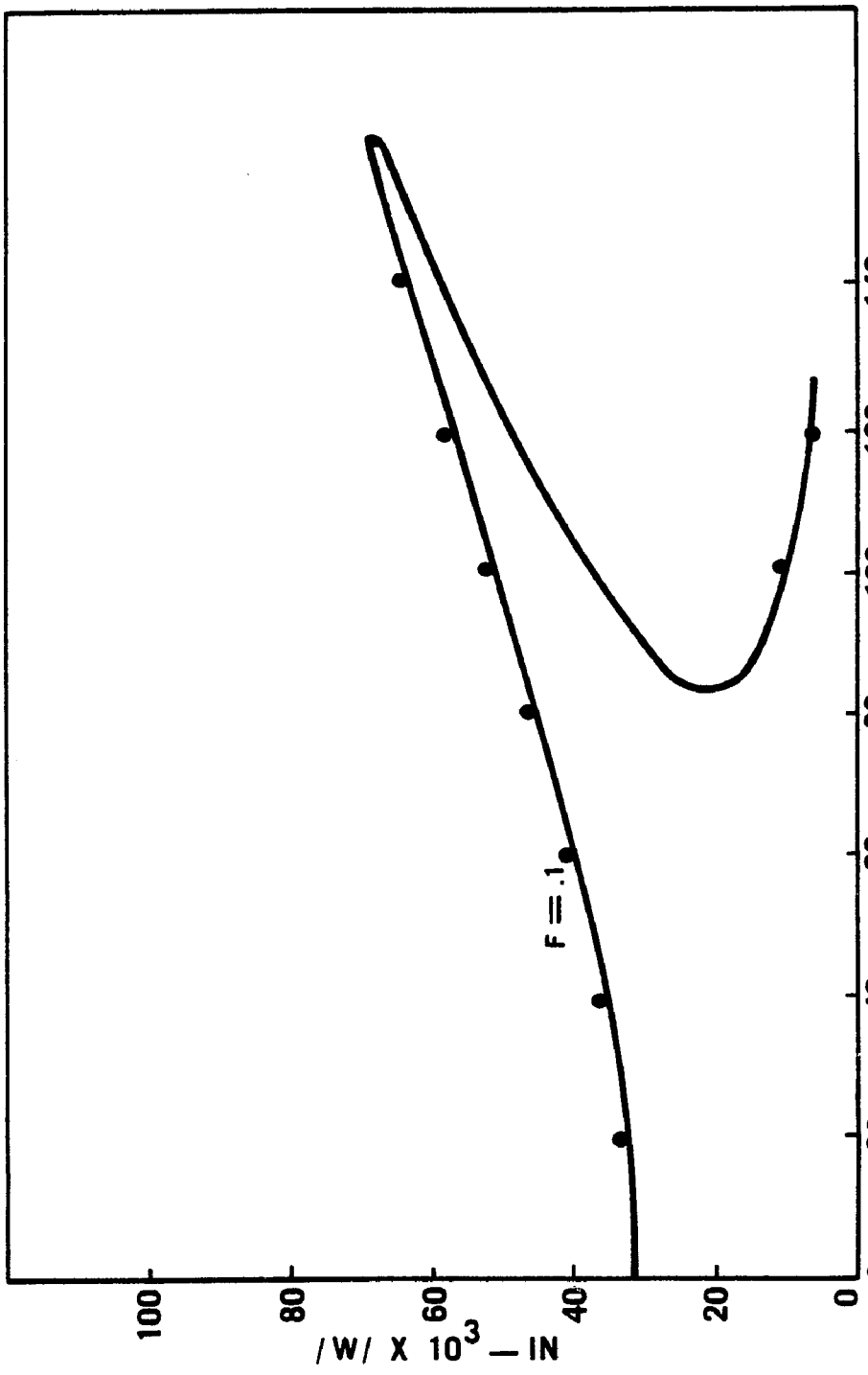


FIGURE 2.8 DAMPED RESPONSE. h = .018", b = 1", L = 12", t = .008" LAYER

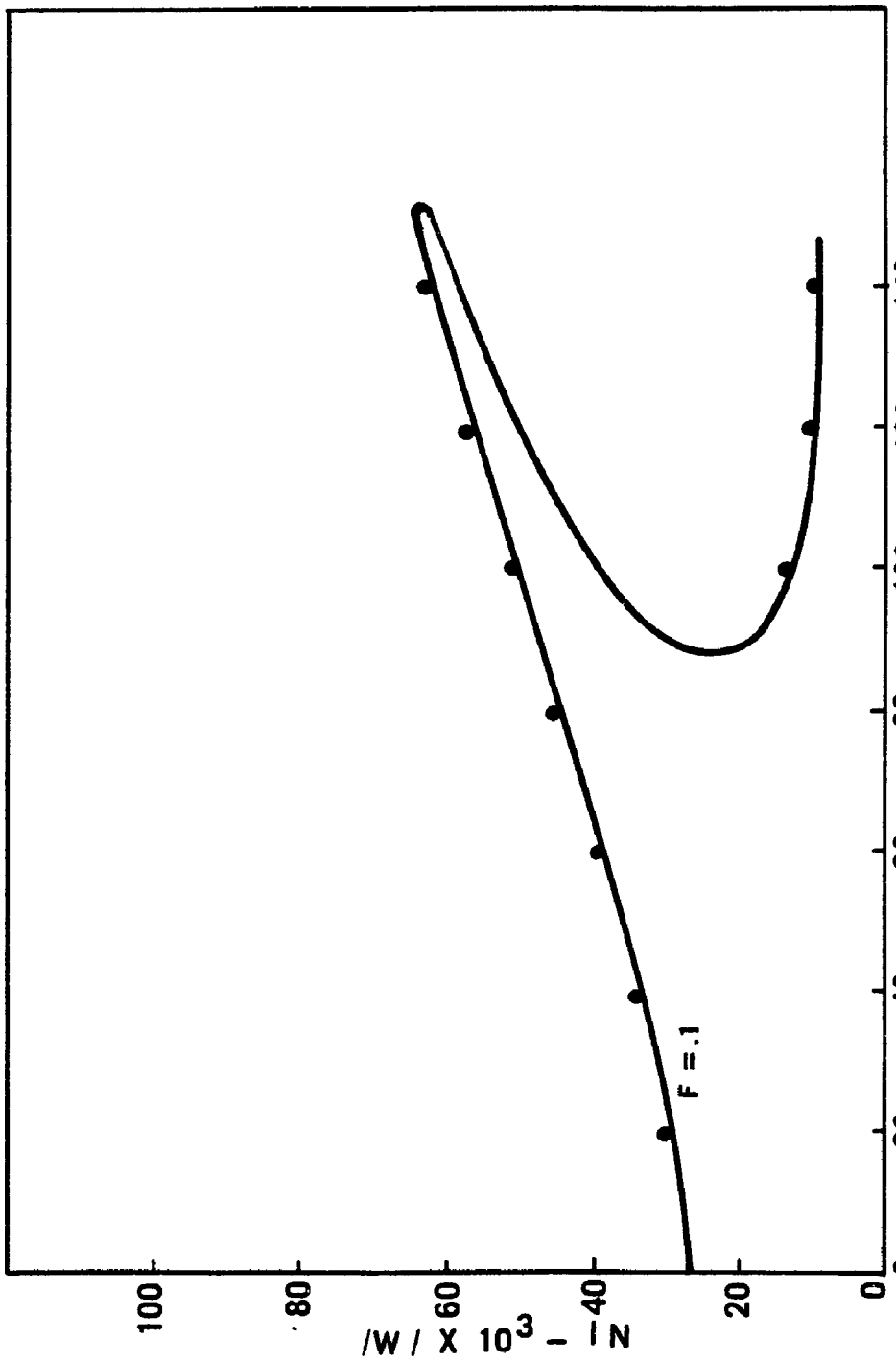


FIGURE 2.9 DAMPED RESPONSE, = .022", b = 1", L = 12", t = .008" LAYER

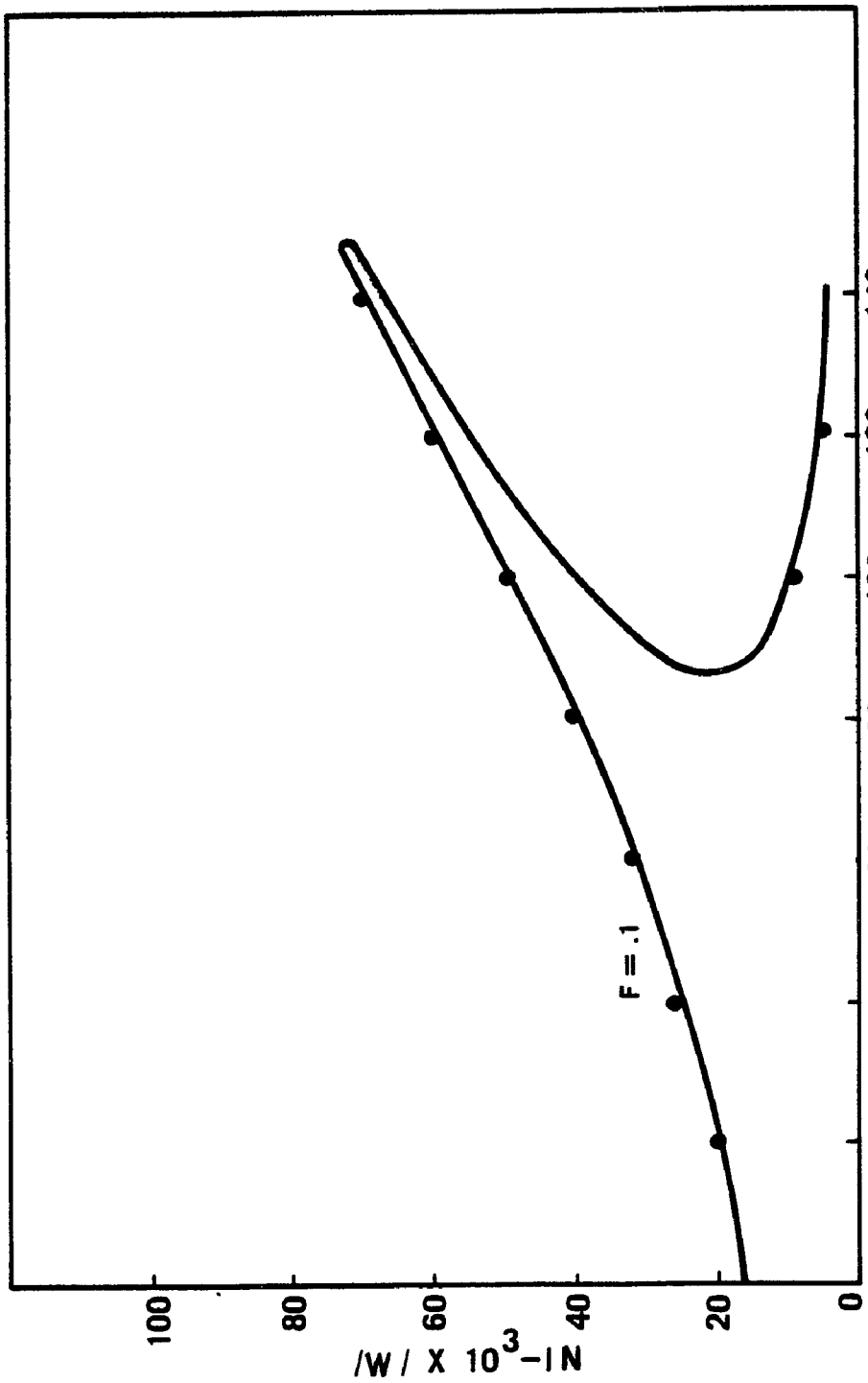


FIGURE 2.10 DAMPED RESPONSE. h = .035", b = 1", L = 12", t = .008" LAYER

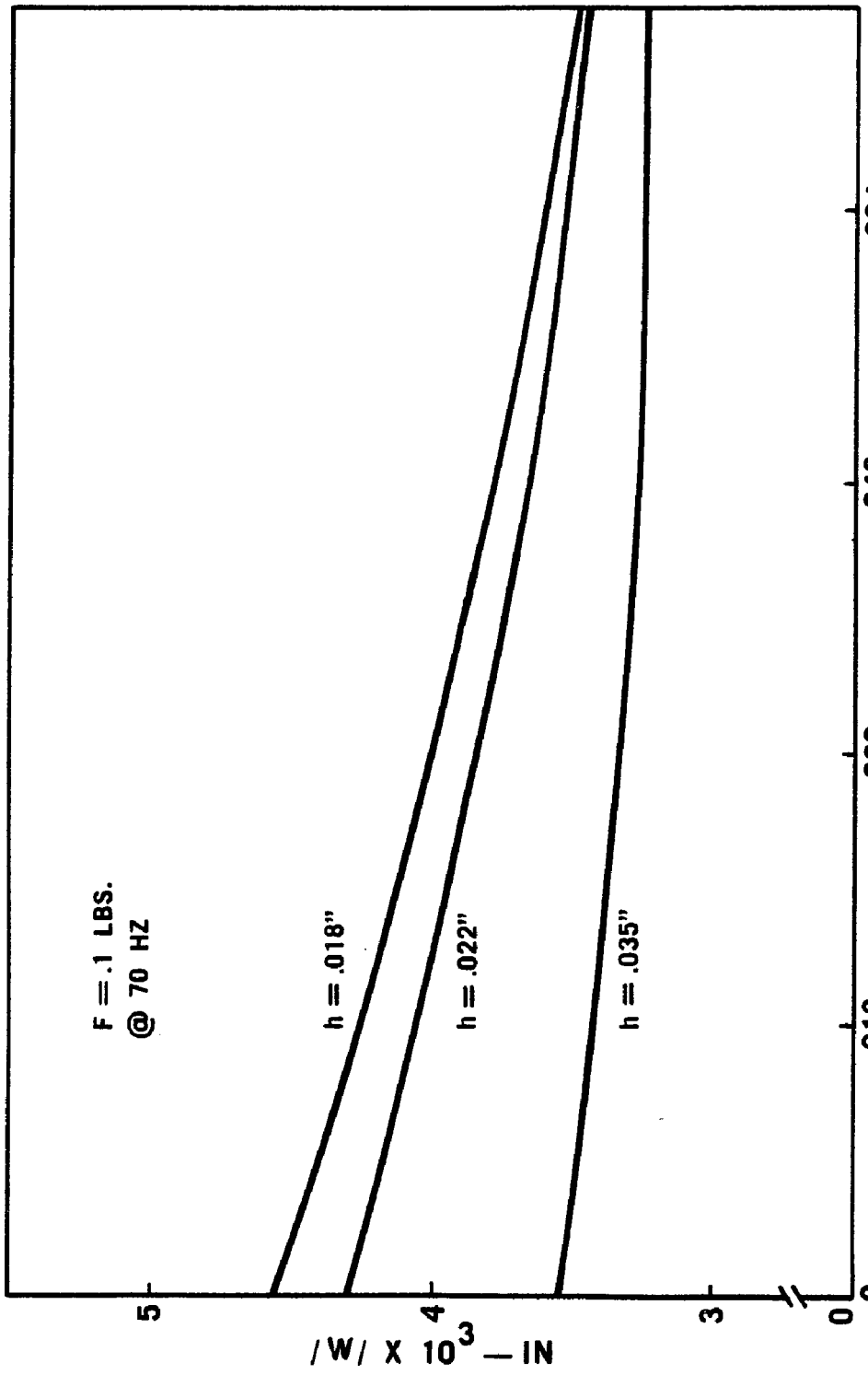


FIGURE 2.11 ISPD III VISCOELASTIC LAYER THICKNESS — IN

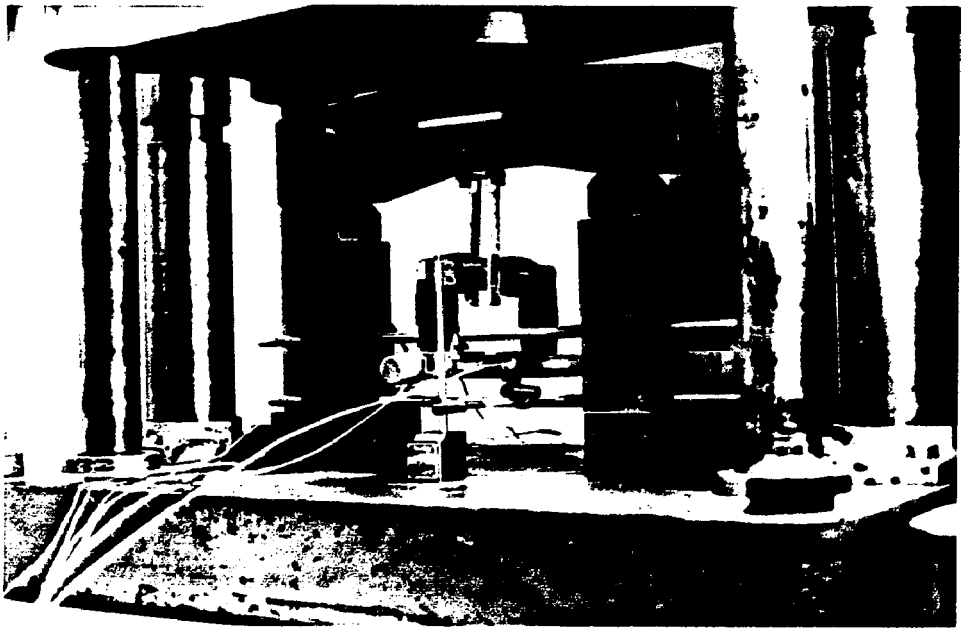


FIGURE 2.12. EXPERIMENTAL TEST SET-UP

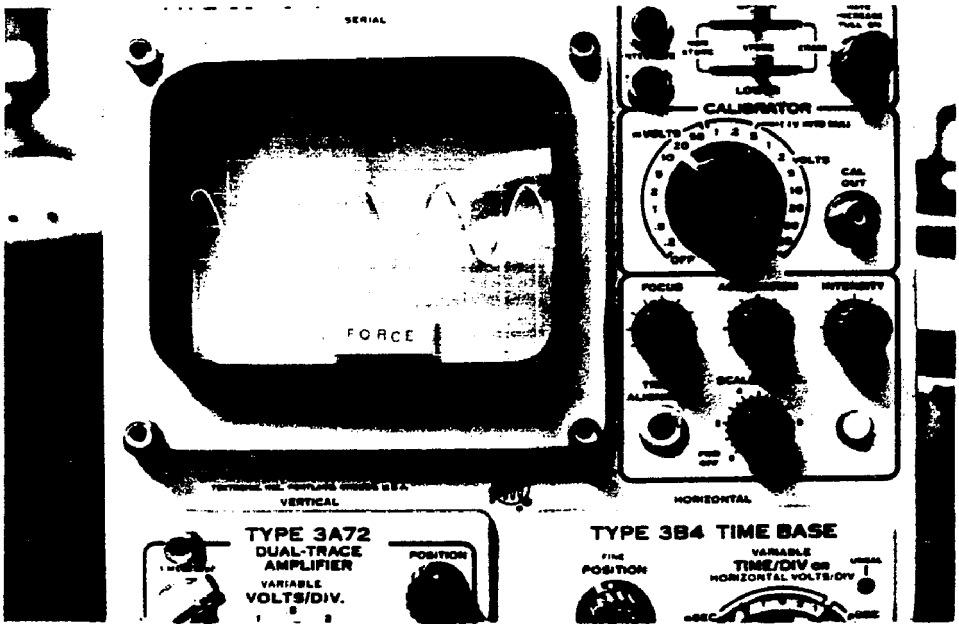


FIGURE 2.13. EXCITATION FORCE

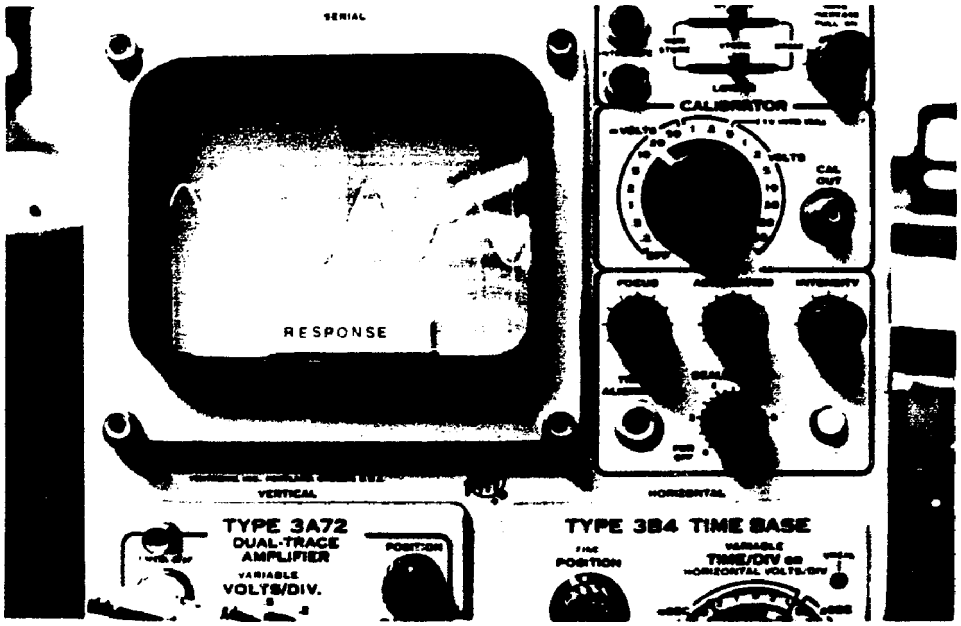


FIGURE 2.14. RESPONSE

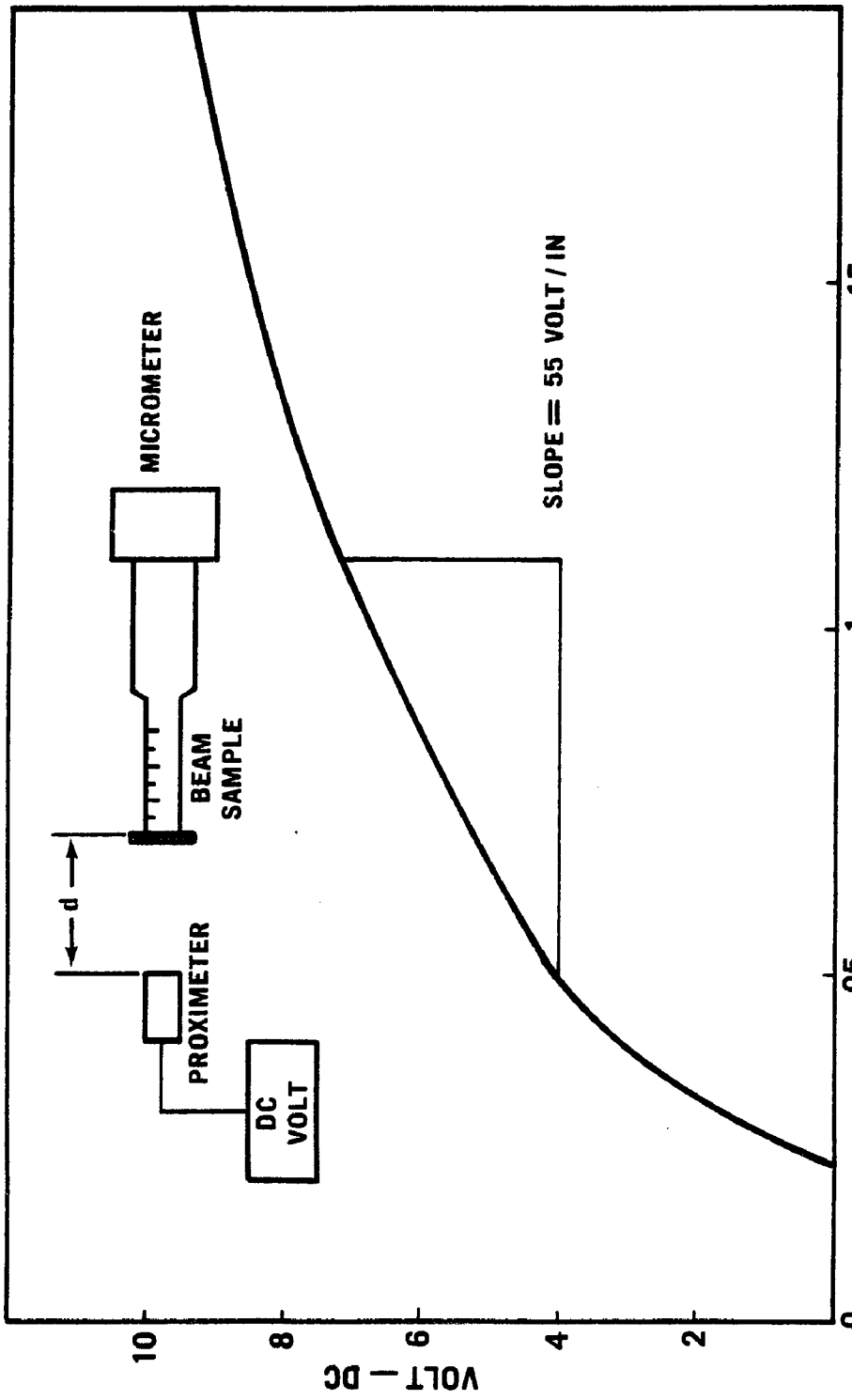
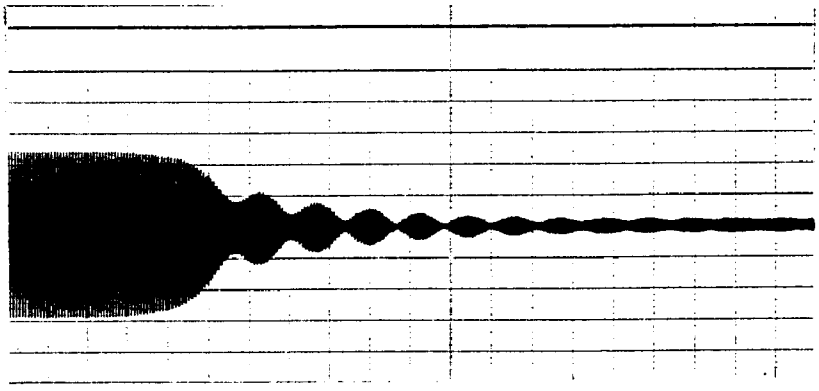
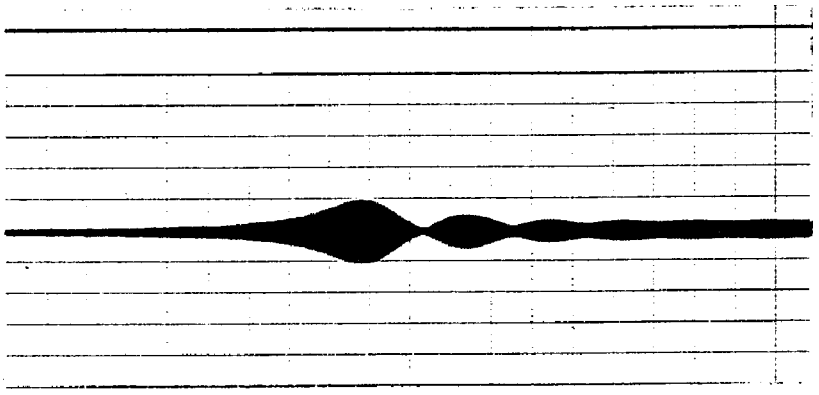


FIGURE 2.15 CALIBRATION CURVE OF PROXIMETER.



A. JUMP FROM HIGH - LOW AMP.



B. JUMP FROM LOW - HIGH AMP.

FIGURE 2.16. JUMP-BEATING PHENOMENA